DETAILED STUDIES OF THE STRUCTURE, TECTONICS, NEAR BOTTOM MAGNETIC ANOMALIES AND MICROEARTHQUAKE SEISMICITY OF THE MID-ATLANTIC RIDGE NEAR 37°N

by

KEN C. MACDONALD

B.S., University of California at Berkeley
(1970)

SUBMITTED IN PARTIAL FULFILLMENT OF THE
REQUIREMENTS FOR THE DEGREE OF
DOCTOR OF PHILOSOPHY

at the

MASSACHUSETTS INSTITUTE OF TECHNOLOGY

and the

WOODS HOLE OCEANOGRAPHIC INSTITUTION

September, 1975
(i.e. February, 1976)

Signature of Author .....
Joint Program in Oceanography, Department of Earth and Planetary Sciences, Massachusetts Institute of Technology and Department of Geology and Geophysics, Woods Hole Oceanographic Institution, September, 1975

Certified by .....
Thesis Supervisor

Accepted by .....
Chairman, Joint Oceanography Committee in the Earth Sciences, Massachusetts Institute of Technology and Woods Hole Oceanographic Institution

TABLE OF CONTENTS

Page

LIST OF FIGURES

CHAPTER II

LIST OF TABLES

DETAILED STUDIES OF THE STRUCTURE, TECTONICS, NEAR-BOTTOM MAGNETIC ANOMALIES AND MICROEARTHQUAKE SEISMICITY OF THE MID-ATLANTIC RIDGE NEAR 37°N

by

Ken C. Macdonald

Submitted to the Massachusetts Institute of Technology-Woods Hole Oceanographic Institution Joint Program in Oceanography on September 22, 1975, in partial fulfillment of the requirements for the degree of Doctor of Philosophy

ABSTRACT

The Mid-Atlantic Ridge is one of the most well known and yet poorly understood spreading centers in the world. A detailed investigation of the Mid-Atlantic Ridge crest near 37°N (FAMOUS) was conducted using a deeply towed instrument package. The objective was to study the detailed structure and spreading history of the Mid-Atlantic Ridge median valley, to explore the roles of volcanism and faulting in the evolution of oceanic crust, and to study the morphologic expression and structural history of the zone of crustal accretion. In addition, microearthquake surveys were conducted using arrays of free-floating hydrophones.

The most recent expression of the accreting plate boundary in the Famous Rift is an alternating series of linear central volcanoes and depressions 1.5 km wide which lie within the inner floor. This lineament is marked by a sharp maximum in crustal magnetization only 2-3 km wide. Magnetic studies indicate that over 90% of the extrusive volcanism occurs within the rift inner floor, a zone 1 to 12 km wide, while volcanism is extremely rare in the rift mountains. Volcanoes created in the inner floor are transported out on block faults, becoming a lasting part of the topography. Magnetic anomaly transition widths vary from 1 km to 8 km with time and appear to reflect a bi-stable median valley structure. The valley has either a wide inner floor and narrow terraces, in which case the volcanic zone is wide and magnetic anomalies are poorly recorded (wide transition widths); or it has a narrow inner floor and wide terraces, the volcanic zone is then narrow and anomalies are clearly recorded (narrow transition widths). The median valley of any ridge segment varies between these two structures with time. At present the Famous Rift has a narrow inner floor and volcanic zone (1-3 km) while the south Famous Rift is at the opposite end of the cycle with a wide inner floor and volcanic zone (10-12 km).

Over 95% of the large scale (> 2 km) relief of the median valley is accounted for by normal faults dipping toward the valley axis. Normal faulting along fault planes dipping away from the valley begins just past the outer walls of the valley. Outward facing normal faulting accounts for most of the decay of median valley relief in the rift mountains while crustal tilting accounts for less than 20%. The pattern of normal faulting creates a broad, undulating horst and graben relief. Volcanic features contribute little to the large scale relief, but contribute to the short wavelength (<2 km) roughness of the topography.

Spreading in the Famous area is highly asymmetric with rates twice as high to the east as to the west. At 1.7 m.y.b.p. the sense of asymmetry reverses in direction with spreading faster to the west, resulting in a gross symmetry when averaged through time. The change in spreading asymmetry occurred in less than 0.15 m.y. Structural studies indicate that the asymmetric spreading is accomplished through asymmetric crustal extension as well as asymmetric crustal accretion. Spreading in the Famous area is 17° oblique. Even on a fine scale there is no indication of readjustment to an orthogonal plate boundary system. Spreading has been stably oblique for at least 6 m.y., even through a change in spreading direction.

Magnetic studies reveal that the deep DSDP hole at site 332 was drilled into a magnetic polarity transition, and may have sampled rocks which recorded the earth's field behavior during a reversal. The presence of negative polarity crust within the Brunhes normal epoch in the inner floor has been determined, and may be due to old crust left behind or recording of a geomagnetic field event. Crustal magnetization decays to 1/e of its initial value in less than 0.6 m.y. The rapid decay may be facillitated by very intense crustal fracturing observed in the inner floor.

Microearthquake, magnetic and structural studies indicate that both the spreading and transform plate boundaries are very narrow (1-2 km) and well-defined for short periods, but migrate over zones 10-20 km wide through time.

Thesis Advisor: Tanya Atwater
Title: Assistant Professor of Geophysics, Massachusetts Institute of Technology

ACKNOWLEDGEMENTS

Many thanks go to Bruce Luyendyk, John Mudie and Fred Spiess who initiated the deep-tow program on the Mid-Atlantic Ridge. My thesis advisors, Bruce Luyendyk and Tanya Atwater I thank for their inspiration. Steve Huestis, Robert Parker, Kim Klitgord and John Mudie introduced me to techniques and programs for making sense out of near-bottom magnetic data. Steve Huestis, Steve Miller and John Mudie were particularly generous in helping me. Captain Hiller and the crew of the R/V KNORR, and the deep-tow group including Tony Boegeman, Martin Benson, and Steve Miller, were largely responsible for the successful completion of our work on the Mid-Atlantic Ridge under bad to terrible conditions.

I had many helpful discussions ranging from the practical to the philosophical with T. Atwater, B. Luyendyk, H. Schouten, C. Denham, R. Parker, J. Mudie, S. Huestis, S. Miller, J. R. Heirtzler, R. P. Von Herzen, C. Bowin, R. Ballard, W. Bryan, Tj. van Andel, J. Francheteau, J. Phillips (who provided me with data prior to publication) K. Louden, S. Gegg, and A.L. Peirson. Among those who helped me with graphics, art work and typing I am particularly grateful to G. Mosier, S. Bernardo, K. Macdonald, J. Zwinakis, D. Souza, F. Medeiros, and G. Storm.

Special thanks go to Kathy who put up with me.

BIOGRAPHIC NOTE

I was born in San Francisco in 1947 and lived there most of my life until 1970, when I received a B.S. degree in Engineering Geoscience from Berkeley(University of California) and headed east to the MIT/WHOI Joint program. My first contact with oceanography was as an ordinary seaman on the R/V VIRGINIA CITY in 1968. My first mentors here were G. Simmons, R. P. Von Herzen and B. Luyendyk, whom I thank for their inspiration. My research interests at Woods Hole have included heat flow, southwest Pacific tectonics, tracking of bottom currents, microearthquake studies in the Atlantic and Pacific, and deep-tow studies of magnetic anomalies and tectonics of the Mid-Atlantic Ridge. In April of 1975 I married Kathy Gill.

PUBLICATIONS

Macdonald, Ken and Gene Simmons, Temperature coefficient of the thermal conductivites of ocean sediments, Deep-Sea Res., 19, 669, 1972.

Reid, I., and K.C. Macdonald, Microearthquake study of the Mid-Atlantic Ridge near 37°N using sonobuoys, Nature 246, 88, 1973.

Detrick, R., J.D. Mudie, B.P. Luyendyk, and K.C. Macdonald, Near-bottom observations of an active transform fault: Mid-Atlantic Ridge at 37°N, Nature, 246, 59, 1973.

Macdonald, Ken C., B.P. Luyendyk, and R.P. Von Herzen, Heat flow and plate boundaries in Melanesia, J. Geophys. Res., 78, 2537, 1973.

Macdonald, K.C. and C.D. Hollister, Near-bottom thermocline in the Samoan Passage, west equatorial Pacific, Nature, 243, 461, 1973.

Luyendyk, B.P., K.C. Macdonald, and W.B. Bryan, Rifting history of the Woodlark Basin in the southwest Pacific, Bull. Geol. Soc. Amer., 84, 1125, 1973.

Spindel, R.C., S.B. Davis, K.C. Macdonald, R.P. Porter and J.D. Phillips, Microearthquake survey of median valley of the Mid-Atlantic Ridge at 36°30'N, Nature, 248, 577, 1974.

Macdonald, K.C. and J.D. Mudie, Microearthquakes on the Galapagos spreading centre and the seismicity of fast-spreading ridges, Geophysical J.R.astr. Soc., 36, 245, 1974.

Macdonald, Ken C., Marine seismicity, Rev. Geophys. Space Phys., 13, 540, 1975.

Macdonald, Ken C., B.P. Luyendyk, J.D. Mudie and F.N. Spiess, Near-bottom geophysical study of the Mid-Atlantic Ridge median valley near lat. 37°N: Preliminary observations, Geology 3, 211, 1975.

Luyendyk, Bruce P. and Ken C. Macdonald, Physiography and structure of the Famous Rift valley inner floor observed with a deeply towed instrument package, in prep. for Bull. Geol. Soc. Amer. dedicated issue on FAMOUS.

Macdonald, Ken C., Near-bottom magnetic anomalies, asymmetric spreading, oblique spreading, and tectonics of the accreting plate boundary on the Mid-Atlantic Ridge (37°N), in prep. for Bull. Geol. Soc. Amer. dedicated issue on FAMOUS.

Macdonald, Ken C. and B.P. Luyendyk, An intensive deep tow study of the geomorphology and tectonics of the Mid-Atlantic Ridge (37°N), in prep. for Bull. Geol/ Soc. Amer. dedicated issue on FAMOUS.

Macdonald, Ken C., Deep-tow inversion solutions for crustal magnetization at DSDP site 332. International Symposium on the Nature of the Oceanic Crust (submitted).

Chapter 1

Introduction

The visual fit of the continents on opposite sides of the Atlantic inspired Wegener (1924) over fifty years ago to hypothesize continental drift, and yet our knowledge of the tectonics of the spreading center between the Atlantic continents has remained obscure to this day. Even detailed, intensive surface ship studies of the Mid-Atlantic Ridge crest have often yielded confusing and ambiguous results (Aumento et al., 1971). It was our objective to study the detailed structure of the Mid-Atlantic ridge median valley and rift mountains, to explore the origin and evolution of the rugged terrain, and to study the morphologic expression and history of the zone of crustal accretion relative to the ridge structure. To this end we made precise topographic and magnetic field measurements near the seafloor, and located microearthquakes with floating hydrophone arrays.

Early studies of the Mid-Atlantic ridge median valley showed that it is a 20-30 km wide 1.5 to 2.5 km deep cleft in the seafloor, but the poor resolution of wide beam surface echo sounders limited interpretation as to its origin (Heezen et al., 1959; Loncarevic et al., 1966; van Andel

and Bowin, 1968; Aumento and Loncarevic, 1969; van Andel and Heath, 1970; Phillips et al., 1969). Deep tow studies of the Gorda Rise (Atwater and Mudie, 1968, 1973) and focal mechanism solutions (Sykes, 1967) suggested that the median valley is formed by block faulting, and later work showed that normal faulting was also the origin of the Mid-Atlantic Ridge valley (Barrett and Aumento, 1970; Macdonald et al., 1975). Recently there have been a number of detailed surveys on the Mid-Atlantic ridge (at 45°N, Aumento et al., 1971; at 37°N, Needham and Francheteau, 1974; Phillips and Fleming, in prep.; at 26°N, McGregor and Rona, 1975), and yet, even the identification of key magnetic anomalies is still often difficult. Several fundamental problems have remained unsolved: 1) the roles of volcanism and faulting in the median valley; 2) the structure of the rift valley through time; 3) the level of tectonic and volcanic activity away from the rift valley; 4) the evolution and decay of median valley relief in the rift mountains; and 5) the detailed spreading history and kinetics of the plate near the crustal accretion zone, in particular, the problems of highly asymmetric and oblique spreading.

To address ourselves to these problems we conducted a detailed survey of the Mid-Atlantic ridge at 37°N (the

Famous area) using the Marine Physical Laboratory (Scripps Institute of Oceanography) deep tow fish (Spiess and Tyce, 1973). We collected topographic, side-looking sonar, sediment thickness, magnetic, and photographic data near the seafloor in a navigation framework with relative accuracies of 50 m or better. We precisely located microearthquakes in the survey area using arrays of sono-buoys (free floating hydrophones). With this unique suite of data we were able to make significant progress in solving the problems mentioned earlier. We have found that:

1. The most recent expression of the accreting plate boundary is an alternating series of linear central volcanoes and depressions. This lineament is less than 1.5 km wide in the Famous rift. Within 500 m of the floor axis, intense faulting and fracturing of the crust begins (up to 25 faults per km^2).
2. The accreting plate boundary is marked by a narrow (2-3 km) maximum in crustal magnetization. The axial magnetization maximum is highest over central volcanoes and decreases over the central depressions. While volcanism may cover most of the inner floor with a veneer of recent lavas, the magnetization maximum delineates the major recent volcanic center. It lies near the center of the Famous rift and well off to the east side of the south Famous rift (fig. 1, chapter 2).

3. Inward and outward facing block faults and tilting of fault blocks account for almost all the depth of the median valley. Volcanic relief dominates in the inner floor of the rift valley but is secondary to faulting in creating large scale relief outside the inner floor.
4. The Mid-Atlantic Ridge in the Famous area is characterized by highly asymmetric spreading; 7.0 mm/yr to the west and 13.4 mm/yr to the east. The sense of asymmetry reversed at 1.7 m.y.b.p.; 10.8 mm/yr to the east and 13.4 mm/yr to the west. The grossly symmetric spreading previously reported for the Mid-Atlantic ridge (e.g., Pitman and Talwani, 1972; Phillips et al., 1975) is probably composed of highly asymmetric episodes of spreading.
5. The reversal in asymmetric spreading and change in total spreading rate occurred almost instantaneously (geologically); less than 0.15 m.y.
6. Asymmetric spreading appears to be accomplished through asymmetric crustal extension as well as asymmetric crustal accretion. Horizontal crustal extension out to the beginning of the terraces is 11% to the west and 18% to the east. The zone of active extension appears to be at least 16 km wide.

7. While the Mid-Atlantic Ridge is grossly symmetrical, nearly every aspect of the median valley is asymmetrical: the position of the inner and outer rift walls relative to the axis, the dips of faults, the density of faulting, the structure of the inner walls, sediment distribution, crustal extension rates, and short term seafloor spreading rates.
8. Median valley relief appears to decay in the rift mountains primarily through outward facing normal faulting occurring outside the median valley (about 80%) and to a much lesser extent by crustal tilting (about 20%).
9. Faulting accounts for nearly all the large scale relief in the rift mountains while volcanic relief is important in the small scale roughness of the topography (< 2 km wavelength).
10. The Mid-Atlantic ridge here is spreading obliquely at an angle of 17°. Detailed studies of the strikes of faults, fissures, recent volcanic zones, and fine scale magnetic trends, as well as microearthquake distribution all indicate that spreading is stably oblique. There is no indication of reorientation to an orthogonal system in the transform faults or in

the rift inner floor. Oblique spreading apparently has been stable for millions of years, even through a change in spreading direction. At least out to anomaly 5 (10 m.y.) the Famous area is sufficiently removed from the Azores triple junction so that oblique spreading cannot be explained by its influence. Oblique spreading may be stable for many or even most slow spreading centers.

11. High magnetizations of the youngest crust (20 to 30 amps/m) decay very rapidly to 1/e in only 0.6 m.y. Most of the decay occurs in and near the inner floor where the crust is intensely fractured and faulted almost immediately after formation. This intense fracturing may accelerate the alteration of magnetic minerals through seawater contact and circulation.

12. The magnetization of topographic features (from deep-tow modeling), combined with surface tow magnetic anomalies suggests that the magnetized layer is 700 m thick. This is assuming constant magnetization with depth in the crust.

13. Deep tow magnetic modeling of topographic magnetic anomalies suggests that over 90% of the volcanism and

crustal accretion occurs within the 2-12 km wide inner floor. Central highs which mark the volcanic zone are transported out of the inner floor on block faults becoming a lasting part of the topography. They frequently occur as lips at the edges of fault blocks.

14. There are several zones in the inner floor, within the Brunhes normal epoch in which the crust is negatively polarized. Perhaps a short reversal such as the Blake event was recorded, or perhaps seafloor created during the Matuyama reverse epoch was somehow left behind. At present there appears to be no satisfying explanation.

15. The unusually low magnetic inclinations observed throughout the first deep DSDP hole (332) may be explained by its location in a wide polarity transition zone which may consist of more than one reversal. Results from the hole and from the inversion solution near the site suggest that volcanism is highly episodic and that the entire magnetized layer can be created in a short period of time. The deep hole here may be invaluable in studying the earth's magnetic field during a field reversal.

16. Magnetic anomaly transition widths vary from 1 km to 8 km with time and appear to reflect a bi-stable median valley structure. The valley has either a wide inner floor in which case the volcanic zone is wide and magnetic anomalies are poorly recorded (wide transition widths); or it has a narrow inner floor, the volcanic zone is then narrow and anomalies are clearly recorded (narrow transition widths). The median valley of any ridge segment may vary between these two structures with time.

17. The accreting plate boundary over short periods of time ($\sim 10^5$ years) is sharply defined in space ($\sim$1.5 km). Over millions of years, however, the valley structure changes and the plate boundary may shift about inside a zone approximately 10 km wide.

18. Transform faults are also sharply defined in space (1 to 2 km wide) as delineated by microearthquakes and near bottom mapping. However, over millions of years the faults migrate over a zone 10-20 km wide, a zone wide enough to disrupt lineated magnetic anomalies generated at the ridge crests.

19. Major block faults in the Famous rift appear to bend longitudinally toward the fracture zones about a point

midway between the two fracture zones. This suggests that rift zone tectonics are influenced by fracture zone tectonics at least 20 km away from the fracture zones.

The research summarized in this thesis is part of a larger project, FAMOUS (French-American mid-ocean undersea study; Heirtzler and LePichon, 1974). Other unique methods were employed to address the difficult tectonic problems of the Mid-Atlantic ridge including long range sonar (Gloria; Laughton and Rusby, 1975), novel underwater camera systems (LIBEC; Brundage et al., in prep.) and deep diving submersibles including the Alvin (Heirtzler and van Andel, submitted), the Archimede and the Cyana. The submersible work occurred after the deep tow survey was completed, however, discussions with the divers and data collected from the submersibles was valuable in interpreting the deep tow data and vice versa. (Belliache et al., 1974; Ballard et al., in press; Arcyana, in press; Bryan and Moore, in prep., Ballard and van Andel, in prep.). Submersible results of immediate relevance are cited in the text and all Famous area investigations are referenced in the bibliography.

A note on format: Some of the results in this thesis were presented in a preliminary form by Macdonald and others (1975). Very detailed work on bottom photographs and side looking sonar within the inner floor is being published by Luyendyk and Macdonald (in prep.) and is not a part of this thesis. Chapter 2 is being published by Macdonald and Luyendyk (in prep.), and Chapter 3 is being published by Macdonald (in prep.). Thus, in Chapter 2 "Macdonald (in prep.)" refers to Chapter 3 and in Chapter 3 "Macdonald and Luyendyk (in prep.)" refers to Chapter 2. Results of the sonobuoy/microearthquake studies have been published by Reid and Macdonald (1973) and Spindel and others (1974), reprints of which can be found in Appendix 2.

References and Bibliography, Chapter 1

Arcyana, X.Y., Transform fault and rift valley geology by bathyscaphe and diving saucer, Science, in press.

Atwater, T.M. and J.D. Mudie, Block faulting on the Gorda Rise, Science, 159, 729, 1968.

Atwater, T.M. and J.D. Mudie, Detailed near bottom geophysical study of the Gorda Rise, J. Geophys. Res., 78, 8665, 1973.

Aumento, F., B.D. Loncarevic, and D.I. Ross, Hudson geotraverses: geology of the Mid-Atlantic Ridge at 45°N, Roy. Soc. London, 268, 623, 1971.

Aumento, F. and B.D. Loncarevic, The Mid-Atlantic Ridge near 45°N, III. Bald Mountain, Can. J. Earth Sci., 6, 11, 1969.

Ballard, R.D., W.B. Bryan, J.R. Heirtzler, G. Keller, J.G. Moore, Tj. van Andel, Manned Submersible Observations in the FAMOUS Area Mid-Atlantic Ridge, Science, in press.

Ballard, R.D. and T.H. van Andel, Project FAMOUS: the Mid-Atlantic Rift at 36-37°N, operational techniques of the U.S. submersible operation, in prep. for Bull. Geol. Soc. Amer. dedicated issue on FAMOUS.

Ballard, R. and T.H. van Andel, Project FAMOUS: the Mid-Atlantic Rift valley at 36-37°N, morphology and tectonics of the inner rift valley at 36°50'N on the Mid-Atlantic Ridge, in prep. for Bull. Geol. Soc. Amer. dedicated issue on FAMOUS.

Barrett, D.L. and F. Aumento, The Mid-Atlantic Ridge near 45°N, XI. Seismic velocity, density and layering in the crust, Can. J. Earth Sci., 7, 1117, 1970.

Bellaiche, G., J.L. Cheminee, J. Francheteau, R. Hekinian, X. Le Pichon, H.D. Needham, R.D. Ballard, Rift valley's inner floor: First submersible study, Nature, 250, 558-560, 1974.

Bougault, H., and R. Hekinian, Rift Valley in the Atlantic Ocean near 36°50'N: Petrology and Geochemistry, Earth Planet. Sci. Lett., 24(2), 249-261, 1974.

Bryan, W.B., and J.G. Moore, Project FAMOUS: The Mid-Atlantic Rift valley at 36-37°N, volcanism, petrology and geochemistry of the basalts of the inner floor of the rift valley at 36°50'N on the Mid-Atlantic Ridge, in prep. Bull. Geol. Soc. Amer., dedicated issue on FAMOUS.

Detrick, R., J.D. Mudie, B.P. Luyendyk, and K.C. Macdonald, Near Bottom Observations of an Active Transform Fault: Mid-Atlantic Ridge at 37°N, Nature, 246, 59, 1973.

DSDP Drilling Team, Leg 37 - The Volcanic Layer, Geotimes, 16, 1974.

Fowler, C.M.R., and D.H. Matthews, Seismic refraction experiment using ocean bottom seismographs and sono-buoys in the FAMOUS Area, Nature, 249, 752, 1974.

Greenewalt, D., and P.T. Taylor, Deep-tow magnetic measurements across the Axial Valley of the Mid-Atlantic

Ridge, Jour. Geophys. Res., 79, 4401-4405, 1974.

Heezen, B.C., M. Tharp, and M. Ewing, The floors of the oceans, 1, The North Atlantic Ocean, Geol. Soc. Am. Spec. Paper 65, 122, 1959.

Heirtzler, J.R., Project FAMOUS Planning Mid-Atlantic Ridge Investigation, Marine Tech. Soc. Jour. 7(1), 14-15, 1973.

Heirtzler, J.R., and X. Le Pichon, FAMOUS: A plate tectonics study of the genesis of the lithosphere, Geology, 2(6), 273-378, 1974.

Heirtzler, J.R., and T.H. van Andel, Project FAMOUS: The Mid-Atlantic rift valley at 36-37°N, project history and geologic setting, in prep. for Bull. Geol. Soc. Amer. dedicated issue on FAMOUS.

Hekinian, R., M. Chaigneau, and J.L. Cheminee, Popping rocks and lava tubes from the Mid-Atlantic Rift valley at 36°N, Nature, 245, 371-373, 1974.

Hekinian, R., and M. Hoffert, Rate of palagonitization and manganese coating on basaltic rocks from the Rift Valley in the Atlantic Ocean near 36°50'North, Marine Geology, in press.

Keller, G.H., S.H. Anderson, D.E. Koelsch, and J.W. Lavelle, Near bottom currents in the Mid-Atlantic Ridge rift valley, Can. J. Earth Sci., in press.

Laughton, A.S., and J.S. Rusby, Long range sonar and photographic studies of the median valley in the Famous Area of the Mid-Atlantic Ridge near 37°N, Deep-Sea Research, in press.

Loncarevic, B.D., C.S. Mason, and D.H. Matthews, The Mid-Atlantic Ridge near 45°N, I. The Median Valley, Can. J. Earth Sci., 3, 327, 1966.

Luyendyk, Bruce P., and Ken C. Macdonald, Physiography and structure of the Famous rift valley inner floor observed with a deeply towed instrument package, in prep. Bull. Geol. Soc. Amer. dedicated issue on FAMOUS.

Macdonald, Ken C., Near-bottom magnetic anomalies, asymmetric spreading, oblique spreading, and tectonics of the accreting plate boundary on the Mid-Atlantic Ridge (37°N), in prep. Bull. Geol. Soc. Amer. dedicated issue on FAMOUS.

Macdonald, Ken C., and B.P. Luyendyk, An intensive deep-tow study of the geomorphology and tectonics of the Mid-Atlantic Ridge (37°N), in prep. Bull. Geol. Soc. Amer. dedicated issue on FAMOUS.

Macdonald, Ken C., B.P. Luyendyk, J.D. Mudie, and F.N. Spiess, Near-bottom geophysical study of the Mid-Atlantic Ridge median valley near lat. 37°N: Preliminary observations, Geology, 211, 1975.

McGregor, B.A., and P.A. Rona, Crest of the Mid-Atlantic Ridge at 26°N, J. Geophys. Res., 80, 3307, 1975.

Melson, William G., Fabrizio Aumento, et al., Deep Sea Drilling Project, Leg 37 - The Volcanic Layer, Geotimes, 16-18, 1974.

Moore, J.G., H.S. Fleming, and J.D. Phillips, Preliminary model for extrusion and rifting at the axis of the Mid-Atlantic ridge, 36°48' North, Geology, 2 (9), 437-440, 1974.

Needham, H.D., and J. Francheteau, Some characteristics of the Rift Valley in the Atlantic Ocean near 36°48' North, Earth and Planet. Sci. Lett., 22, 29-43, 1974.

Phillips, J.D., and H.S. Fleming, The Mid-Atlantic Ridge west of the Azores 35°-39°N, in prep. Bull. Geol. Soc. Amer. dedicated issue on FAMOUS.

Phillips, J.D., H.S. Fleming, R. Feden, W.E. King, and R. Perry, Aeromagnetic study of the Mid-Atlantic Ridge near the Oceanographer Fracture Zone, Geol. Soc. Am., in press.

Phillips, J.D., G. Thompson, R.P. Von Herzen, and V.T. Bowen, Mid-Atlantic Ridge near 43°N latitude, J. Geophys. Res., 74, 3069, 1969.

Pitman, W.C., III, and M. Talwani, Sea-floor spreading in the North Atlantic, Bull. Geol. Soc. Amer., 83, 619, 1972.

Poehls, K., Seismic refraction on the Mid-Atlantic Ridge at 37°N, Jour. Geophys. Res., 79, 3370-3373, 1974.

Reid, I., and K.C. Macdonald, Microearthquake study of the Mid-Atlantic Ridge near 37°N using sonobuoys, Nature, 246, 88-90, 1973.

Schilling, J.G., Azores mantle blob: Rare-earth evidence, Earth and Planet. Sci. Lett., in press.

Spiess, F.N., and R.C. Tyce, Marine Physical Laboratory Deep-Tow instrumentation system, Scripps Inst. Oceanography Ref. 73-4, 1973.

Spindel, R.C., S.B. Davis, K.C. Macdonald, R.P. Porter, and J.D. Phillips, Microearthquake survey of median valley of the Mid-Atlantic ridge at 36°30'N, Nature, 248, 577-579, 1974.

Sykes, L.R., Mechanism of earthquakes and nature of faulting on the mid-ocean ridges, J. Geophys. Res., 72, 2131, 1967.

van Andel, Tjeerd H., and Carl O. Bowin, Mid-Atlantic ridge between 22° and 23° north latitude and the tectonics of mid-ocean rises, J. Geophys. Res., 73,1279,1968 .

van Andel, Tjeerd H., and G. Ross Heath, Tectonics of the Mid-Atlantic Ridge, 6°-8° south latitude, Mar. Geophys. Res., 1, 5, 1970.

Wegener, A., The Origin of Continents and Oceans, Methuen, London, 1924.

Whitmarsh, R.B., Median valley refraction line, Mid-Atlantic ridge at 37°N, Nature, 246 (5430), 297-299, 1973.

Whitmarsh, R.B., Axial intrusion zone beneath the median valley of the Mid-Atlantic ridge at 37°N detected by explosion seismology, Geophys. Journal, in press.

CHAPTER II

AN INTENSIVE DEEP TOW STUDY OF THE GEOMORPHOLOGY AND TECTONICS OF THE MID-ATLANTIC RIDGE (37°N)

1. MORPHOLOGY AND STRUCTURE OF THE FAMOUS RIFT

The portion of the median valley studied consists of two segments each 40 km long trending N 17°E (Fig. 1). Fracture zones A, B, and C each right-laterally offset the valley about 20 km and trend east-west. The Famous Rift was studied in greatest detail and will be discussed first. Then the south Famous Rift will be compared to the Famous Rift using available deep-tow data and supplementary surface ship data.

Macdonald and others (1975) divide the Famous Rift into four physiographic provinces: 1) the inner floor, 2) the inner walls, 3) the terraces, relatively flat regions between the inner and outer walls, and 4) the outer walls which form the boundary between the median valley and the rift mountains (Fig.2).

DATA INTERPRETATION

The tectonic maps and profiles are based on interpretation of three types of deep tow sonar records: high frequency (40 kHz) narrow beam sonar for depth, low frequency (4.0 kHz) sonar for sediment penetration, and left and right side-looking sonar

Figure 1A. Regional setting and plate boundaries in the Famous area (unpublished navy bathymetric chart courtesy of W. Perry). E-E''' is the long deep tow traverse into the east rift mountains.

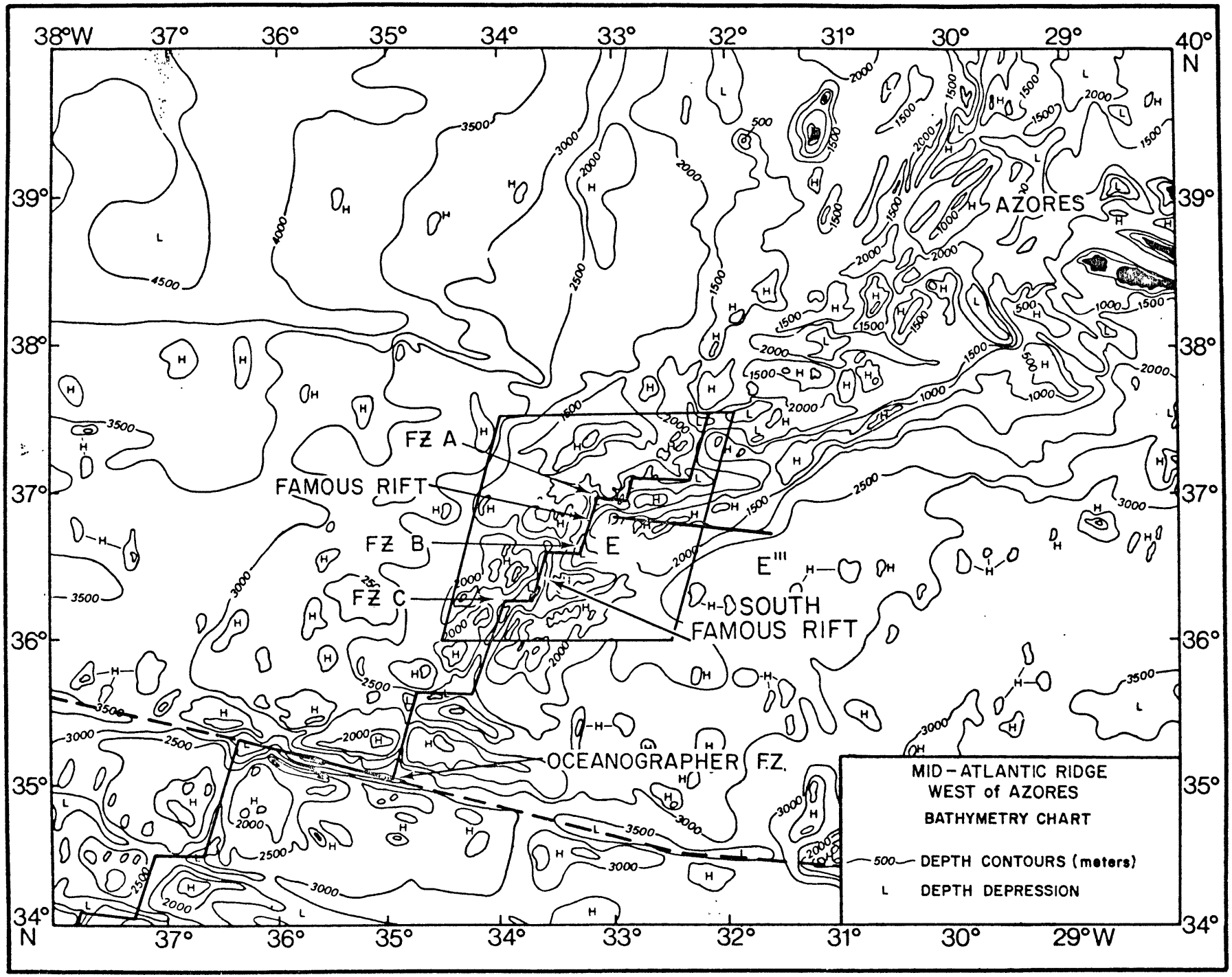
38°W
37°
36°
35°
34°
33°
32°
31°
30°
29°
40° N
39°
38°
37°
36°
35°
34° N
AZORES
FZ A
FAMOUS RIFT
FZ B
FZ C
E
E'''
SOUTH FAMOUS RIFT
OCEANOGRAPHER F.Z.
MID-ATLANTIC RIDGE
WEST of AZORES
BATHYMETRY CHART
500 DEPTH CONTOURS (meters)
L DEPTH DEPRESSION

Figure 1B. Bathymetric chart of Famous area 100 fm. contour interval (after Phillips & Fleming, in prep.). Location of geophysical profiles shown by solid lines. Strike parallel lines in median valley not shown (see Figure 3). Dashed lines show location of supplementary surface ship bathymetric profiles shown in Figure 20.

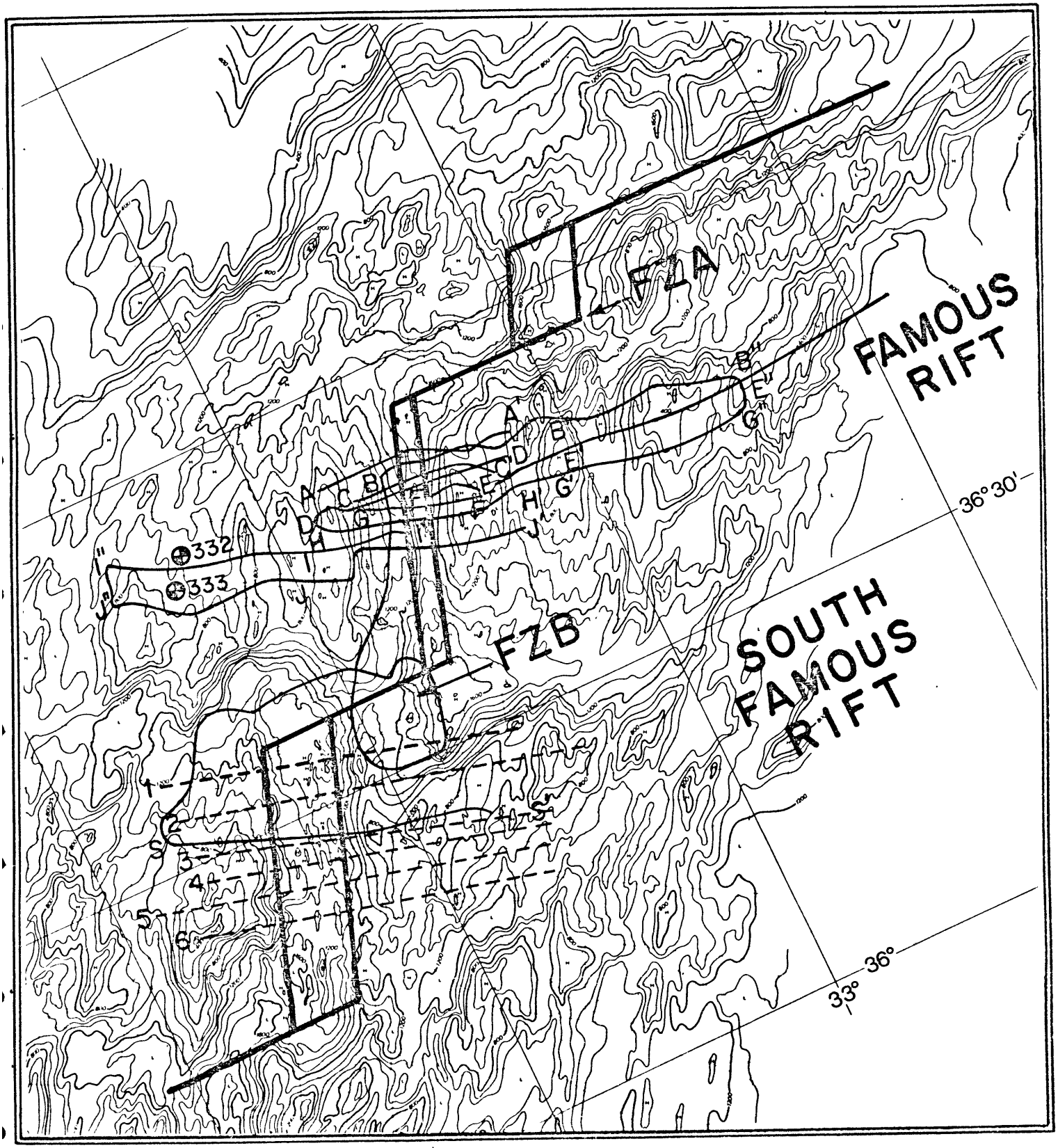
FZA
FAMOUS RIFT
FZB
SOUTH FAMOUS RIFT
36° 30'
36°
33°
332
333
A
B
C
D
E
F
G
H
J
1
2
3
4
5
6

Figure 2. Near-bottom bathymetric profiles across the Famous valley. Physiographic provinces are labelled. Sediment ponds are shown with numbers indicating the maximum thickness in meters. Volcanic constructions perched at the edges of faulted blocks are labelled L for "lip" (see text) and other volcanic constructions outside the inner floor are labelled V. Major faults discerned from near bottom echo sounder and side-looking data are shown with dashed lines. Vertical exaggeration is 2X to reduce distortion.

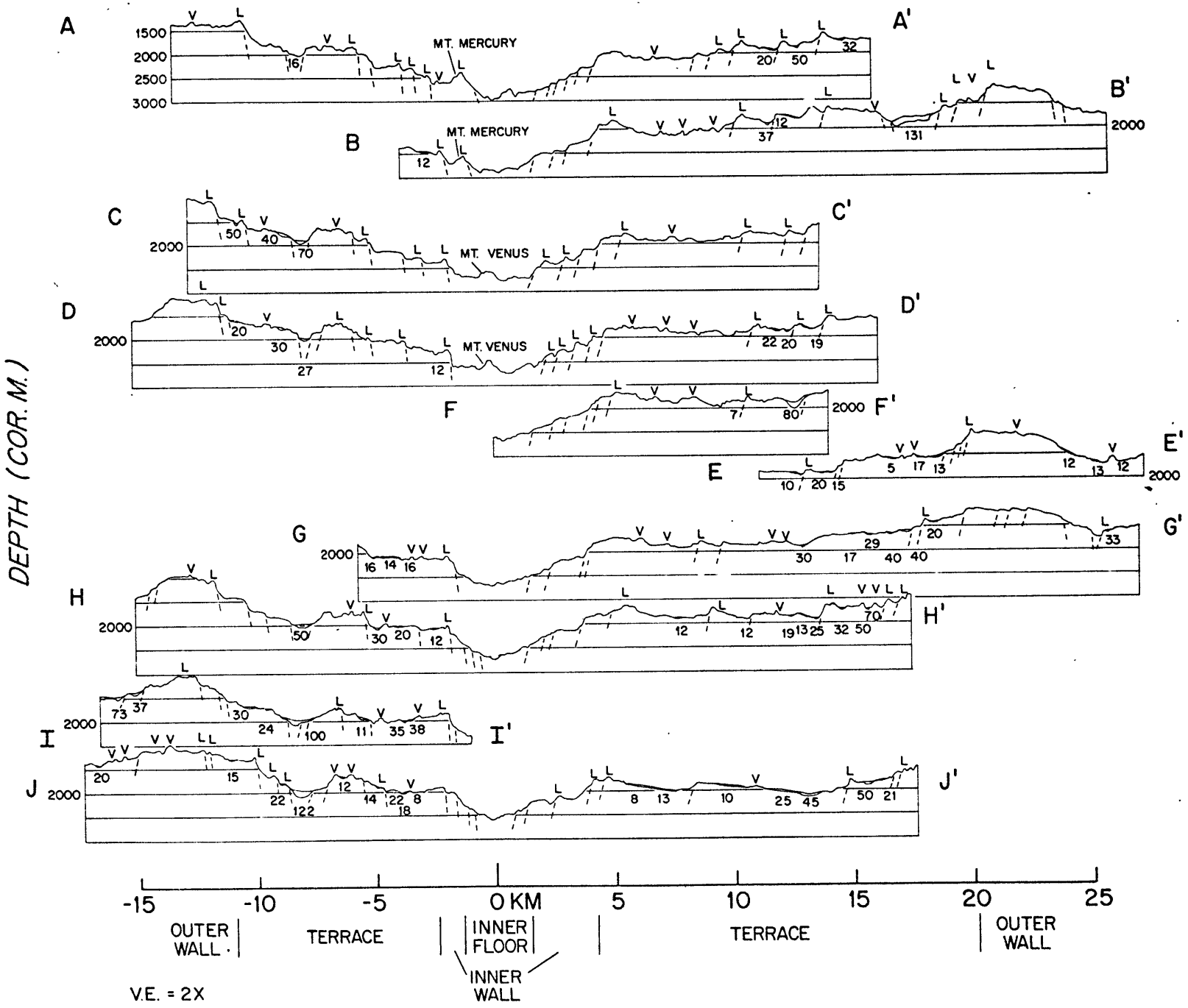
A
A'
B
B'
C
C'
D
D'
E
E'
F
F'
G
G'
H
H'
I
I'
J
J'
MT. MERCURY
MT. VENUS
1500
2000
2500
3000
DEPTH (COR. M.)
-15
-10
-5
0 KM
5
10
15
20
25
OUTER WALL
TERRACE
INNER FLOOR
INNER WALL
TERRACE
OUTER WALL
V.E. = 2X

Figure 3. Tectonic map of the Famous Rift and its intersection with FZA. The height of the the scarps is indicated by the thickness of the lines, and horizontal extent of the scarps by the hatchures. FZA physiography is after Detrick (1974). Notice the asymmetry in structure of the inner walls and terraces; the large graben on the west terrace; and the sharp intersection between the west inner wall and FZA forming "corner cliffs."

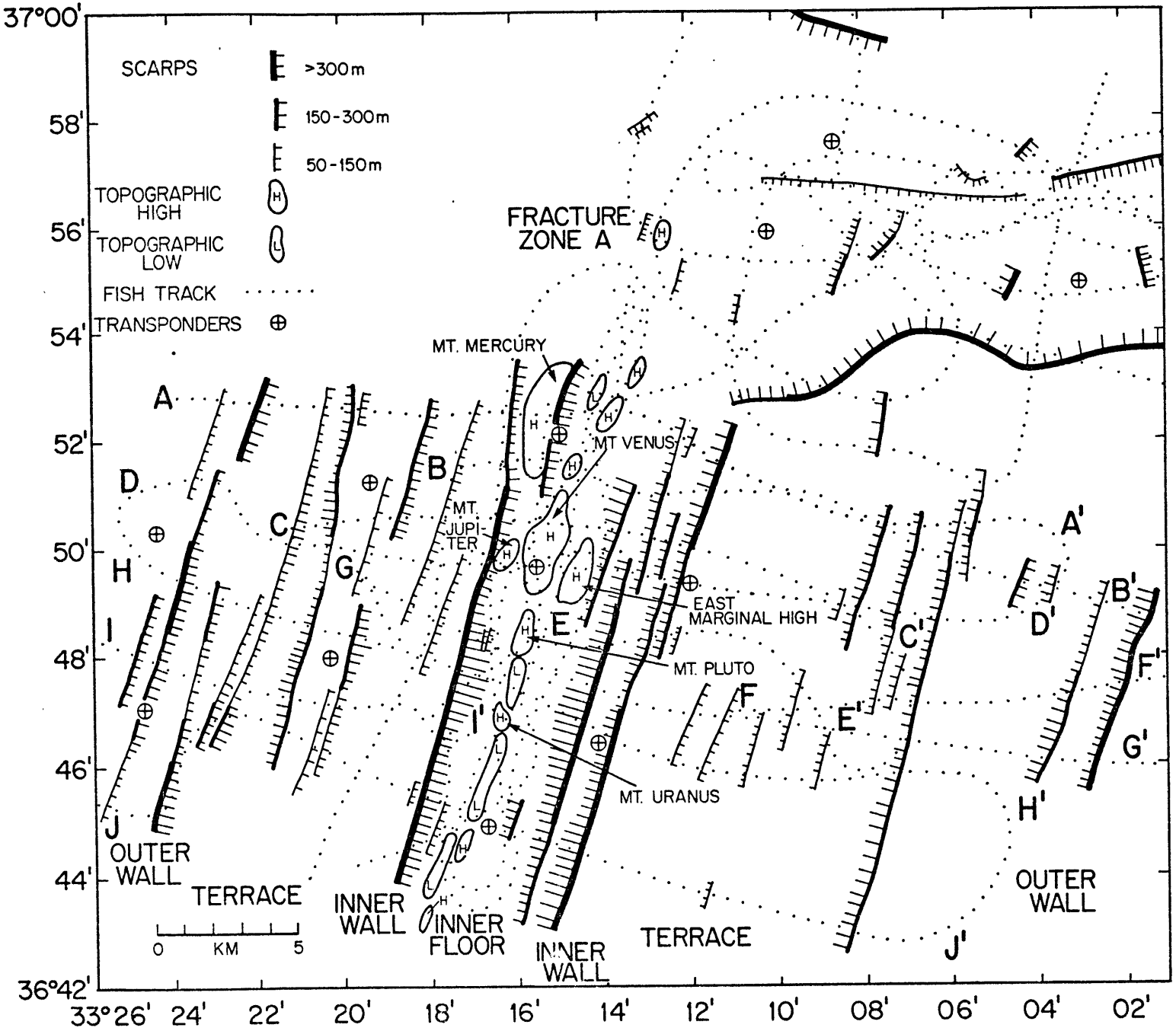
37°00'
58'
56'
54'
52'
50'
48'
46'
44'
36°42'
33°26'
24'
22'
20'
18'
16'
14'
12'
10'
08'
06'
04'
02'
SCARPS
>300m
150-300m
50-150m
TOPOGRAPHIC HIGH
TOPOGRAPHIC LOW
FISH TRACK
TRANSPONDERS
FRACTURE ZONE A
MT. MERCURY
MT VENUS
MT. JUPI-TER
EAST MARGINAL HIGH
MT. PLUTO
MT. URANUS
A
B
C
D
E
F
G
H
I
J
I'
A'
B'
C'
D'
E'
F'
G'
H'
J'
OUTER WALL
TERRACE
INNER WALL
INNER FLOOR
INNER WALL
TERRACE
OUTER WALL
0 KM 5

(110 kHz). When the fish is towed at normal heights above bottom (50-150 m) the 40 kHz sonar can track slopes greater than 75°, as verified by submersible observations of the same scarps (FAMOUS diving team, personal comm.). The 4.0 kHz sonar reliably penetrates and detects sediment thicknesses from 5-100 m. Nowhere in the inner floor was sediment thick enough to be detected by this system. Photographs of the inner floor suggest a thin sediment veneer of 0 to 50 cm. thickness.

Four types of returns were observed on the side-looking sonar and mapped. The most common is a sharp dark band in front of a white shadow area. They are quite linear, often occur in sets, and can be traced up to 2-3 km. These are interpreted as small throw (2-30 m) step faults (Fig. 4). Lineations can be traced out to a range of 400-600 m from the fish giving an effective search path 800-1200 m wide. The second most common are sharp returns with lobate outlines (Fig. 4) which are interpreted as volcanic flow fronts or lava ridges and are generally 2 to 10 m high. The flow direction is assumed to be perpendicular to the flow front, directed toward the steep face of the front. Discrete or point targets were observed which were tens of meters across and 2-25 m high. These are interpreted as small volcanic constructions

Figure 4. Right and left side-looking sonar records from just east of Mt. Pluto and Uranus following the 1400 fm. contour (lat 36°47'N; long 33°16'W). This record shows step faults of the east inner wall on the left and flow fronts or ridges, and discrete targets associated with the two central highs on the right. The contact between the valley floor and inner wall is seen at the top left center where the smooth returns are in contact with the step faults.

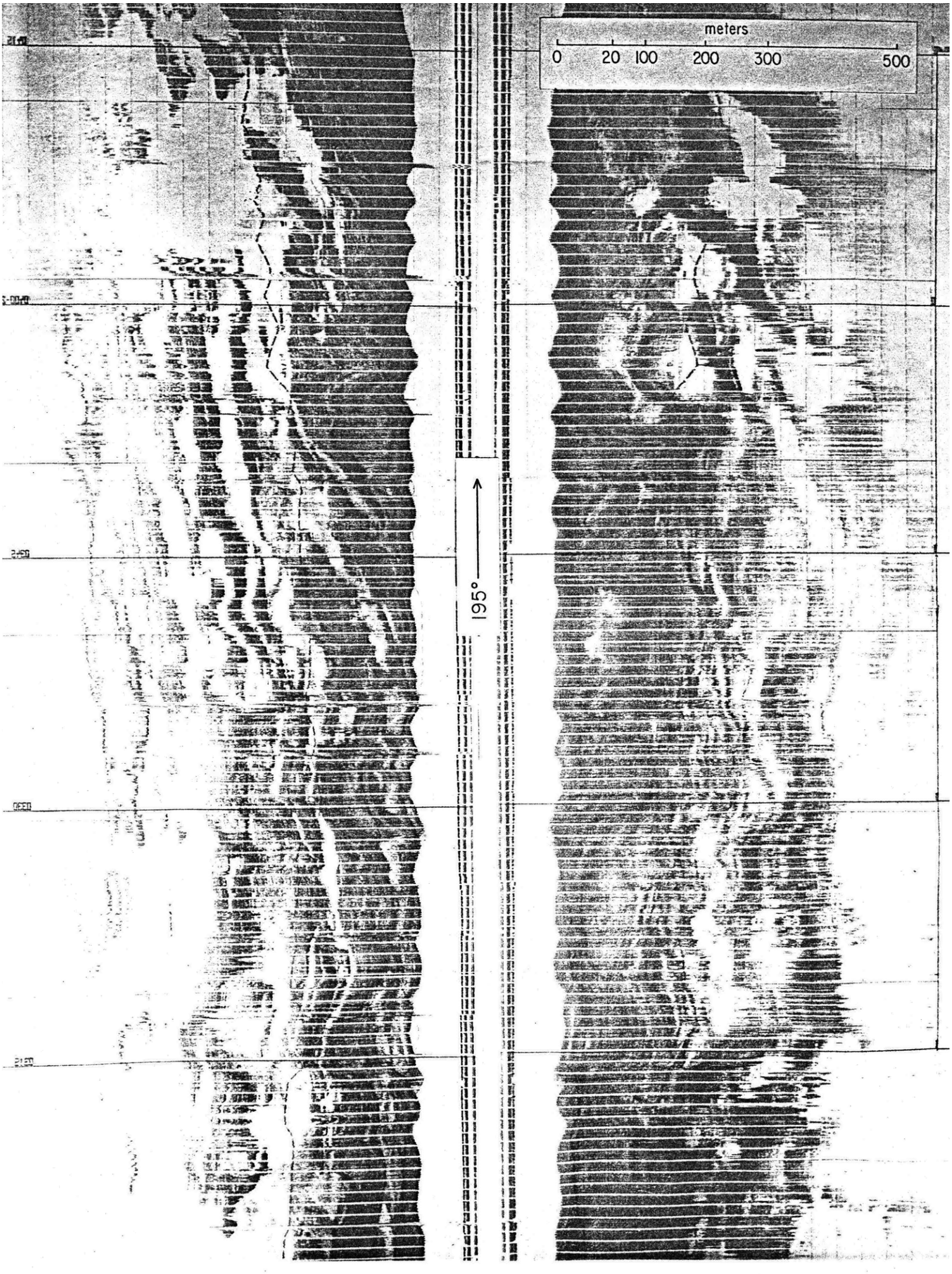
meters
0 20 100 200 300 500
195°

or "haystacks." Submersible observations and bottom photographs indicate that they are formed by a symmetrical, conical piling of basalt pillows (FAMOUS team, personal comm.). The least common type of return shows a thin grey strip in a darker background. These are interpreted as open fissures with little or no vertical offset similar to the "gjas" of Iceland. The fact that few gjas were detected in spite of the fact that they were commonly observed by the divers (Ballard and van Andel, in prep.) shows that the system is relatively insensitive to this type of target.

Within the median valley outer walls the fish was navigated using bottom moored acoustic transponders (Spiess and Tyce, 1973). Relative accuracy is 10 to 50 m. Outside the transponder net the fish was tracked using satellite navigation and a cable trajectory program by Ivers and Mudie (1973). Location accuracy is 500-1000 m. Location relative to latitude and longitude was accomplished by comparing some 40 satellite fixes to transponder navigated ship positions. However, so that the deep tow work could be compared to submersible work directly, the coordinates were shifted 0.7' west to match the submersible base map.

THE INNER FLOOR

The inner floor of the median valley is from 1 km to 4 km wide and is bounded by the first major scarps forming the inner walls. The axis of the valley is marked by alternating topographic central highs and lows (Needham and Francheteau, 1974; Moore, et al. 1974). There are about 8 major topographic highs, which are largest and most numerous in the northern half of the inner floor. Central depressions separate the highs and dominate in the southern portion of the valley (Fig. 3). Mt. Venus, the most prominent central high, was studied in detail (Fig. 6).

Mt. Venus

Mt. Venus is 3.7 km long, 1.1 km wide, and rises up to 250 m above the surrounding floor (Figs. 2, C-C' and D-D'; 3, 5; 6a, b). Studies of crustal magnetization using deep tow magnetic anomalies show that the most highly magnetized rocks occur along the axis of the inner floor, and that the magnetization is particularly high over Mt. Venus and other central highs (Macdonald, in prep.). The freshest rock samples have been collected from Mt. Venus and Mt. Pluto (Belliache et al., 1974; Ballard et al., in press). Ages inferred from the thickness of manganese and palagonite coatings calibrated

Figure 5. Bathymetric chart of the northern portion of the Famous rift inner floor (uncorrected fathoms, 25 fm. contour interval). Data from deeptow supplemented by a U.S. Navy narrow beam survey (Phillips and Fleming in prep.). Track of the fish is shown.

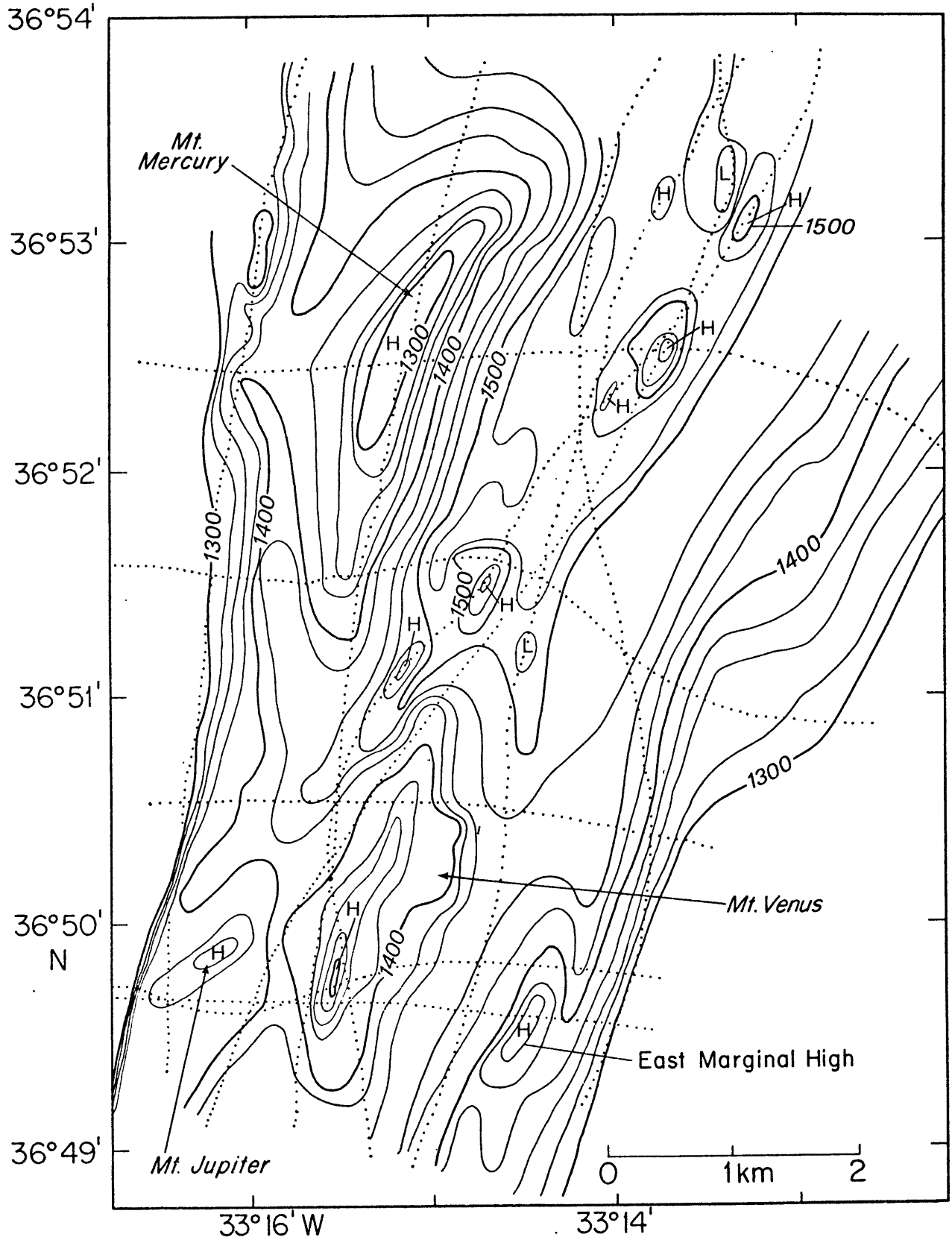
36°54'
36°53'
36°52'
36°51'
36°50'
N
36°49'
33°16' W
33°14'
Mt. Mercury
Mt. Venus
Mt. Jupiter
East Marginal High
1300
1400
1500
H
L
0
1km
2

Figure 6A. Map of the inner floor near Mt. Venus showing flow fronts (solid lines) and discrete targets (open circles) detected by near-bottom side-looking sonar. The targets are probably volcanic conelets or "haystack" lava formations (see text). Arrows indicate the inferred flow direction. Note that the flow fronts subparallel the gross N17E trend of the inner floor suggesting linear fissure eruptions as a major source for the flows.

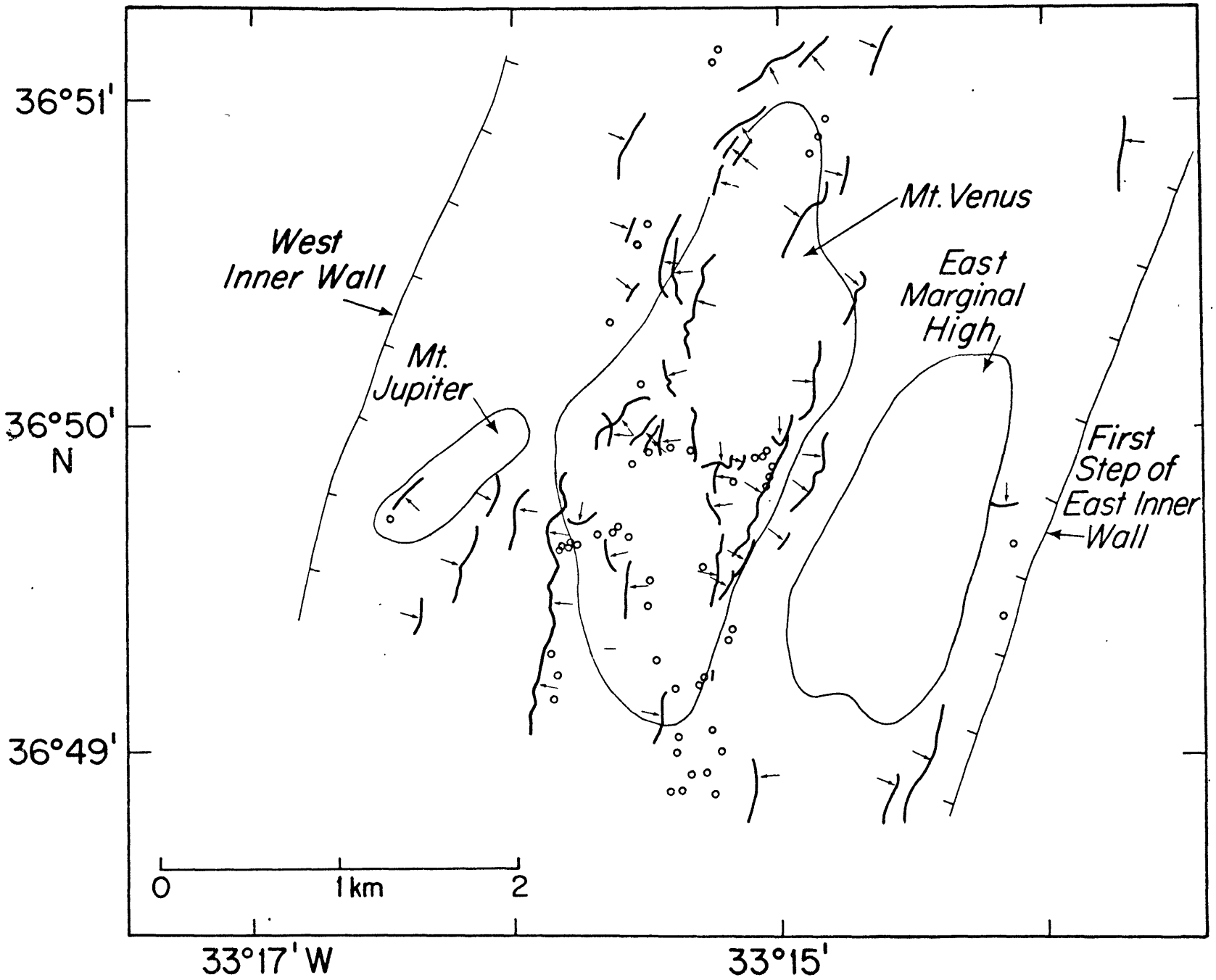
36°51'
36°50'
N
36°49'
West
Inner Wall
Mt.
Jupiter
Mt. Venus
East
Marginal
High
First
Step of
East Inner
Wall
0
1 km
2
33°17' W
33°15'

Figure 6B. Tectonic map of the inner floor near Mt. Venus. Scarps interpreted as small throw normal faults shown by hatchured lines, open fissures with little or no throw shown by lines with dots.

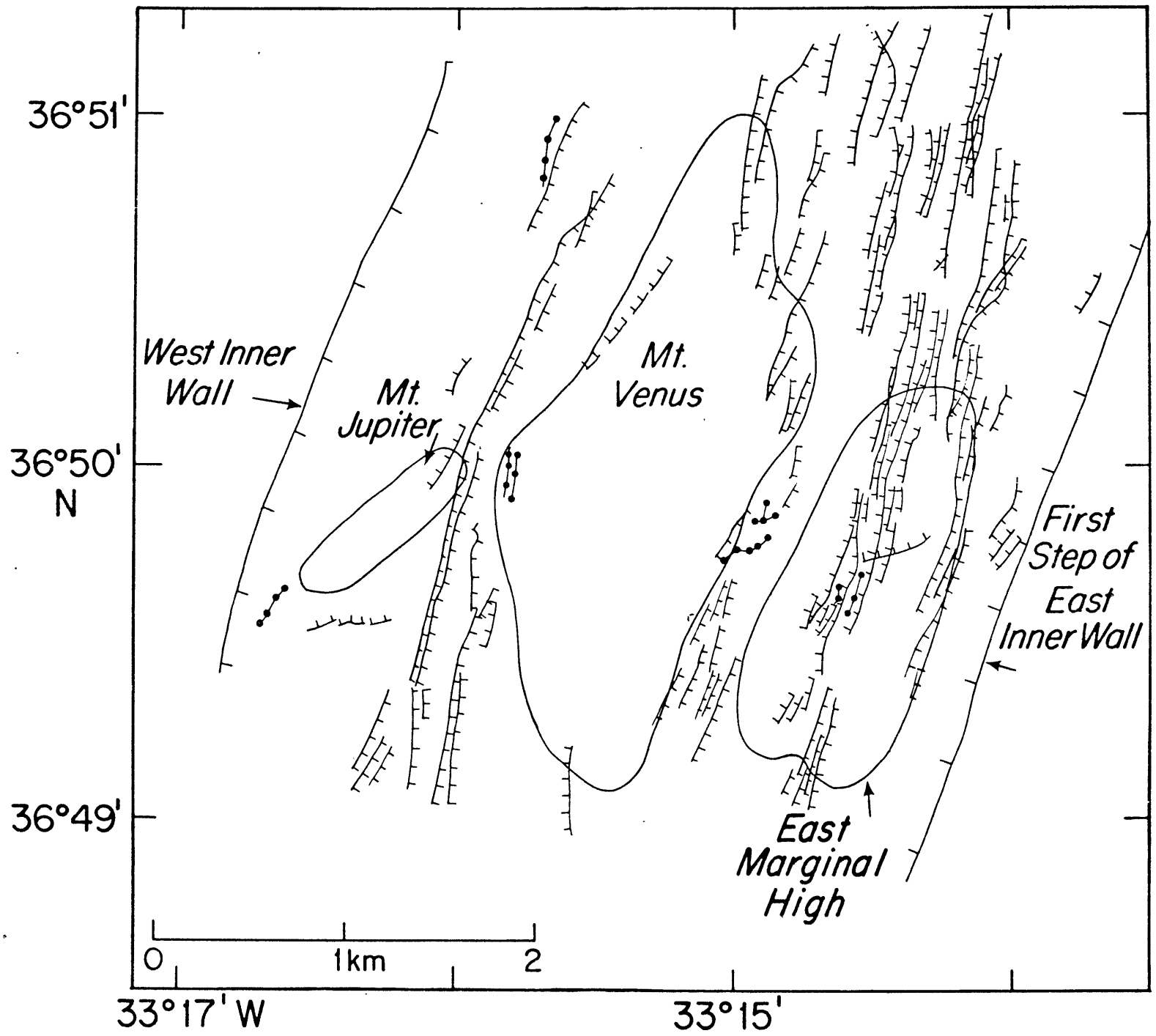
36°51'
36°50'
N
36°49'
West Inner
Wall
Mt.
Jupiter
Mt.
Venus
First
Step of
East
Inner Wall
East
Marginal
High
0
1km
2
33°17' W
33°15'

against C^{14} dates on coral indicate that the youngest basalts at the center of the floor may be only a few hundred years old (Bryan and Moore, in prep.). For these and other reasons discussed in the following, it is thought that the active spreading center plate boundary lies along the inner floor axis and passes through or near central highs such as Mt. Venus.

Average slopes on Mt. Venus are generally between 20° and 40°, but within the regional slopes there are 5 m-50 m steps with dips of 50° to 70°. Such steep slopes suggest small scale normal faulting at first glance; however, side-looking sonar mapping shows that most of the apparent steps are actually lobate and sinous along strike (Fig. 6a), suggesting that even the steepest slopes of Mt. Venus are constructed by volcanic flow fronts. Several deep-tow photographic traverses as well as observations from submersibles (Belliache et al., 1974) show fields of coherent basalt pillows and steep flow fronts (Fig. 7). Such steep slopes can occur in submarine eruptions due to rapid quenching and has been observed during formation for shallow submarine flows (Moore, 1975). A small number of linear steps interpreted as faults occur on the northern flanks of Mt. Venus, mostly on the east side, but make up very little of the total relief (Fig. 6b).

Most of the flows are parallel to and directed away from the crest of Mt. Venus (Fig. 6). This suggests that most of the flows have erupted from a single major system of vents along the en echelon axis of Mt. Venus (Figs. 5, 6a). A few flow fronts occur near the inner floor edges and are directed toward the axis, but still have a NNE trend. In fact, most volcanic flow fronts , even those away from the axial vent, are sub-parallel to the gross trend of Mt. Venus, and the median valley as a whole. Only two east-west flow fronts were mapped. Thus even small scale volcanic activity is largely controlled by the regional stresses associated with seafloor spreading.

Over fifty discrete targets were mapped on and near Mt. Venus. They range in height from 2 to 25 m and in width from 15 m to 70 m. Features with almost exactly the same size and shape have been observed by the U.S. FAMOUS dive team and have been called "haystacks" (Ballard et al., in press). They are conical piles of very elongate basalt pillows which appear to have stacked up about a small central vent. Even many of these small discrete eruptions occur in linear groups trending NNE (Fig. 6a).

Flow directions suggest that there may be volcanic activity away from Mt. Venus at the edges of the valley floor. Particularly west of Mt. Venus, flows appear to have their origin near the west inner wall (Fig. 6a). Mt. Jupiter may be the source for some of the flows, but several occur further north with no prominent topographic high to the west. These are probably pahoehoe sheet eruptions of small volume.

While the very center of the inner floor is dominated by volcanism, the crust becomes highly fractured by closely spaced, small throw normal faults within 1 km of the center (Fig. 6b). Fault density increases from less than 3 per km^2 along the axis to more than 20 faults per km^2 on the east and more than 10 faults per km^2 on the west. The lateral spacing between fault scarps is 20 to 100 m for the intensely fractured areas away from Mt. Venus. Throws average approximately 8m, and rarely exceed 40 m within the inner floor. The east marginal high is flanked by closely spaced faults. It appears to be a horst, with the scarps all dipping away from its axis. However, the summed relief of the faults account for at most half of the total elevation (about 80 m). This suggests a volcanic origin with post-volcanic faulting and tectonic uplift.

Figure 7A. Open fissure north of Mt. Pluto trending along the strike of the inner floor. This is an example of the vertically sided tensional cracks which are common in the inner floor.

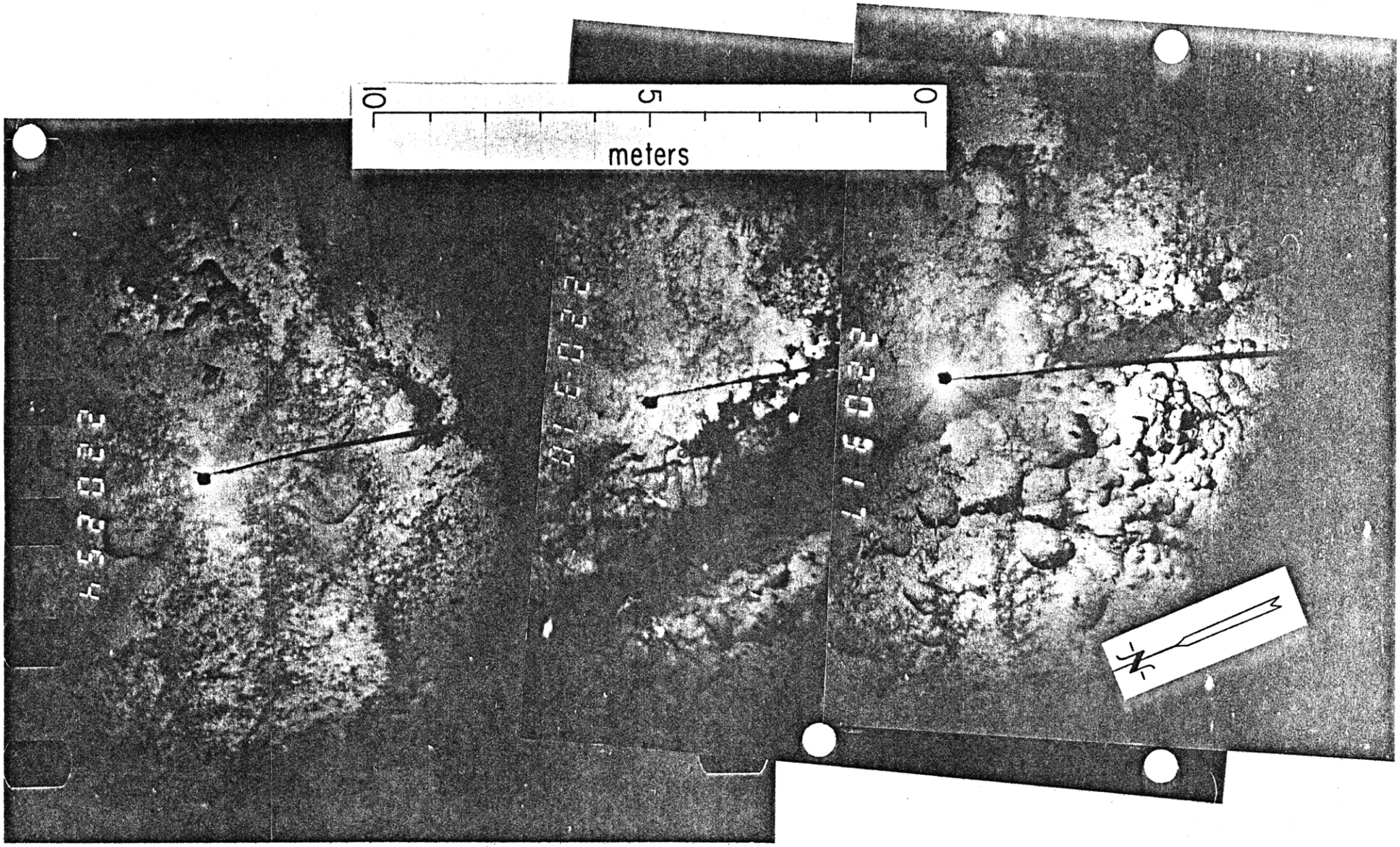
10
5
0
meters

Figure 7B. A gja on the Reykjanes peninsula in Iceland. Gjas are tensional cracks generally parallel to the tectonic grain and are numerous on the Icelandic portion of the Mid-Atlantic Ridge. The tensional cracks in the Famous inner floor may have the same origin and structure as the gjas. Apparently these vertically sided tensional cracks may occur in the floor of the MAR median valley where there is significant hydrostatic pressure. The gja shown here is 1-2 m. wide.

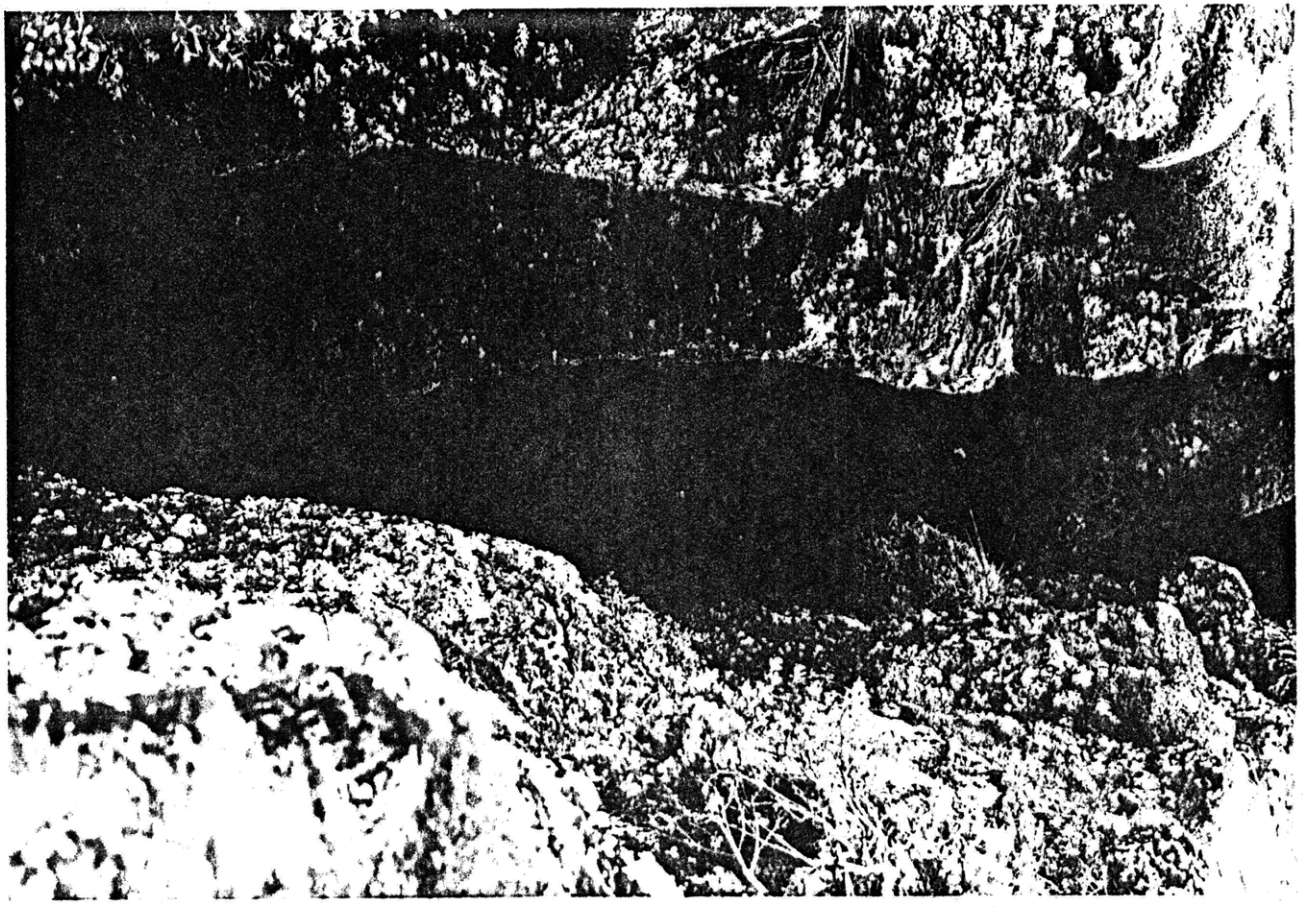

Only 12 tectonic fissures were observed in the Mt. Venus region (Fig. 6b). They are probably more common than this since the side-looking sonar is rather insensitive to this type of target. Correlation with photographs suggest that these features are similar to the vertical tension cracks or gjas observed in Iceland (Fig. 7). Some extend for more than 300 m along strike.

The Central Lows

Just south of Mt. Pluto and Mt. Uranus are two well-developed central lows, each about 2 km long and 100 m deep (Figs. 3, 8). They are 600 m to 800 m wide with floors that range from being flat to U or V-shaped (Fig. 8). These central lows could be grabens, created by inward facing normal faults, topographic troughs, caused by a gap between flows erupted near the inner floor edges, or regions of caldera collapse. Side-looking sonar records indicate that the lows are bounded by linear scarps (Fig. 9) so it is unlikely that the depression is simply a gap between flows emanating from the floor edges. The difference between a central high and central low is probably the presence of a local magma source. Where a magma source is not present, continual normal faulting and fracturing of the crust concommitant with spreading results in a graben and

Figure 8. Tracing of near bottom bathymetric profiles across the central lows south of Mt. Pluto (H-H') and south of Mt. Uranus (J-J'). These may be grabens or caldera collapse structures (see text). Vertical exaggeration is approximately 2.6x for H-H' and 1.5x for J-J'.

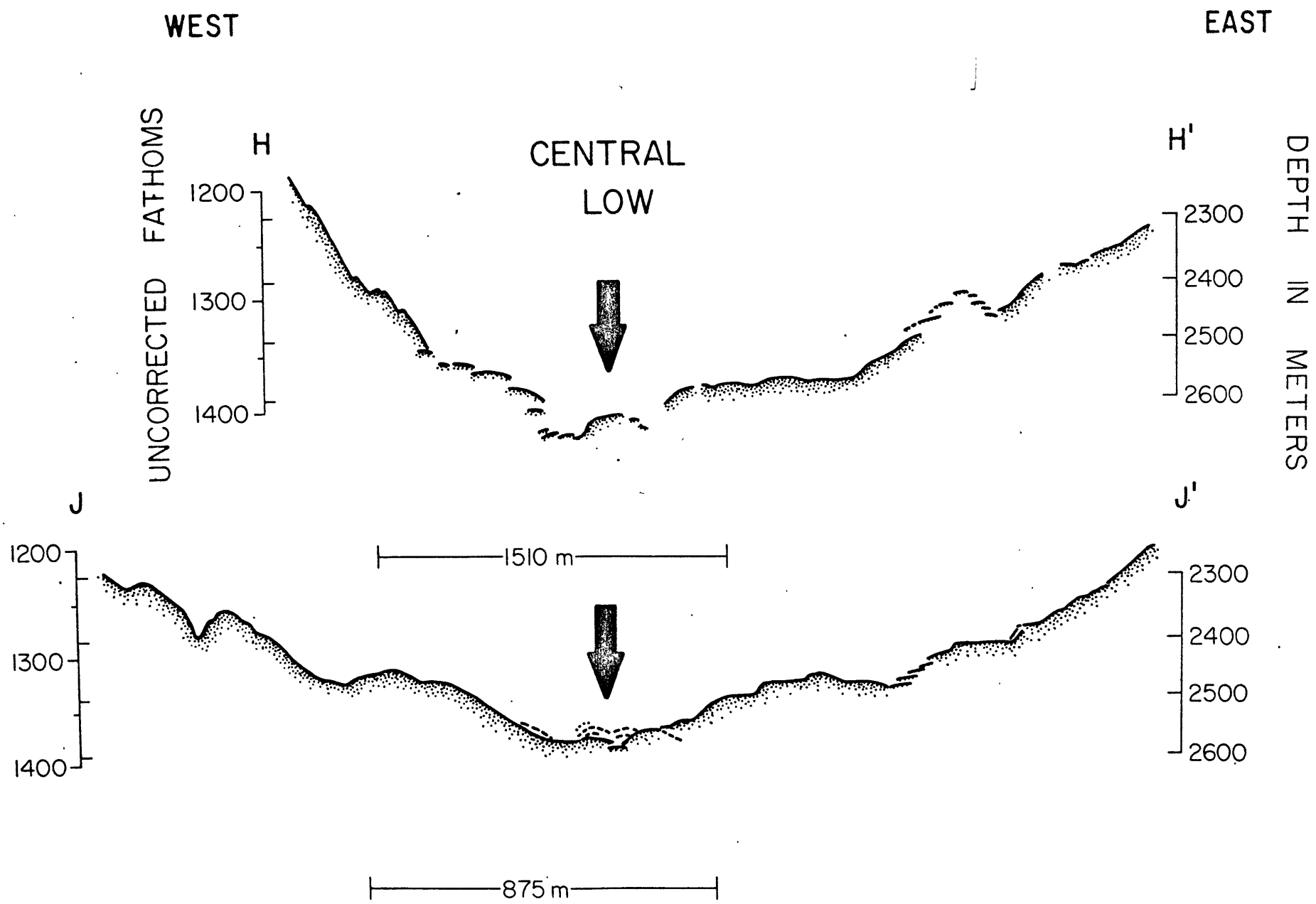
WEST
EAST
H
H'
CENTRAL
LOW
UNCORRECTED FATHOMS
1200
1300
1400
2300
2400
2500
2600
DEPTH IN METERS
J
J'
1510 m
875 m

down dropping of the floor. Alternatively, the low may be caused by caldera collapse due to a pressure drop in an underlying magma chamber. Magma may migrate along the strike of the floor with sources concentrating at the central highs. For example, the recent eruption at Heimaey in Iceland began as a linear fissure eruption several km long. Within a few days magma sources migrated along strike resulting in a linear fissure eruption less than half its original length (Samuelsson, personal comm.). Crust overlying the depleted zone may collapse, giving rise to an alternating central high/central low morphology.

Tectonic Grain of the Inner Floor

Intense faulting and fracturing commences within 1 km of the inner floor axis (Fig. 9). Faults mapped in the inner floor have small vertical offsets (5 to 40 m) but extend for hundreds of meters to kilometers. Fault distribution is clearly asymmetric, the density being twice as high on the east side of the floor. Fault density exceeds 25 per km^2 in some areas.

Besides the extremely high density of faulting in the inner floor, the most striking observation is the pervasive NNE trend of tectonic lineations (Fig. 9). The fault trends

Figure 9. Faults and fissures in the Famous inner floor mapped by side-looking sonar. The crust becomes intensely fractured within 500-1000 m. of the inner floor axis. The faulting is asymmetric with a higher density on the east side. Note how parallel these small faults are to the trend of the rift. V is Mt. Venus, M Mt. Mercury, P Mt. Pluto, EMH east marginal high and U is Mt. Uranus.

33° 20' W 18' 16' 14' 33° 12' W

36° 56' N

FAULTS AND FISSURES

FAMOUS AREA

54' 52' 50' 48' 46' 44'

36° 56' N

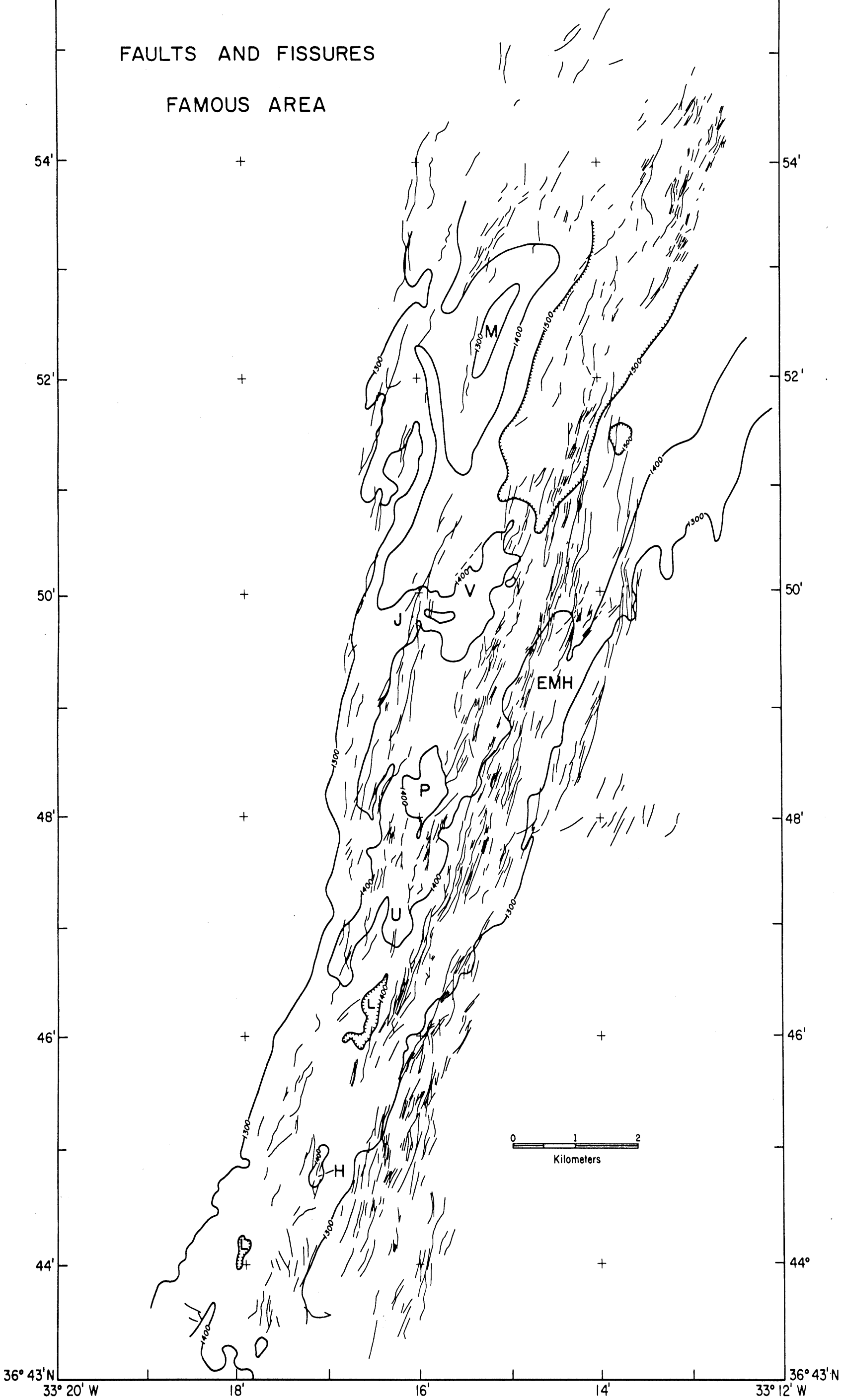

36° 43' N

33° 20' W 18' 16' 14' 33° 12' W

Figure 10. Trends of over 700 tectonic lineations in the inner floor (from Figure 9). Note that the lineations form a normal distribution about a median of N17E. While north-south trends are observed, they are only part of the normal scatter of a natural process. There is no evidence for readjustment to a north-south trend for the ridge which would create an orthogonal plate boundary system.

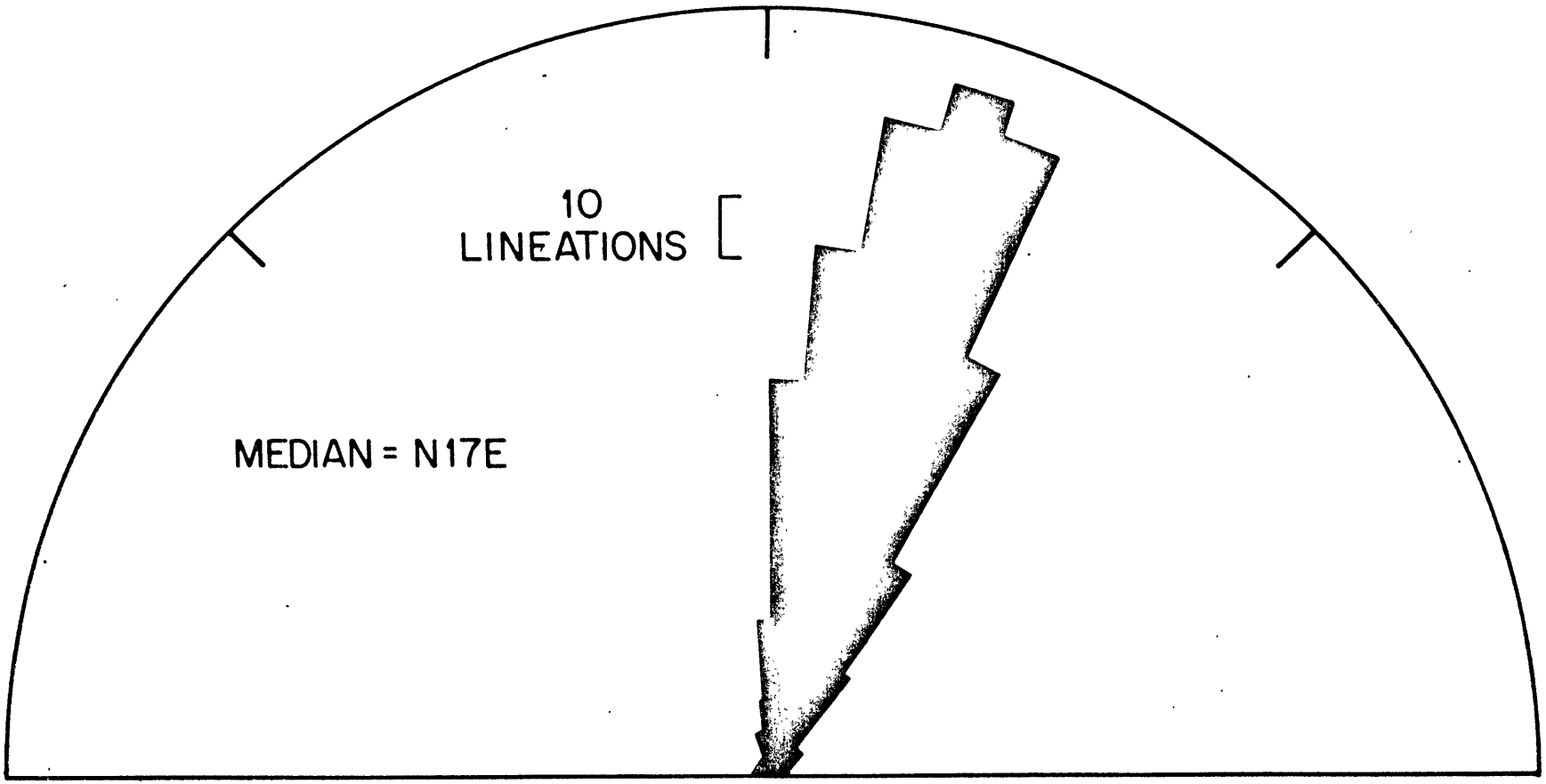

STRIKES OF FAULTS AND FISSURES

form an almost perfect Gaussian distribution about N 17°E with a standard deviation of only 6° (Fig. 10). The faults were mapped along sub-parallel tracks which were transponder navigated (Fig. 3), so the trends are accurate to within about 2°. Some workers in the Famous area have observed north trending lineations and have interpreted them as evidence that the ridge is rotating to a north-south direction to form an orthogonal system with east-west transform faults (Brundage et al., in prep.; Phillips and Fleming, in prep.). We too have mapped over 40 N-S trending faults and fissures. However, they appear to be only part of the expected scatter of a natural process, and are quite consistent with a normal distribution of lineations about a median of N 17°E (Fig. 10). Thus, even on a scale of tens of meters there is no indication of readjustment to an orthogonal system. This is most important, for this observation (and others discussed later) indicates that the Mid-Atlantic ridge in this area has a stable spreading obliqueness of approximately 17°.

THE INNER WALLS

The inner floor is bounded by the inner walls (Figs. 2, 3). The walls strike approximately N 17°E and are continuous throughout the length of the valley right up to the transform

fault intersections. The northern end of the east inner wall actually forms a corner with the major east-west scarp marking the southern boundary of FZA (Fig. 3). Such "corner cliffs" have also been observed at the intersection of the west inner wall with FZB (Laughton and Rusby, 1975).

The structure of the inner walls is very asymmetric. East of the valley axis, the floor rises at a slope of 9° for 2.2 km before meeting the first major scarp marking the inner wall (Figs. 2, 11). This slope is composed of 13 steps which are lineated in a N 17°E direction (Fig. 11a). The fault scarps have an average dip of at least 60° and some are essentially vertical. Throws range from 5 m to 30 m. This intense faulting commences within 400 m of the inner floor axis. In places, this series of small steps is replaced by marginal highs, some of tectonic origin as discussed in the previous section (e.g. Fig. 2, B-B', D-D'). Scarp dimensions increase abruptly at the first major block fault of the inner wall with throws of 150 to 350 m and block widths of 500 to 1500 m (Figs. 2, 3, 11b). The wall looks like a staircase in cross section consisting of three to six major blocks (Fig. 11b).

Faulting is not as intense on the west side of the inner floor and there is no gradual slope composed of small step faults leading up to the wall. Instead the floor is abruptly

Figure 11A. Tracing of a near-bottom bathymetric profile showing intense small throw normal faulting on the east side of the inner floor leading up to the east inner wall. Faults inferred from bathymetric and side-looking sonar data shown by dashed lines. Depth is in meters.

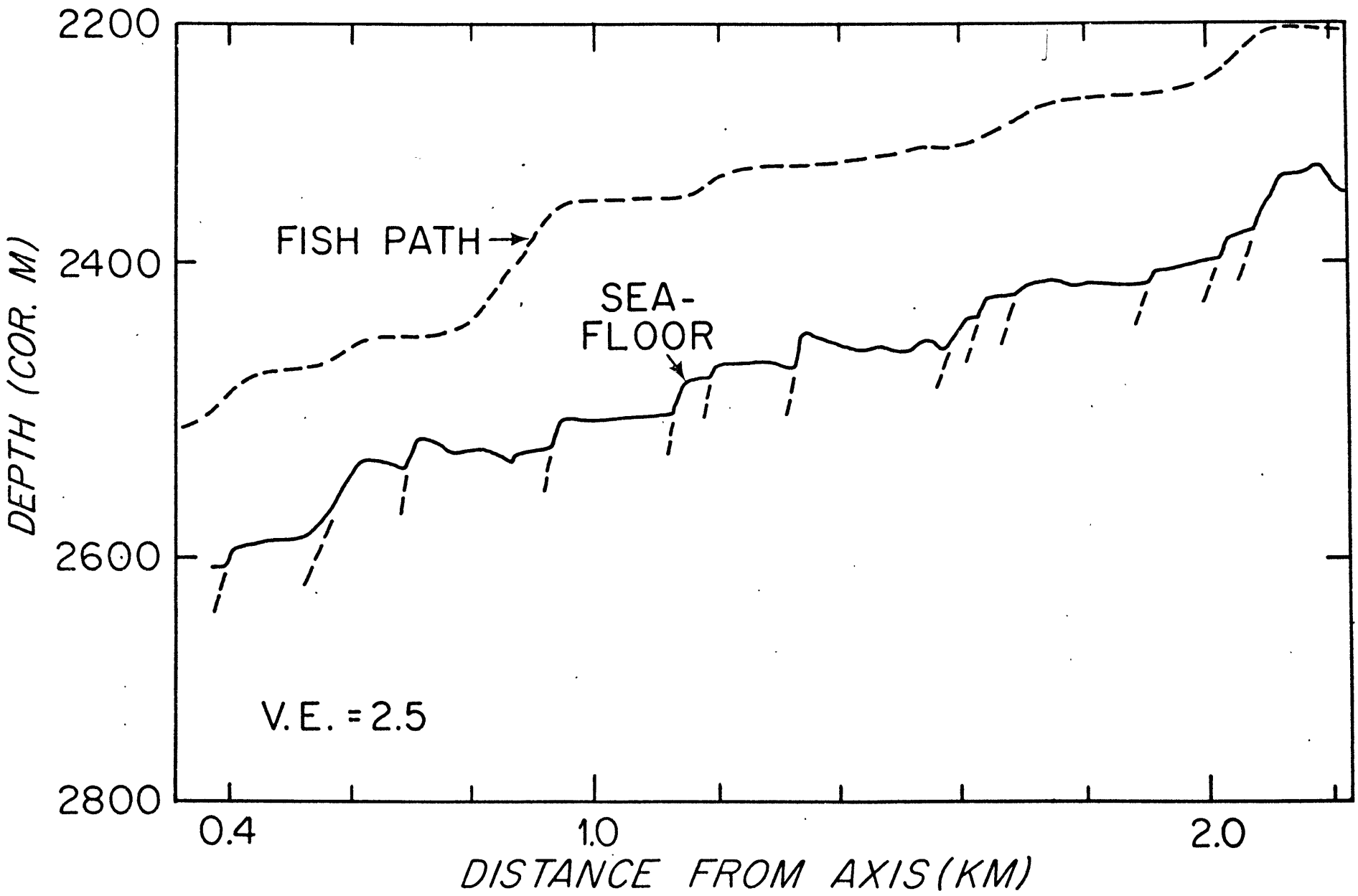
2200
2400
2600
2800
DEPTH (COR. M)
FISH PATH
SEA-
FLOOR
V.E. = 2.5
0.4
1.0
2.0
DISTANCE FROM AXIS (KM)

Figure 11B. Original near-bottom echo-sounding record showing the stair-step block faulted profile of the east inner wall (along D-D'). Notice tilting of the blocks away from the rift axis.

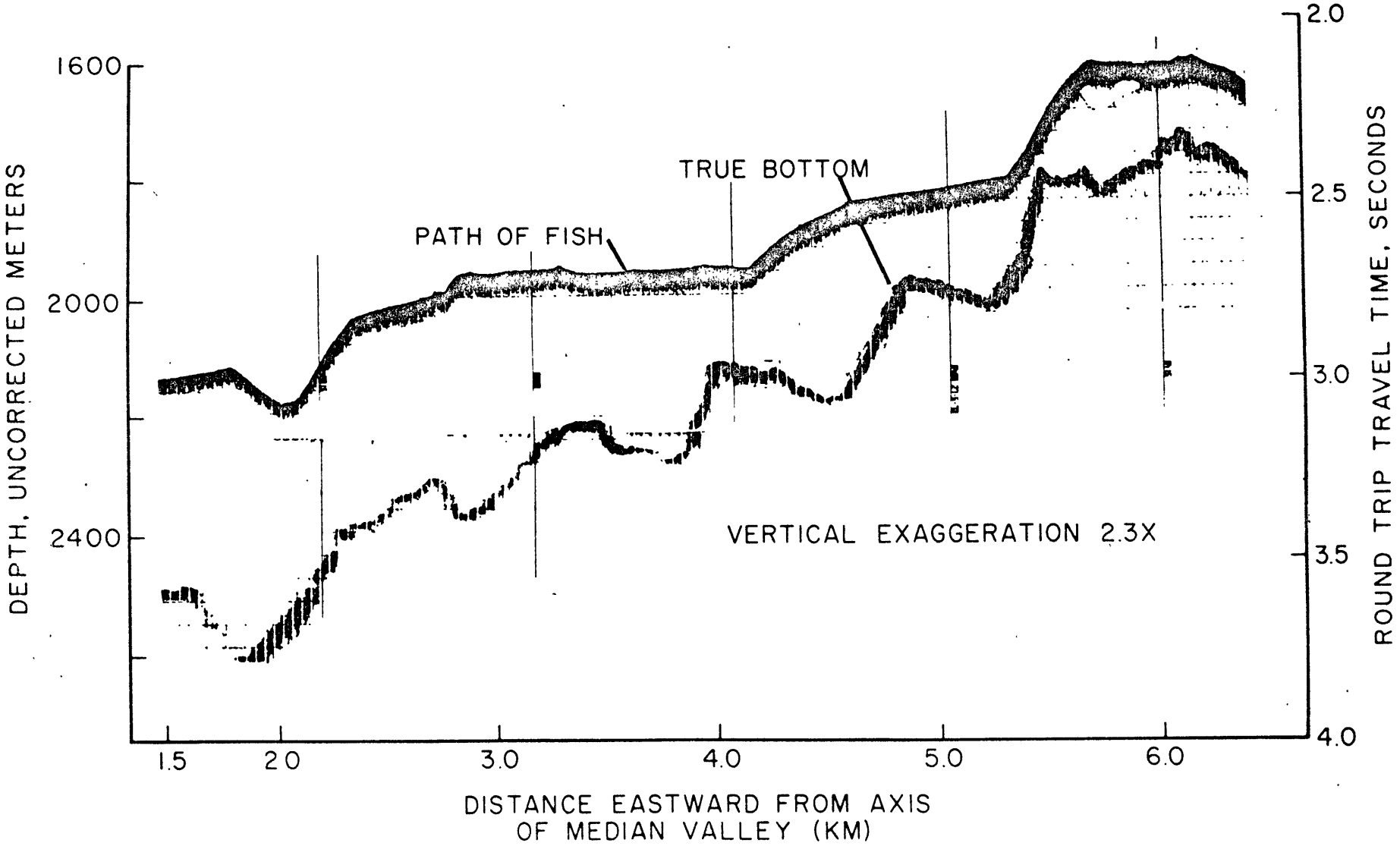
1600
2000
2400
DEPTH, UNCORRECTED METERS
2.0
2.5
3.0
3.5
4.0
ROUND TRIP TRAVEL TIME, SECONDS
TRUE BOTTOM
PATH OF FISH
VERTICAL EXAGGERATION 2.3X
1.5
2.0
3.0
4.0
5.0
6.0
DISTANCE EASTWARD FROM AXIS
OF MEDIAN VALLEY (KM)

Figure 12A. Tracing of near-bottom record showing the narrow slivers of crust composing steep west inner wall (along G-G'). Notice the prominent volcanic lip at the top of the scarp.

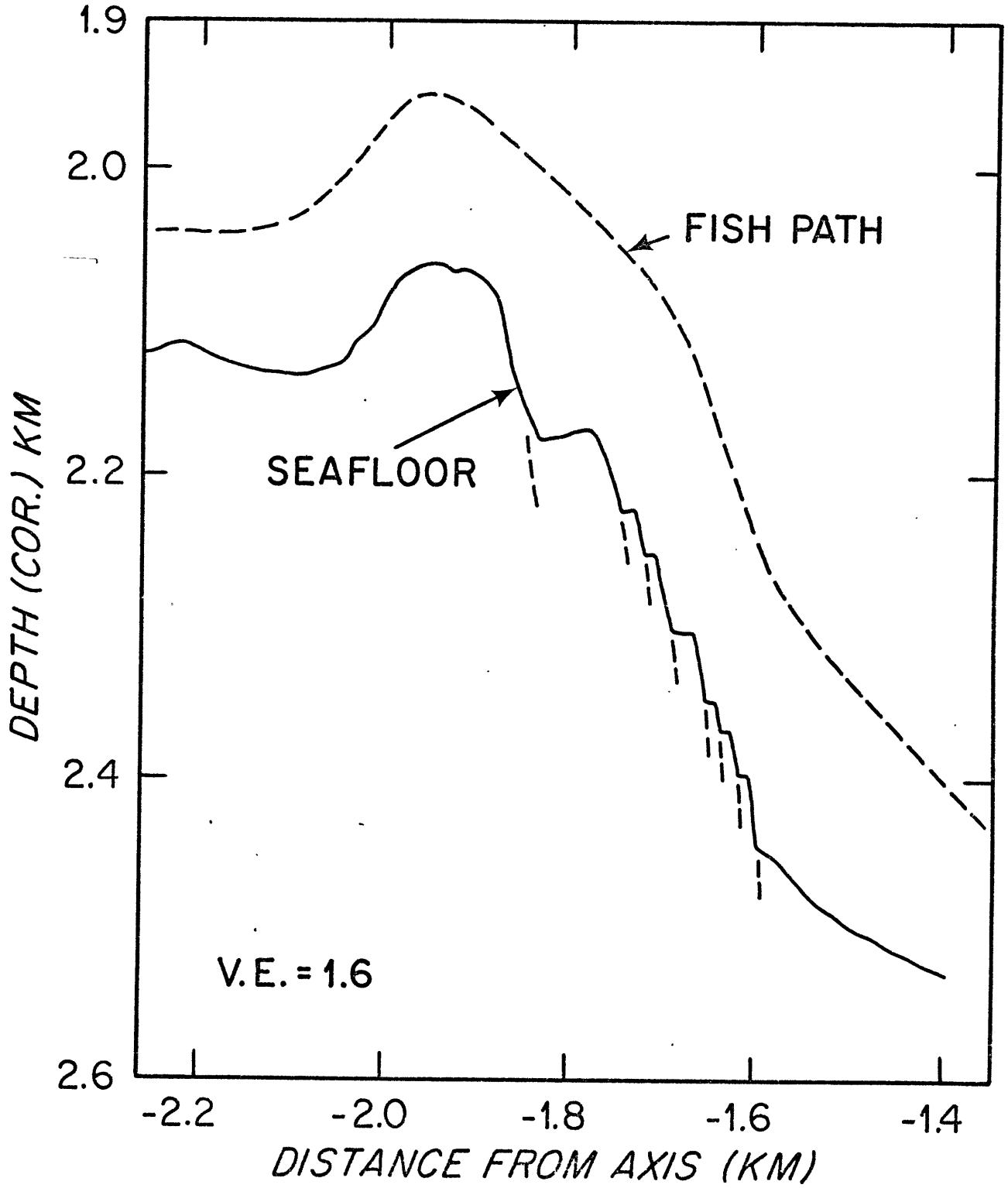
1.9
2.0
2.2
2.4
2.6
DEPTH (COR.) KM
FISH PATH
SEAFLOOR
V.E. = 1.6
-2.2
-2.0
-1.8
-1.6
-1.4
DISTANCE FROM AXIS (KM)

Figure 12B. The west inner wall (along H-H'), again showing the narrow slivers of crust composing this massive block. Notice that here the blocks are tilted back away from the valley axis. Again there is a lip at the top of the fault scarp.

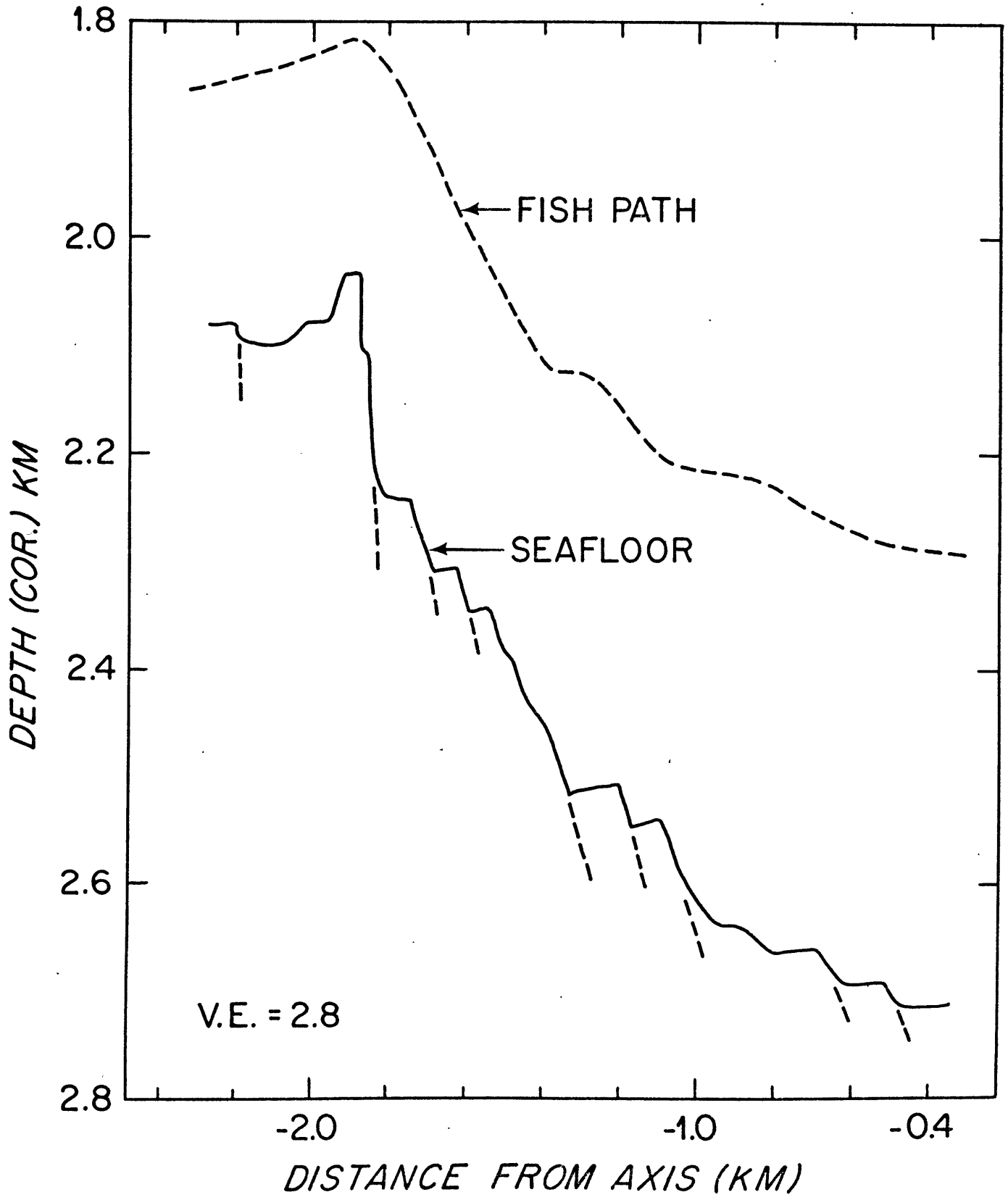
1.8
2.0
2.2
2.4
2.6
2.8
DEPTH (COR.) KM
FISH PATH
SEAFLOOR
V.E. = 2.8
-2.0
-1.0
-0.4
DISTANCE FROM AXIS (KM)

truncated by the west inner wall (Figs. 2, 12). To a first approximation, the west wall is a single massive block fault with a throw of up to 600 m. In detail it is composed of a series of narrow slivers of faulted crust (Figs. 12a, b).

Microearthquakes recorded in the median valley cluster at the first and second steps of the inner walls and not along the valley axis (Fig. 15) (Reid and Macdonald, 1973; Spindel et al., 1974). This suggests that the quakes are associated with the incipient and ongoing uplift of fault blocks forming the inner wall rather than with dynamics of intrusion in the inner floor. Of 20 events located on the inner walls, 18 were on the east inner wall (Fig. 15). In a later microearthquake study the west wall was found to have almost an equal level of seismicity (Francis, personal comm.). The level of earthquake activity was high, averaging 10 to 30 events per day (Reid and Macdonald, 1973; Spindel et al., 1974).

Fault scarps were analyzed to determine dip. Scarps exceeding 100 m in throw and with sharp rectlinear cross-sections were considered. Talus piles at the bases of scarps commonly appear in bottom photos (Luyendyk and Macdonald, in prep.), so dip was measured near the top of the scarp, generally on its steepest slope. The average dip toward the valley axis

is 50°. However, the west inner wall is somewhat steeper than the east (Tables 1, 2). The steeper dip of the west wall is largely caused by the prominent scarp responsible for most of the throw of the west wall which has dips exceeding 75° (Figs 2, D-D'; 12).

Most of the blocks face the valley axis and some are tilted back. Of the blocks showing a measurable backward tilt, the average tilt is 6° (standard deviation, S.D. = 2°, standard error, S.E. = 0.7°). The average for all the inner wall blocks, however, including those with zero or forward (negative) tilt, is 2° (S.D. = 20; S.E. = 0.3°). Forward tilts may be due to talus accumulations from adjacent scarps, or to volcanic construction. There is no significant difference in tilt between the east and west inner walls. That the outward slopes of the blocks are indeed caused by tilting has been verified by observation of elongate pillows directed up slope on top of some of the tilted blocks (U.S. FAMOUS team, personal comm.).

The same vertical uplift occurs all along the east inner wall but is accomplished through an overlapping and bifurcating series of faults of varying throw. This has been observed in the Afar Rift and is termed "relay faulting" (Needham, personal comm.). In places, the east inner wall consists of 5 to 6

major steps (Fig. 11b). Along strike it changes to 2 or 3 major faults with a gradual slope at the base of the wall consisting of a series of small steps (Figs. 2, F-F', G-G', H-H'; 11a). A similar type of relay faulting occurs on the west inner wall, so that to the south, the wall is wider consisting of at least 8 slivers with considerable backward tilt (Fig. 12b). To the north, the wall becomes narrower, crustal slivers show less tilt (Fig. 12a), and further north the wall looks like a single massive block (Fig. 2, D-D'). At the north end, the throw of this scarp decreases to 200 m, the remainder of the uplift appearing on the block carrying Mt. Mercury (Figs. 2, A-A', B-B'; 3). This fault is 4.5 km long, has up to 400 m of throw and is only 0.5 km from the valley axis, suggesting that very large scale block faulting can occur within hundreds of meters of the center of the floor.

Horizontal extension was calculated from fault dips and throws on the traverse crossing Mt. Venus (Figs. 2, D-D'; 6). It is highly asymmetric (Fig. 13). The west wall and inner floor represents only 230 m of extension compared to 870 m for the east. Normalized against distance from the floor axis, only 11% of the horizontal movement is due to the extension on the west as opposed to 18% on the east. Extension rates within

Figure 13A. Cumulative horizontal extension of the crust east of the rift axis at the latitude of Mt. Venus calculated from the dips and throws of faults. Extension is 6% of the total distance from the axis in the inner floor, 18% out to the top of the east inner wall, and decreases abruptly on the terraces. (The basic assumption is that the faults are or were active near their present location. As is discussed later, faulting and extension must occur to some extent on the terraces and even outside the median valley, but it is uncertain which faults have been active near their present in crust that old.)

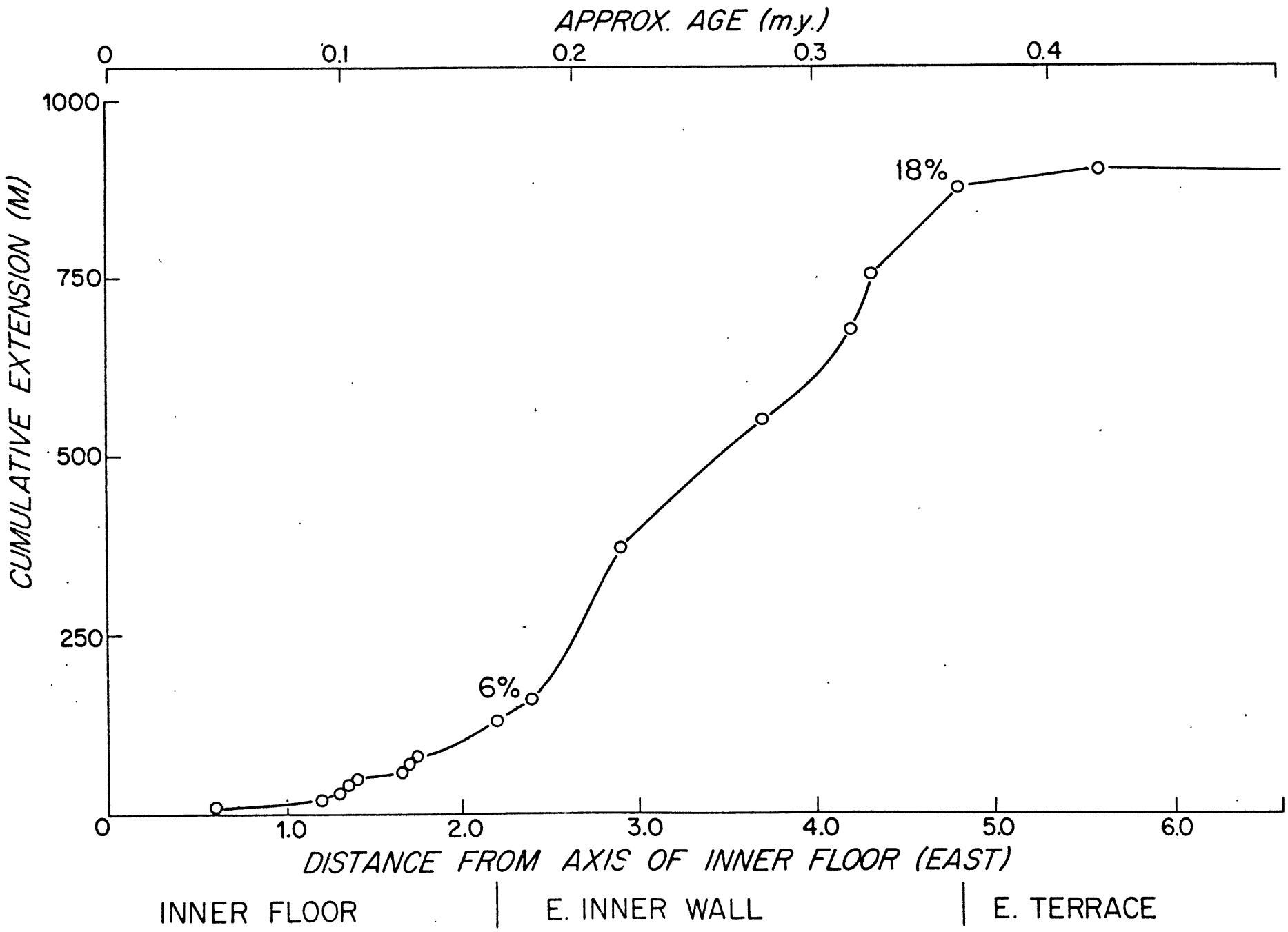
APPROX. AGE (m.y.)
0
0.1
0.2
0.3
0.4
1000
750
500
250
0
CUMULATIVE EXTENSION (M)
18%
6%
1.0
2.0
3.0
4.0
5.0
6.0
DISTANCE FROM AXIS OF INNER FLOOR (EAST)
INNER FLOOR
E. INNER WALL
E. TERRACE

Figure 13B. Horizontal extension west of the inner floor axis at the latitude of Mt. Venus. (similar to Figure 13A.). Notice that the horizontal extension is asymmetric: 4% and 6% for the west and east sides of the inner floor, and 11% and 18% for the west and east inner walls, respectively. This is consistent with the sense of asymmetric spreading and suggests that asymmetric spreading is accomplished through asymmetric extension as well as asymmetric crustal accretion.

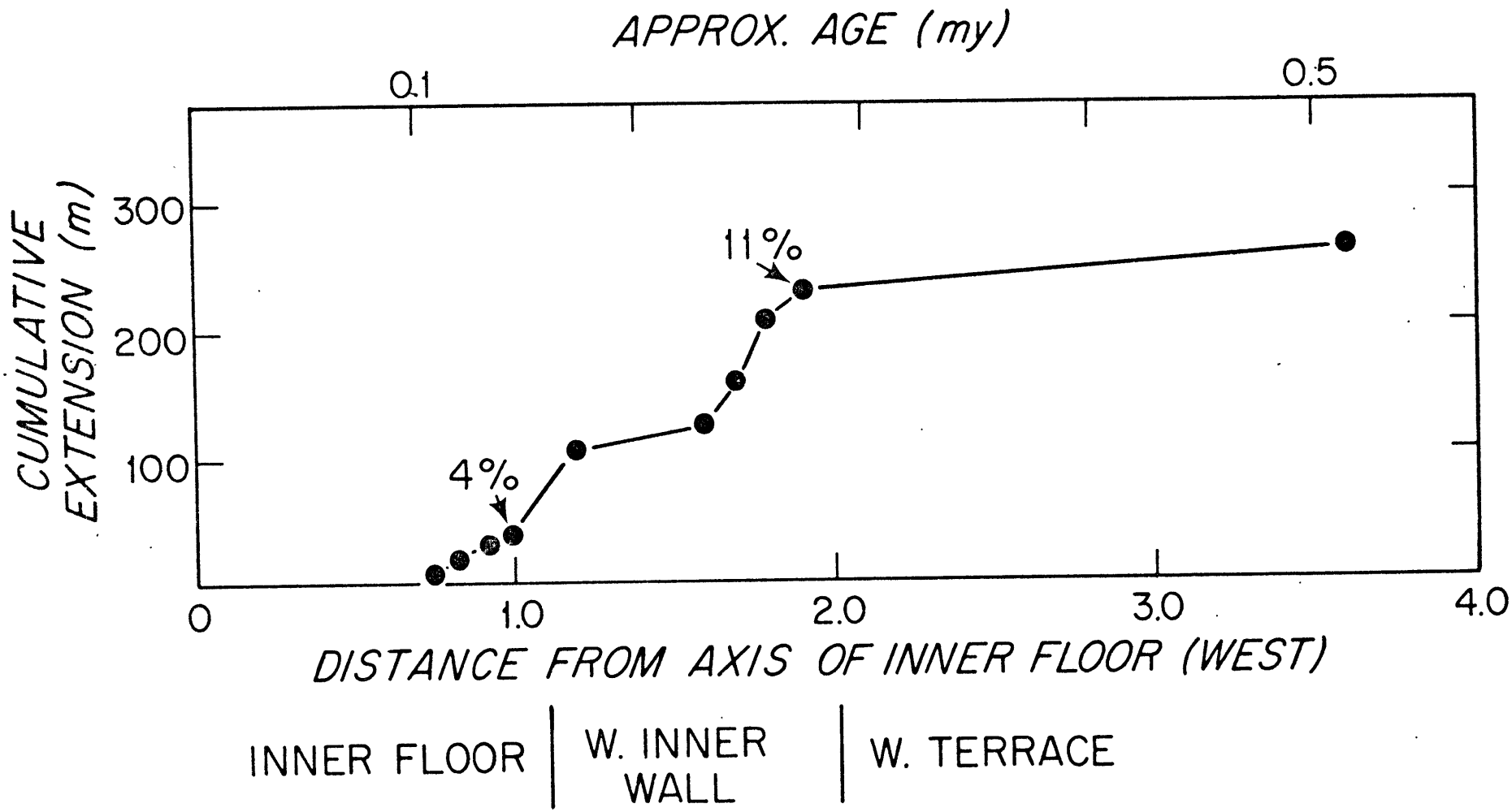
APPROX. AGE (my)
0.1
0.5
CUMULATIVE EXTENSION (m)
300
200
100
11%
4%
0
1.0
2.0
3.0
4.0
DISTANCE FROM AXIS OF INNER FLOOR (WEST)
INNER FLOOR
W. INNER WALL
W. TERRACE

the floor are lower, 4% on the west side and 6% on the east. Most of the extension occurs in the inner walls. The asymmetry in extension is largely caused by the asymmetry in fault density and fault dip between east and west. It is also in keeping with the highly asymmetric spreading rates which prevail out to the outer wall (anomaly 2). The rates are 7.0 mm/yr to the west and 13.4 mm/yr to the east (Macdonald, in prep.). The ratio of east to west spreading rate is close to that of east to west horizontal extension (11% to 18%). Thus the extreme asymmetry in spreading rate may be due to a greater rate of horizontal extension to the east as well as a higher rate of crustal accretion.

THE TERRACES

The median valley terraces between the outer and inner walls are characterized by relatively horizontal, flat topography. The terrace is 14 km wide on the east side and 8 km on the west. Block fault scarps form much of the relief. Fault dips are significantly steeper on the west terrace than on the east terrace (Tables 1, 2). As with the inner walls, this results in greater extension associated with faulting on the east terrace than on the west. This is in keeping with the higher spreading rate on the east side and with the greater width of the east terrace.

TABLE 1:

Average Dips of Fault Scarps

Province	Dip	Standard Deviation	Standard Error	Number of Samples
FAMOUS RIFT				
West Inner Wall	'56°	11.2°	2.8°	17
East Inner Wall	47°	6.1°	1.2°	27
West Terrace	52.5°	7.6°	1.6°	22
East Terrace	44°	5.3°	1.1°	23
West Outer Wall	48.6°	8.1°	2.4°	11
East Outer Wall	46.4°	6.9°	2.4°	7
South FAMOUS Rift	50°	3.7°	1.3°	8

TABLE 2:

Student's T-test of Significance of Differences in Fault Dips*

Provinces Compared	Significance
East and West Inner Walls	96%
East and West Terraces	99%
East Terrace and East Inner Wall	90%
West Terrace and West Inner Wall	96%

* Normal distribution assumed.

The average dip of scarps on both terraces is less than that of the corresponding inner wall. However the significance level of the difference is low and there is no measurable change in tilting of the blocks (Tables 1, 2).

The fault pattern on the terraces is quite different from that on the inner walls. The throw of individual faults is generally less (Fig. 3), and the lateral spacing between faults with throws exceeding 50 m increases from 0.9 km for the inner walls to 2.4 km on the terraces. The change in fault density suggests either that coalescing of faults by reverse faulting occurs in going from the inner walls to the terraces or that the terraces are not steady state. Reverse faulting requires compressional stresses within the median valley. This contradicts focal mechanism solutions (Sykes, 1967), and the observation of normal faulting and graben formation in the median valley. There are also regions as wide as 10 km in the terraces which are almost totally unfaulted, suggesting that large parts of the inner floor were uplifted as single units (e.g. 5 to 15 km, Fig. 2). Thus, it appears that the terraces are not steady state, but are transient features of the median valley structure (discussed later).

Figure 14. a) Graben formation through antithetic faulting due to curved shape of the main fault. b) Tilting of faulted blocks due to shallowing of fault dip with depth. (After de Sitter, 1964).

a

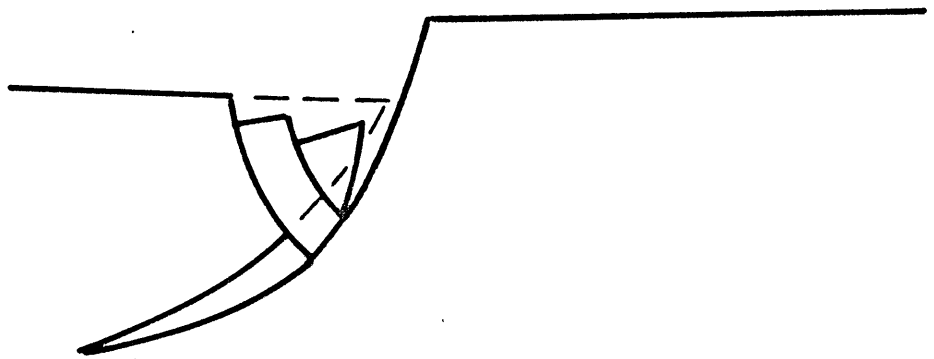

b

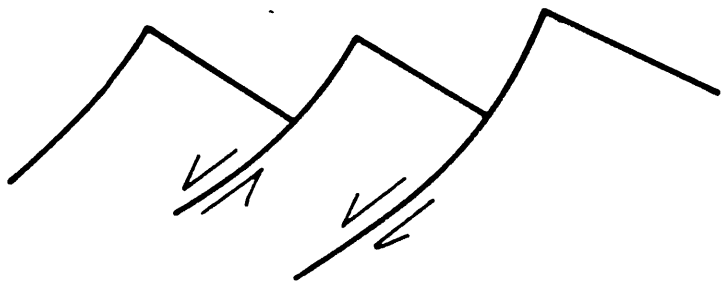

Figure 15. Seismicity of the Famous area. Solid circles are microearthquakes located by Reid and Macdonald (1973) with approximate location accuracies of 2 km. Squares are microearthquakes located by Spindel and others (1974) with a 500m. location accuracy. Large open circles are telesismically located events for 1961-1972 reported by ESSA, with location accuracies of about 20km. Approximate plate boundaries are indicated superposed on the same bathymetric map as in Figure 1B.


33°
34°
36°30'
36°
33°30'

On the west side between -6.5 and -8.0 km from the valley axis there is a graben 200 to 300 m deep (Fig. 3). It extends at least 20 km parallel to the valley and is bounded by scarps with slopes of 45° to 55°. The only earthquake located on the terraces was at the south end of this graben (Fig. 15), indicating that it is still active. This may be very significant for it suggests that the zone of active crustal extension is at least 16 km wide, even though most of the extension occurs at the inner walls in a zone 7 km wide.

The outward facing scarps of the graben may be caused by conjugate normal faulting or by antithetic faulting, both requiring tension. Antithetic faulting could occur if the inward dip of the main fault decreased with depth. Further uplift of the west block would result in a gap at the surface which is filled with antithetic blocks (Fig. 14a). Under increased hydrostatic pressure, the internal friction of rock decreases, resulting in shallower fault dip at depth (de Sitter, 1964). A shallowing of fault dip with depth in the crust has been observed at different erosional levels in the Rhine Graben (Illies, personal comm.). It provides a mechanism for outward tilting of fault blocks, as well as for the formation of grabens and outward facing faults through antithetic faulting (Fig. 14).

Topographic highs 100 to 800 m across and 40 to 200 m high are superposed on many of the blocks (Fig. 2). They are generally symmetric in cross section and range from being equidimensional to having elongation ratios of 6:1. The morphology and dimensions suggests a volcanic origin. They are very similar to the central highs and other volcanic constructions in the inner floor.

Most of the highs are not randomly situated, but form "lips" at the edges of fault blocks. Of 82 highs mapped on the terraces, 51 were lips, i.e., 62% (72 out of 107 for the entire median valley). If highs of average width 500 m were randomly distributed along the fish path on the terrace, only 30% would be lips. It seems likely that volcanic highs, particularly lips, are created in the inner floor like Mt. Pluto or Mt. Venus. If the volcano is dormant, block faulting is likely to be concentrated along its edges where the crust is thinnest, resulting in a volcanic lip perched at the edge of the block fault (e.g. Mt. Mercury, Fig. 2, A-A'). If the volcano has been recently active the crust may be thinnest along its axis and it may be split in two by block faulting. The lip at -1 km on D-D' (Fig. 2) has coherent flows on the west side and truncated pillows on the east, suggesting such splitting (French dive team, personal communication).

If lips were created by volcanism outside the inner floor, their location relative to the blocks might be random. If there were any systematic relationship between volcanism and block faulting, one would expect eruptions to occur at the bases of scarps along fractured fault planes, not at the top of fault blocks on their outer edges. Detailed magnetic studies of the topography concur with an inner floor origin for the lips and volcanoes. Only 7 out of 170 volcanoes in the Famous area either have very high magnetizations or polarities opposite to the surrounding topography, indicative of an origin outside the inner floor (Macdonald, in prep.).

THE OUTER WALLS

The outer walls are located asymmetrically about the valley axis, giving a median valley half-width of 11 ±1 km to the west and 20 ±1 km to the east. Despite the highly asymmetric location of the outer walls, their depth is essentially equal on both sides of the median valley (Fig. 2). Spreading rates of 7.0 mm/yr to the west and 13.4 mm/yr to the east determined from near bottom magnetic data are consistent with the asymmetric position of the walls, and show that the outer walls are essentially isochrons about 1.5 million years old.

The outer walls stand 800 ±100 m above the terraces and 1600 ±100 m above the valley floor. The outer walls appear to be constructed by block faults, the faults dipping toward the valley (Tables 1, 2) and the block tops tilted back 3° to 8° (Fig. 2, F-F', G-G', J-J'). In places, the tilt is replaced by faults which dip away from the valley axis (outward facing faults). In such cases a horst marks the outer edge of the valley (e.g., Fig. 2, B-B', H-H'). The walls are composed of one to three major scarps from 100 m to 550 m in throw. The major scarps forming the outer wall parallel the valley axis. They are linear and continuous at least 18 km on the west and 10 km on the east. Correlation with the surface ship bathymetry suggests in fact that the outer walls are continuous over the 30 to 40 km distance between Fracture Zones A and B (Fig. 1b).

THE ROLE OF BLOCK FAULTING IN CREATING MEDIAN VALLEY RELIEF

To what extent can block faulting account for the depth and relief of the median valley? To quantify the contribution of faulting we tabulated the throws of major block faults (inward and outward facing relative to the rift axis) as well as the change in elevation due to tilting of blocks (Fig. 16).

Figure 16. The east side of the Famous Rift (profile D-D"): The cumulative throw of inward facing normal faults (dipping toward the valley axis), outward facing normal faults (dipping away from the valley axis), and the decrease in elevation due to tilting of blocks. The solid black line is the total tectonic contribution to the relief =I-O-T= (inward facing fault throw)-(outward facing fault throw)-(tilt). Faulting accounts for the entire depth of the median valley as well as for most large scale relief (>2 km. wavelength). Volcanism contributes to the short wavelength roughness but contributes little to long wavelength changes in elevation. Vertical exaggeration is 10X.

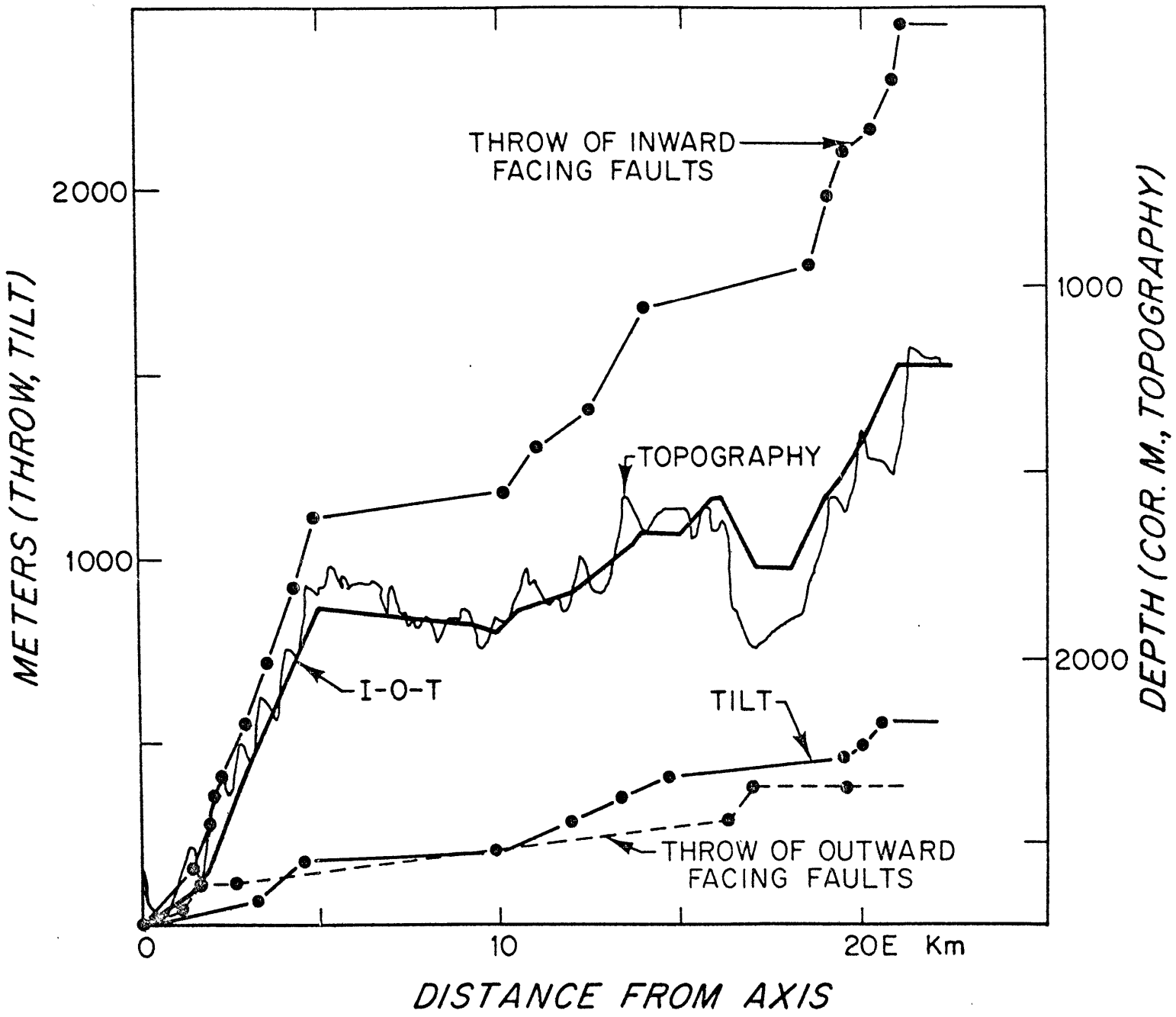
THROW OF INWARD FACING FAULTS
TOPOGRAPHY
I-O-T
TILT
THROW OF OUTWARD FACING FAULTS
2000
1000
0
10
20E Km
METERS (THROW, TILT)
DEPTH (COR. M., TOPOGRAPHY)
DISTANCE FROM AXIS

Inward facing faults increase the depth of the median valley while outward facing faults and outward tilting of blocks decrease the elevation, thus (throw of inward facing faults) - (throw of outward facing faults) - (tilt) equals the contribution of faulting in creating median valley depth. We find that faulting and tilting accounts for nearly all the gross relief of the valley, and in fact, accounts for more than 95% of the depth of the median valley (Fig. 16). Volcanic relief contributes to topographic roughness but very little to large scale relief (i.e., $\geq$ 2 km wavelength). Another interesting observation is that outward facing faulting and tilting contribute almost equally in decreasing median valley depth (discussed later).

2. THE RIFT MOUNTAINS

The rift mountain province begins outside the median valley, just past the outer wall boundary. Topography is still very rugged and is characterized on a large scale by rolling relief with a 6 km to 12 km wavelength (Fig. 17).

As in the median valley, topography is dominated by block faults with throws of up to 300 m. Large block faults and series of faults are linear and continuous over the 4 to 8 km line spacing (Fig. 17). Smaller individual faults of

Figure 17A. Deep-tow geophysical traverse from the Famous Rift outer walls going into the east rift mountains (top 3 profiles) and the west rift mountains (bottom 2 profiles). Major faults indicated by dashed lines. L's denote lips, volcanic features perched at the edges of block faults, and V's denote other volcanic features. Sediment ponds are shown; the numbers indicate the maximum sediment thickness in meters in each pond. Vertical exaggeration is 2X to minimize distortion.

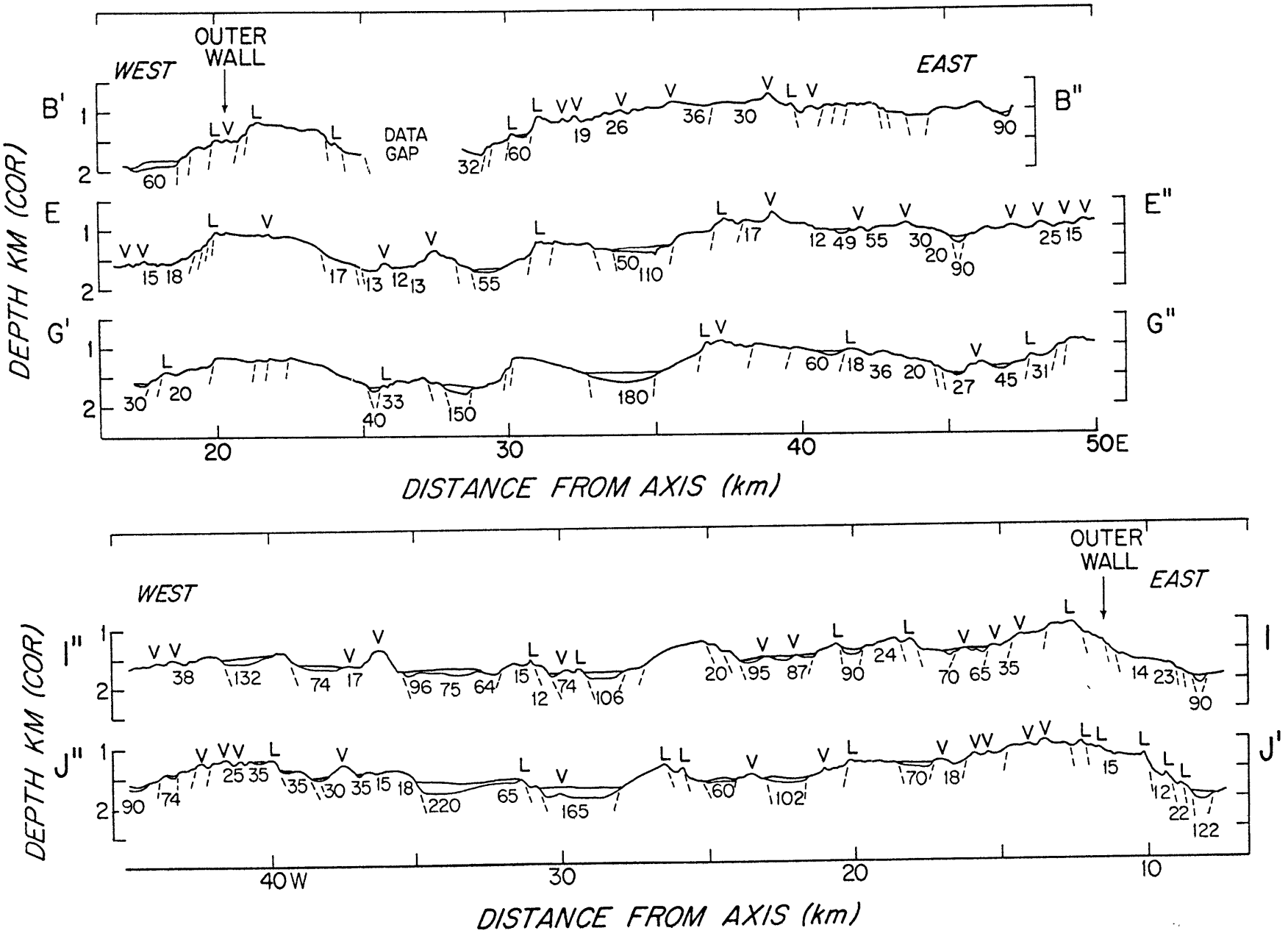
OUTER WALL
WEST
EAST
B'
B"
E
E"
G'
G"
DATA GAP
DEPTH KM (COR)
DISTANCE FROM AXIS (km)
20
30
40
50E
I"
I
J"
J'
40 W
10

Figure 17B. Deep-tow geophysical profile 50 to 130 km. into the east rift mountains (see Figure 1A for track location), key same as in 17A.

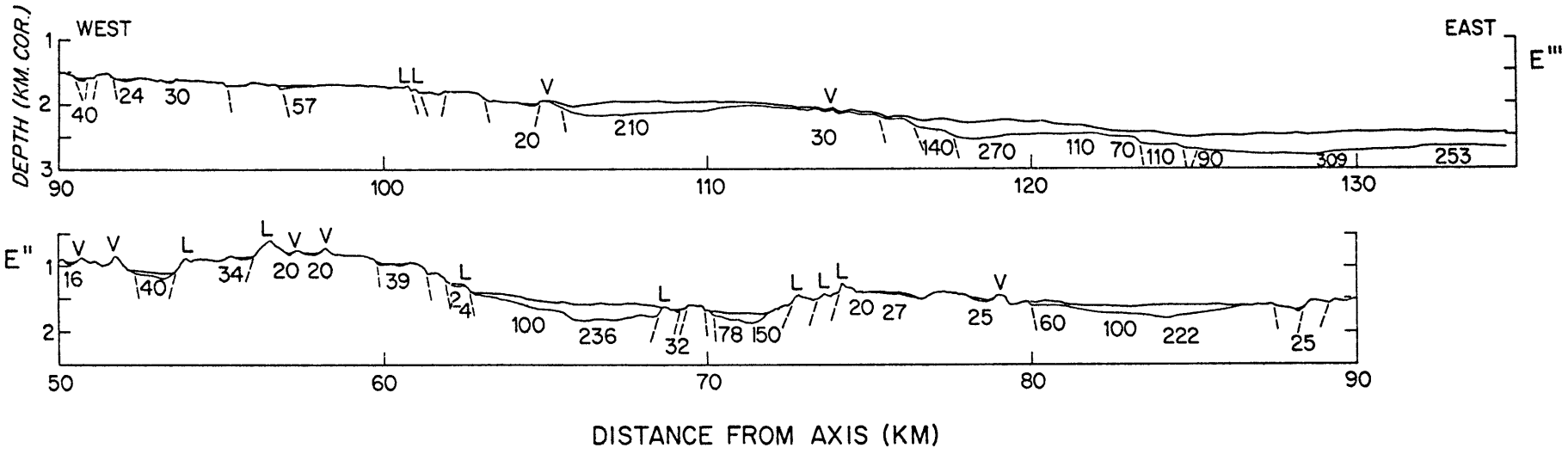
DEPTH (KM. COR.)
WEST
EAST
E'''
E''
1
2
3
40
24
30
57
LL
20
V
210
V
30
140
270
110
70
110
90
309
253
90
100
110
120
130
V
V
16
40
L
34
L
V
V
20
20
39
L
2
4
100
236
L
32
78
150
L
L
L
20
27
V
25
60
100
222
25
50
60
70
80
90
DISTANCE FROM AXIS (KM)

50 to 100 m throw are linear for at least 1 km from side-looking sonar data, but do not appear on adjacent traverses. Lineation direction is generally parallel to the N 17°E strike of the valley.

Major outward facing blocks, which are rare in the median valley, are common in the rift mountains. The average lateral density of outward dipping faults with at least 75 m throw increases from 0.5 per 10 km in the median valley to 2.4 per 10 km in the rift mountains. This further increases to 2.7 per 10 km beyond 80 km from the valley axis. If the median valley is a steady state feature, then outward facing faulting must be occurring outside the valley. Teleseismically located earthquakes do occur in the rift mountains in the FAMOUS area (Fig. 15). Reid and Macdonald (1973) and Spindel et al. (1974) did not locate earthquakes in the rift mountains because their arrays were deployed right over the plate boundaries and their location range was 20 km at best. Francis and Porter's (1973) deployment of a single seismometer in the rift mountains at 45°N lasted only 3 days and recorded little or no activity in the mountains.

However, the dramatic increase in density of outward facing faults suggests that active normal faulting is occurring

in the rift mountains in crust at least 1.5 m.y. old. This is consistent with intraplate earthquake focal mechanism studies by Sykes and Sbar (1973) which suggest that the oceanic crust is still under uniaxial tension out to about 20 m.y. age. In older crust the stresses appear to be compressional.

The cumulative throw of inward and outward facing faults and the effect of tilt was tabulated along traverses I-I' and E-E' in the rift mountains (Fig. 18), similar to the analysis for the median valley (Fig. 16). Once again we find that faulting and tilting of crustal blocks accounts for most of the gross relief and nearly all of the regional change in depth. In contrast with the median valley, the cumulative throw of outward facing faults is as great as that for inward facing faults (Fig. 18). This contrast again indicates active faulting in the rift mountains.

Both outward facing faulting and tilting of the crust results in the decay of median valley relief and increase in depth in the rift mountains. However, outward facing faulting accounts for nearly 80% of the decay of median valley elevation, while tilting of fault blocks accounts for only about 20% (Fig. 18). This is a surprising result because a tilt of only 6° to 7° could account for the cancelation of median valley

Figure 18A. The contribution of normal faulting and tilting of blocks to relief in the east rift mountains on profile E, starting at the rift outer wall (20 km.). Crustal tilt is approximately the same as in the median valley, while outward facing normal faulting increases dramatically, and accounts for over 80% of the decay in median valley elevation in the rift mountains. Less than 20% is due to tilting. Again faulting and tilting accounts for nearly all the large scale relief (I-O-T), while volcanism contributes to short wavelength roughness in the observed topography (bottom).

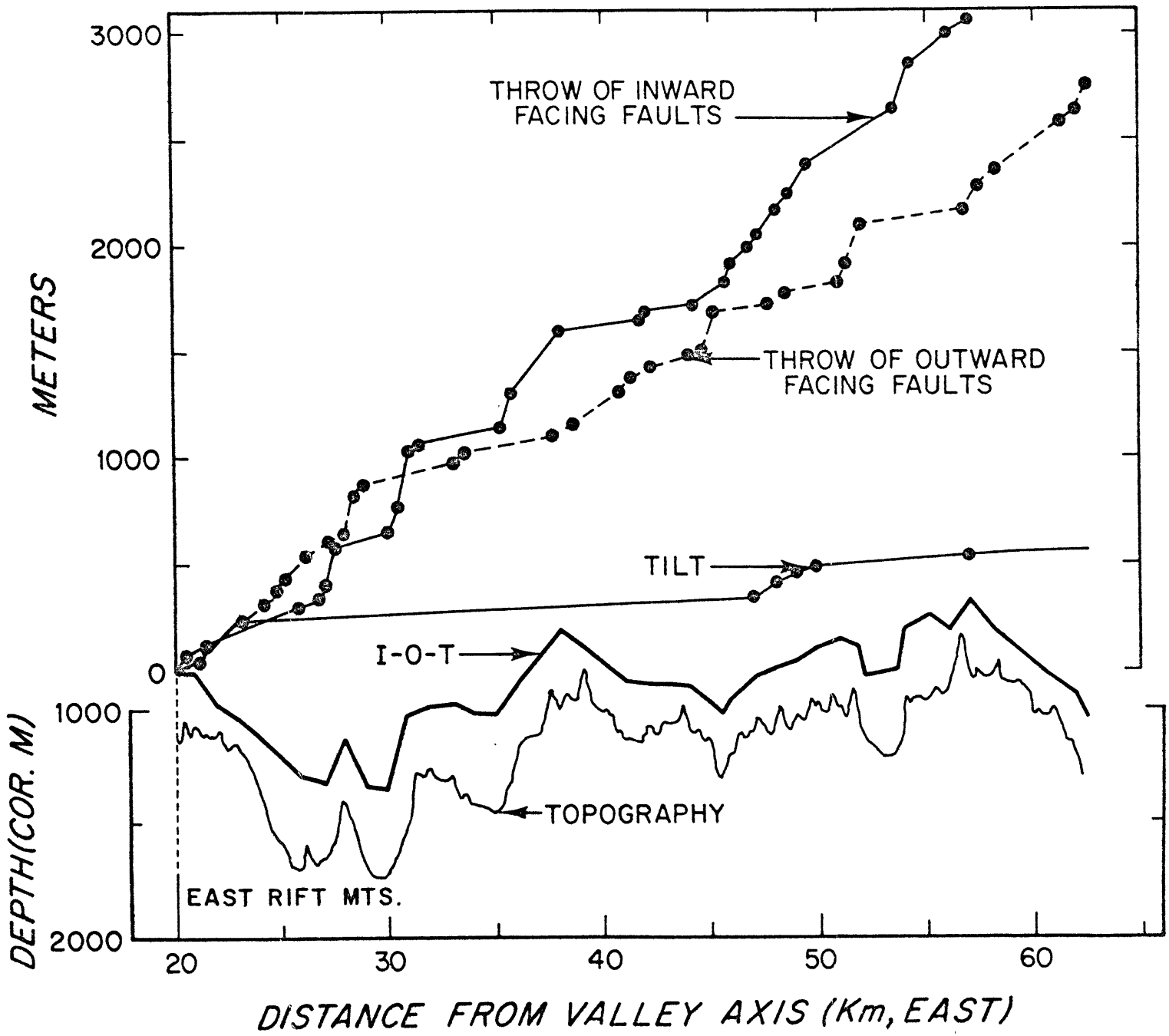
3000
2000
1000
0
1000
2000
METERS
DEPTH(COR. M)
THROW OF INWARD FACING FAULTS
THROW OF OUTWARD FACING FAULTS
TILT
I-O-T
TOPOGRAPHY
EAST RIFT MTS.
20
30
40
50
60
DISTANCE FROM VALLEY AXIS (Km, EAST)

Figure 18B. The contribution of normal faulting and tilting of blocks in the west rift mountains on profile I'-I" starting at the west outer wall (12km.). Results are the same as in Figure 18A. Again outward facing faulting accounts for over 80% of the decay of median valley elevation as opposed to less than 20% due to tilting.

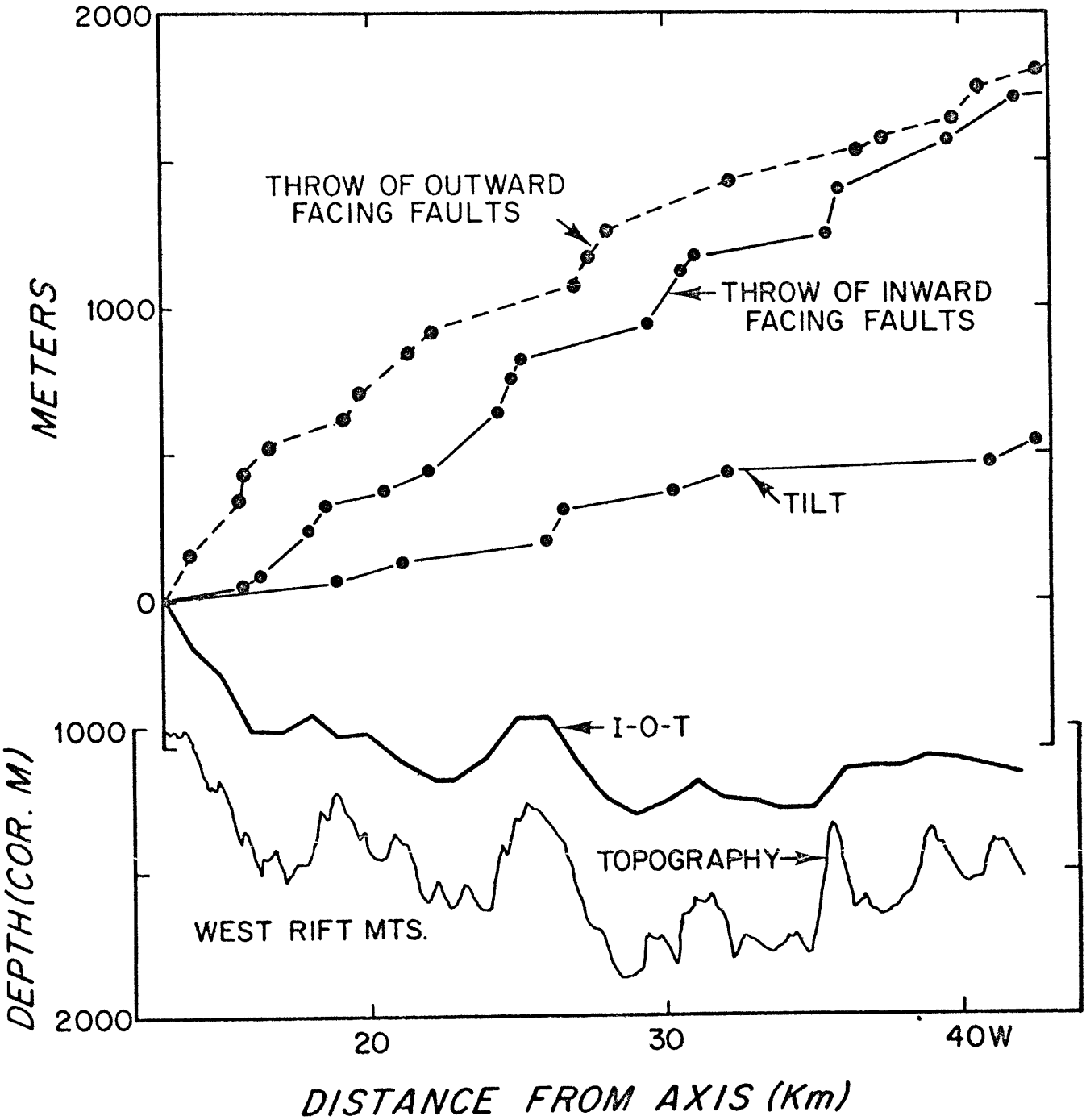
2000
1000
0
1000
2000
METERS
DEPTH(COR. M)
THROW OF OUTWARD FACING FAULTS
THROW OF INWARD FACING FAULTS
TILT
I-O-T
TOPOGRAPHY
WEST RIFT MTS.
20
30
40W
DISTANCE FROM AXIS (Km)

depth. However, the average outward tilt of blocks in the median valley is 2.5° (standard deviation = 2.7° for 126 samples) while that for the rift mountains is 3.8° (standard deviation = 2.5° for 64 samples). Clearly the change in tilt is statistically insignificant and in any case is five times too small. Locally, however, tilt may be an important mechanism for the decay of topographic relief. For example, on several traverses across the outer walls, subsidence of crust is accommodated by tilting of 8° to 12° (Fig. 17, E-E', G-G'). However, outward facing faulting is by far the most important mechanism for the decay of rift valley elevation in the rift mountains.

The outward facing scarps rarely form antithetic faults or conjugate pairs with the inward facing scarps but generally occur in series of outward facing steps (Fig. 17). Some of the long wavelength topography (6 to 12 km) appears to correlate with alternating groups of inward and outward facing scarps resulting in a large scale, undulating horst and graben terrain (Fig. 17).

Equidimensional and slightly elongate volcanic highs including lips occur almost as often in the rift mountains as in the median valley and have similar dimensions and morphology.

As in the rift valley volcanic features contribute to small scale relief, but are secondary to faulting in creating large scale relief. The only very large volcanic feature is at -36 km (Fig. 17). Magnetic studies indicate that this feature and nearly all other volcanic topography was created in the median valley (Macdonald, in prep.)

3. SEDIMENT DISTRIBUTION

Photographic and side-looking sonar data suggest that most of the seafloor, even in the inner floor, is covered with a thin veneer of sediments (Luyendyk and Macdonald, in prep.) Outside the inner floor we have tabulated sediment thickness using the 4 kHz sediment penetration system on the fish (reliable for sediment thicknesses of 5 to 100 m) and air gun reflection profiles where sediment thickness exceeded 100 m.

Sediment thickness generally increases with distance from the valley axis (Fig. 19). Close to the axis, the increase in thickness with distance shows the same asymmetry as the spreading rates, the sediments being thinner on the east side due to the faster spreading half-rate. On both sides of the ridge the increase in sediment thickness is highly erratic, unlike the Pacific (Larson, 1971; Klitgord and Mudie, 1974). The sediment accumulates in ponds, mostly in faulted depressions

Figure 19. Sediment thickness as a function of distance from the valley axis (from profiles I-I", G-G', E-E'''). Note how the sediment cover is very localized and spotty, yet still shows the expected increase in thickness away from the axis. Within 30 km. of the axis, the sediment cover is asymmetric, reflecting asymmetric spreading half-rates.

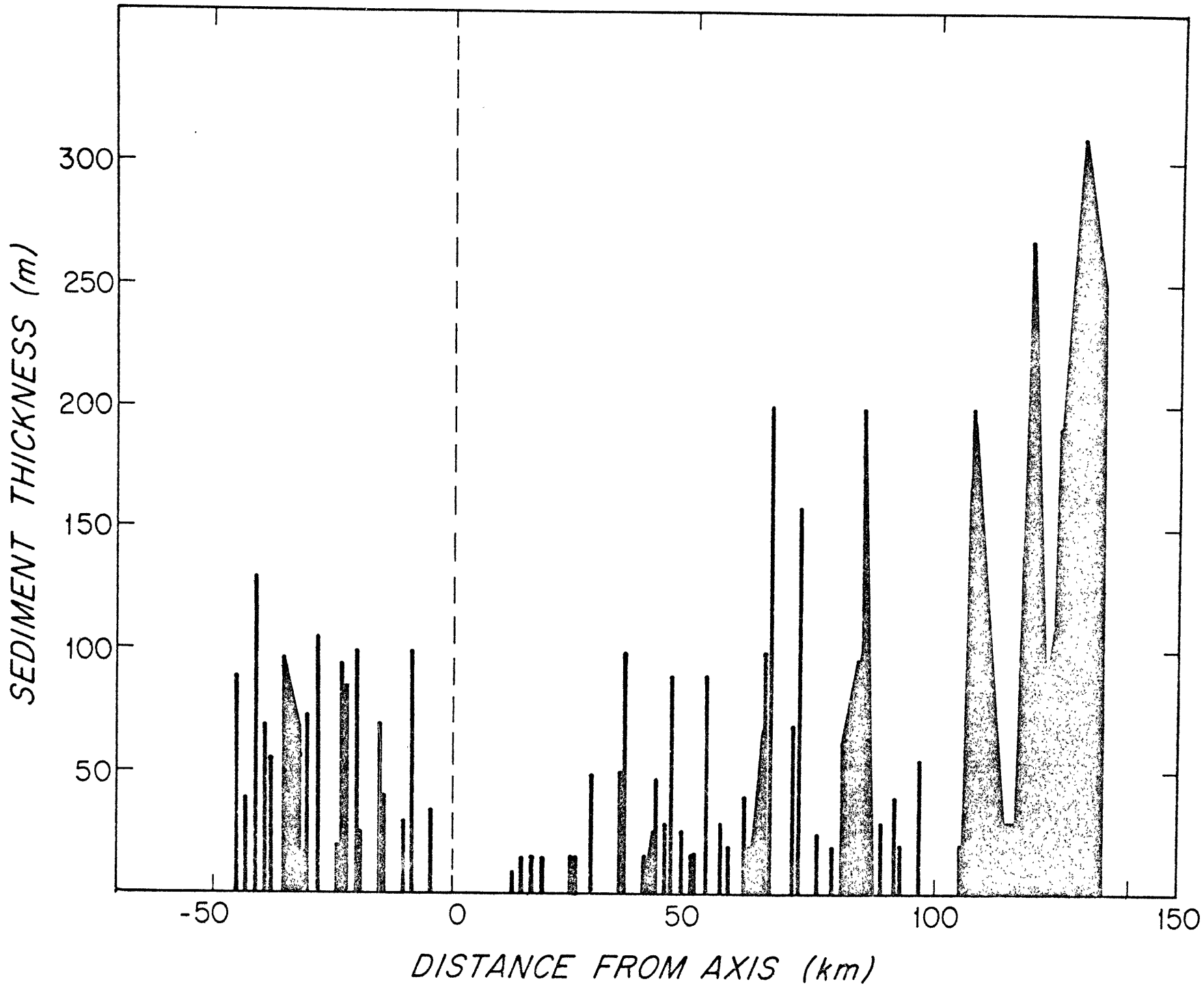
SEDIMENT THICKNESS (m)
300
250
200
150
100
50
-50
0
50
100
150
DISTANCE FROM AXIS (km)

and on the back sides of tilted fault blocks (Figs. 2, 17). Apparently sediment distribution is dominated by downslope transport. Ponding of sediments has also been observed at 22°N on the Mid-Atlantic Ridge (van Andel and Komar, 1969). Bottom currents of up to 20 cm/sec (Keller et al., 1975), and a continuous pulse of faulting activity (Reid and Macdonald, 1973; Spindel et al., 1974) on a rugged block faulted terrain results in a thorough redistribution of sediments downslope into ponds. For example on the west terrace the graben at -8 km (Fig. 2) has up to 120 m of sediment while the average sediment thickness of the terrace is about 20 m. This thorough redistribution of the sediments helps to explain the absence of internal reflectors on the fish and air gun records, and makes it difficult to use displacement of sediment horizons as detectors of tectonic movements.

4. THE SOUTH FAMOUS RIFT

The south Famous Rift, south of fracture zone B, extends 30 km before being offset right-laterally 12 km by fracture zone C (Fig. 1). Like the Famous median valley, it strikes approximately N 17°E, oblique to the east-west trend of FZB. However, the two valleys are morphologically very different.

While the Famous Rift is a double valley with a narrow inner floor and two sets of walls separated by broad horizontal terraces, the south Famous Rift is essentially a single valley with a wide floor and one well-defined set of walls. A narrow terrace (5 km) can be traced on the east side between the blocks at 10 km and 15 km, but there is no terrace on the west side. The median valley is approximately 24 km wide, extending asymmetrically from -9 to +15 km (Figs. 20, 21). (The center of the valley is taken as midway between the inner walls.)

The floor of the valley averages 11 km in width, five times the average width of the Famous inner floor. There is no well-defined valley axis marked by a distinct central high or central low. In cross section, the floor has 4 to 6 topographic highs with more than 100 m of relief (Figs. 20, 21). There are more than 35 topographic highs in the south Famous Rift, some over 10 km long (Fig. 28, Laughton and Rusby, 1975). Side-looking sonar records on our only deep tow traverse indicate that these highs have lobate boundaries along strike (Fig. 21). Their symmetrical profiles and lobate edges suggest that the highs are volcanoes. No single eruptive center or group of volcanoes dominate the morphology. Instead the volcanoes seem to be randomly situated throughout the 11 km wide floor.

Figure 20. Bathymetric profiles across the south Famous Rift picked from a U.S. Navy bathymetric chart using multi-narrow beam data (Phillips and Fleming, in prep.). The deep-tow profile S-S' is almost at the same place as profile 3. Physiographic provinces are as shown. Notice the very wide inner floor and poorly developed terraces relative to the Famous Rift.

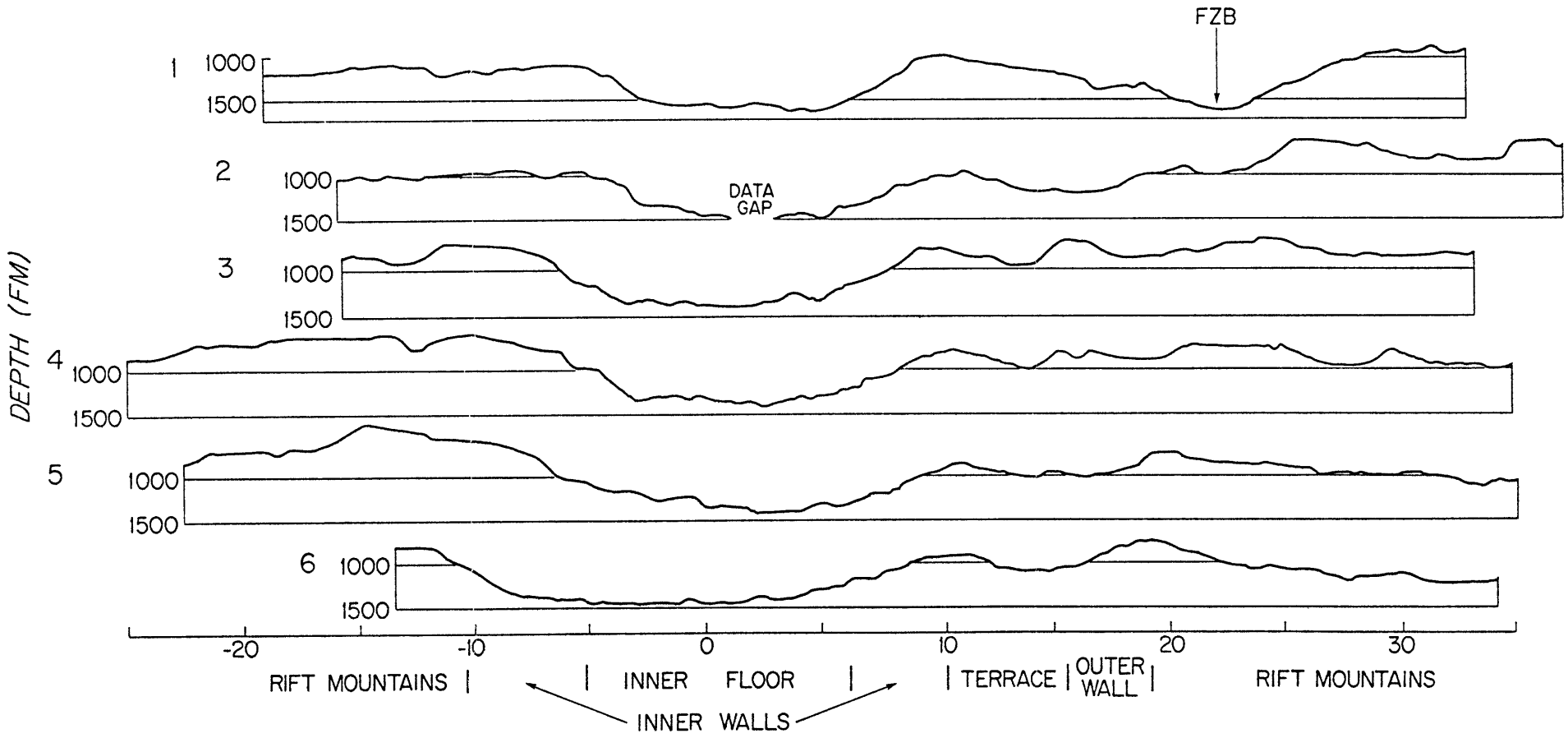
FZB
1
1000
1500
2
1000
1500
DATA
GAP
3
1000
1500
4
1000
1500
5
1000
1500
6
1000
1500
DEPTH (FM)
-20
-10
0
10
20
30
RIFT MOUNTAINS
INNER FLOOR
TERRACE
OUTER WALL
RIFT MOUNTAINS
INNER WALLS

Figure 21. Deep-tow geophysical profile S-S' across the south Famous Rift. Mt. Saturn, the most recent site of volcanism is denoted by S. Sediment and side-looking sonar data is shown, sediment thickness in meters denoted by numbers.

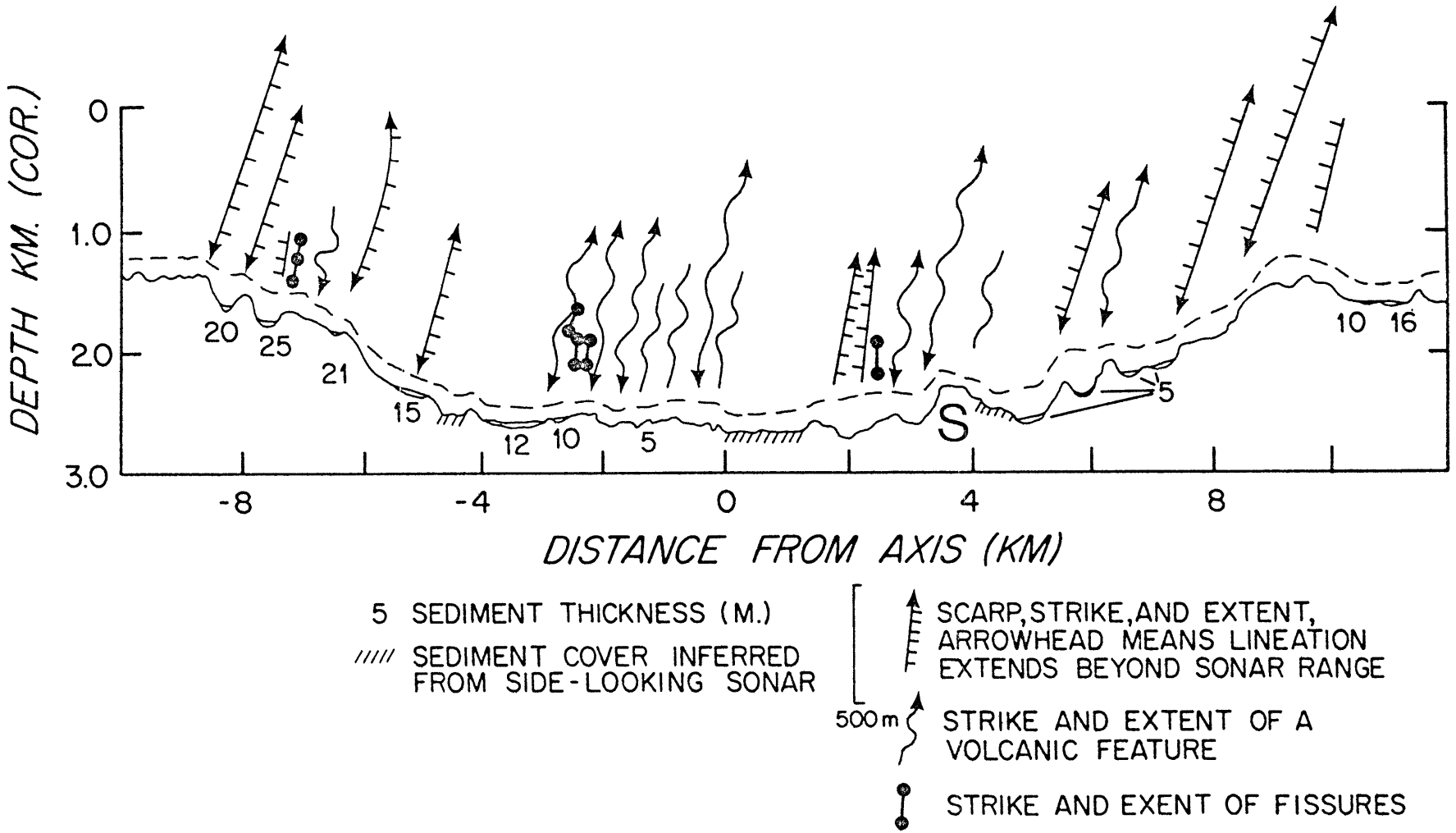
DEPTH KM. (COR.)
0
1.0
2.0
3.0
-8
-4
0
4
8
DISTANCE FROM AXIS (KM)
20
25
21
15
12
10
5
S
5
10
16
5 SEDIMENT THICKNESS (M.)
////// SEDIMENT COVER INFERRED FROM SIDE-LOOKING SONAR
SCARP, STRIKE, AND EXTENT, ARROWHEAD MEANS LINEATION EXTENDS BEYOND SONAR RANGE
500 m
STRIKE AND EXTENT OF A VOLCANIC FEATURE
STRIKE AND EXENT OF FISSURES

Mt. Saturn (at +3.7 km, Fig. 21) appears to be the most recent site of extrusive volcanism in the floor. It is up to 300 m high and is at least 3 km long (sonograph II-JJ, Laughton and Rusby, 1975), about the same size and shape as Mt. Venus in the Famous Rift. The 4.0 kHz sediment penetration system and side-looking sonar system indicate sediment cover, up to 12 m thick in the valley floor except between +2 and + 4 km in the vicinity of Mt. Saturn. The thin veneer of sediments (less than 1-2 m) detected on the east flank of Mt. Saturn is consistent with down slope transport of sediment from the nearby east walls. If Mt. Saturn were an older feature created near the valley axis, the sediments should be more symmetrically distributed on its flanks and thicker. Mt. Saturn is also the most highly magnetized feature in the valley floor suggesting that it is the freshest accumulation of pillow basalts (Macdonald, in prep.). Thus, sediment and magnetic data both suggest that the most recent site of extrusive volcanism is well over on the east side of the valley floor, almost on the east wall. This suggests that volcanism may occur anywhere within the 11 km wide valley floor, and that the numerous volcanoes in the floor were not necessarily erupted along the valley center line.

Faulting is rare in the valley floor. There is no near-bottom side-looking sonar coverage parallel to the strike of the floor, so mapping of scarps as small as 4 m is not possible as it was further north. However, scarps and lineations 20 m or higher should be detected easily, yet only 2 were found, while up to 25 faults per km^2 were mapped in the Famous Rift (Luyendyk and Macdonald, in prep.) There are two scarps forming what appears to be a graben, 50 m deep and 400 m wide (Fig. 21, +2 km). Several tectonic fissures or gjas were mapped. Perhaps most of the small throw faults are masked by the wide volcanic zone.

Large scale faulting with throws exceeding 100 m, begins abruptly at the walls at ±5 km. The walls consist of 4 to 5 major steps with 100 m to more than 500 m of throw. Volcanic lips perched at the edges of fault blocks occur here as in the Famous Rift (e.g. Fig. 21; -8 km, +6 km). Dip of major fault blocks is essentially the same as that in the Famous Rift (Table 1).

5. DISCUSSION AND OBSERVATIONS CONCERNING THE STRUCTURE AND EVOLUTION OF THE MEDIAN VALLEY

In order to understand the evolution of the median valley in time and space, and to set the tectonic framework for

magnetic studies (Macdonald, in prep.) we summarize and discuss our observations.

a. Location and morphologic expression of the center of spreading.

The center of spreading in the Famous median valley is currently a narrow plate boundary lying near the axis of the inner floor. Its location is well defined by: 1) the pattern of inward facing fault blocks bordering a deep, narrow inner floor, 2) the pattern of thinning sediments toward the axis, 3) the relatively unfractured nature of crust along a 1 km wide band, 4) the recovery of extremely fresh unaltered basalt samples from this zone, and 5) the location of a narrow crustal magnetization maximum in this zone (Macdonald, in prep.). The plate boundary lies within an inner floor only 1.0 to 4.0 km wide. Beyond the boundaries of the inner floor, the crust has been block faulted, transported either east or west, and attached to the lithospheric plate. The most recent expression of the accreting plate boundary is an alternating series of linear central volcanoes and central depressions. This lineament of volcanoes and depressions is less than 1.5 km wide and lies a few hundred meters west of the inner floor center line.

b. Expression of asymmetry in the median valley

On a gross scale one is impressed by the symmetry of the Mid-Atlantic ridge; its "Mid"-Atlantic position between the continents, its symmetric increase in depth, and its symmetrical spreading rate over long periods of time (Pitman and Talwani, 1972). However, on a scale of kilometers or hundreds of thousands of years, it is difficult to find any parameter which is symmetrical. This asymmetry can be seen in: 1) the position of the inner and outer walls relative to the inner floor axis, 2) location of the central volcanoes, 3) width of the terraces, 4) fault dips, 5) density of faulting in the inner floor, 6) the stair-step versus the massive block nature of the east and west inner walls, 7) sediment distribution, 8) crustal extension rates, and 9) short term seafloor spreading rates. All these asymmetries are consistent with a skewness of seafloor spreading and related tectonism and volcanism toward the east. The asymmetries must from time to time reverse so that the system is symmetric when time-averaged over long periods.

c. The roles and interaction of volcanism and faulting in the Famous Rift.

The greatest concentration of recent volcanism lies near the inner floor axis and is represented by features such as

Mt. Venus and Mt. Pluto. Most of the recent volcanoes occur in a narrow band 1.0 to 1.5 km wide which is relatively unfractured and unfaulted. Flow fronts are strikingly parallel to the N 17°E trend of the valley. Most of the flows appear to be directed away from the axes of volcanic highs. The strike of flow fronts and inferred direction of flow all suggest that most of the volcanism occurs as linear fissure eruptions hundreds of meters to several km in length. Flow directions suggest that a number of parallel and en echelon fissure eruptions construct a feature like Mt. Venus. Analogous linear en echelon fissure eruptions are responsible for much of the volcanic relief in Iceland (Walker, 1964). Some volcanism occurs along the edges of the floor, with lava flows directed toward the inner floor axis. These flow fronts also have a N 15°E to N 20°E trend. They generally do not build up large volcanic edifices, but are small volume eruptions from flanking fissures. Submersible samples document the existence of recent flank eruptions (FAMOUS dive team, personal comm.), and near-bottom magnetic studies suggest that they are of small volume and thickness relative to axial eruptions (Macdonald, in prep.).

The central volcanic highs are transported out of the inner floor on block faults. These fossil central highs form prominent volcanic lips at the edges of fault blocks (e.g., Mt. Mercury). The occurrence of lips in the valley and in the rift mountains is far too common to be accounted for by random volcanism away from the inner floor. As mentioned earlier, if there were any systematic relationship between block faulting and volcanism, eruptions might be expected at the bases of the blocks along fault planes, and not coincidentally perched at the edges of the blocks. Lips can be explained if fracturing in the inner floor occurs where the crust is thinnest, which would probably be near the edges of the central volcanoes. The volcano is transported to either side by spreading and then uplifted by block faulting, creating a lip at the edge of the scarp. Such lateral transport of the volcanoes away from the median valley provides a mechanism for extremely asymmetric spreading on a small scale. Repeated fracturing along one side of the volcanoes preferentially would create an asymmetry in spreading rate detectable in magnetic anomalies. Magnetic studies also indicate that volcanism is extremely rare outside the floor. Thus, morphologic, tectonic, and magnetic data

(Macdonald, in prep.) all suggest that nearly all the volcanic topography is created in the inner floor of the valley.

Tensional cracks, similar to gjas in Iceland, and steep faults with only a few meters of throw, occur right along the inner floor axis. The intensity of fracturing and faulting of the crust increases dramatically less than 1 km from the axis reaching fault densities of 25 per km^2. Cumulative throw due to the faulting is small, rarely more than 40-50 m. Throughout the inner floor, topography is dominated by volcanism, while faulting is secondary, acting primarily to fracture the crust.

At the inner wall boundaries and beyond, block faulting dominates the relief. Almost the entire depth of the median valley is created by block faulting (Fig. 16). Volcanic topography is generally of smaller amplitude and rides on top of the fault blocks. At the inner walls, fault throws increase from meters to hundreds of meters. On a fine scale, some of the massive upthrust blocks consist of series of narrow slivers. A high level of microearthquake activity is associated with incipient block faulting at the base of the wall.

The dip of the faults, averaging approximately 50°, is close to the average dip of large normal faults on land (de Sitter, 1964). The dips are consistent with shear failure

along the fault planes, whereas the vertically sided gjas in the inner floor indicate failure under tension. The difference in failure is a matter of depth. The crust is intensely fractured (Fig. 9), thus the effective pressure equals the lithostatic pressure minus the hydrostatic pressure. (If the crust were totally impermeable, the effective pressure would equal the lithostatic plus the hydrostatic pressures.) For very shallow cracks and faults in the floor the effective pressure is only a few bars and failure occurs under tension, resulting in vertical cracks and small steep step faults. The large faults of the inner walls may extend 2 to 3 km in the crust (Wiedner and Aki, 1973). At such depths the effective pressure is about 0.8 to 1.2 kilobars. This is sufficiently high to cause shear failure under uniaxial tension, resulting in non-vertical fault dips.

Alternatives to block faulting have been proposed for formation of the valley walls including thrusting (Osmaston, 1971), construction by flow fronts, and caldera collapse. Focal mechanism solutions (e.g., Sykes, 1967) and the very steep fault dips facing the valley axis make thrusting unlikely. Formation of the walls by stacking flow fronts would require tremendous volcanic flows originating from outside the inner floor. This is unlikely since the most recent zone of large

scale volcanism lies near the inner floor axis. The linearity and angular shape of the scarps would also require unrealistic order in stacking the flow fronts. Francis (1974) has drawn an analogy between the 1968 Fernandina caldera collapse in the Galapagos and the formation of the median valley floor and walls. However, formation of the inner walls through caldera collapse contradicts several observations. There is a fine scale, uniform increase in the density of faulting (Figs. 6, 8) and in fault throw (FAMOUS dive team) with distance from the inner floor axis. In addition, microearthquakes of magnitudes -1 to +1 occur on a day by day basis associated with apparently continuous faulting at the base of the inner walls. In contrast, the Fernandina caldera collapse was a highly episodic phenomenon involving an intense swarm of 295 magnitude 4 and greater earthquakes. The collapse occurred over a period of only 11 days involving a 300 m subsidence of the floor, equivalent to half the relief of the inner walls. Furthermore, this and other caldera collapses result in circular or elliptical collapses. However, the walls should then have lobate outlines, which contradicts the striking linearity observed (Fig. 3). Alternatively, collapse of a linear caldera extending the length of the valley may occur. However, the Famous valley

consists of a number of volcanic centers and alternating central lows, and the south Famous valley has an even greater number of eruptive centers (35 or more). These observations preclude the collapse of a single large linear caldera forming the valley. Thus a block faulted origin of the inner and outer walls is most likely. As discussed earlier, however, caldera collapse may be the origin of the 600-800 m wide depressions between the central highs (Fig. 8).

d. Crustal extension

Block faulting accommodates some horizontal extension in the floor and inner walls. Extension is only 4% of the horizontal distance in the inner floor on the west side and 6% on the east. Including the inner walls, horizontal extension is 11% to the west and 18% to the east. This is a small but significant portion of the local spreading rate and has the same asymmetry. The zone of active extension may be at least 16 km wide. Thus asymmetric spreading is accomplished through asymmetric extension as well as asymmetric accretion.

e. The decay of rift valley relief and the evolution of topography in the rift mountains

The 1.6 km deep rift valley decays in the rift mountains by normal faulting along planes dipping away from the valley axis and also by outward tilting. The decrease in elevation due to outward facing normal faulting is about four times that due to tilting. The dramatic increase in outward dipping faults outside the median valley suggests that most of this faulting occurs outside the valley in the rift mountains. This is important for it means that the rift mountains are tectonically active and that the decay of median valley relief is accomplished by a new set of faults originating outside the rift valley.

The slope of the line indicating decay of relief through outward facing faulting in the rift mountains is essentially constant (Fig. 18). This may be important for it suggests that most of the faulting occurs right at the median valley/rift mountain boundary. If faulting continued significantly further out in the rift mountains, the slope of the line representing outward facing faulting should continue to increase with distance from the axis but this is not observed. Thus most of the median valley relief may be cancelled right near the edges of the valley.

The occurrence of outward facing faults in groups rather than in conjugate pairs with the inward facing scarps, gives rise to a broad undulating horst and graben relief with a wavelength of 6 to 12 km. Volcanic topography, including the ubiquitous lips, occurs on top of the fault blocks as it does in the valley. However, nearly all the large scale relief is tectonic, created by inward and outward facing normal faults, and by tilting.

f. Microearthquakes and plate boundaries

Although the transform fault valleys of FZA and FZB are wide, the active transform plate boundaries are linear and narrow. Reid and Macdonald (1973) located a narrow band of microearthquakes in FZA which ended abruptly at the intersection of FZA and the Famous Rift (Fig. 15). A subsequent tectonic map based on deep tow data showed that these earthquakes occurred on 2 linear scarps which also mark a discontinuity in sediment thickness. This single scarp system appears to define the current transform fault, a zone of active faulting less than 1 km wide within the 4 km to 10 km wide transform valley (Fig. 22A)(Detrick et al., 1973). A swarm of seven microearthquakes was located at the west end of the active fault (Fig. 22A). The scarp and the microearthquake activity abruptly stops at a point well into the Famous Rift/FZA intersection.

Figure 22A. Microearthquake epicenters on FZA and its intersection with the Famous Rift. Tectonic map from deep-tow data (after Detrick, 1974), epicenters from Reid and Macdonald (1973). Circle with cross denotes a swarm of at least seven events which were located on the west end of the active FZA transform fault scarp. Note that the active seismic zone continues well into the FZA/Famous Rift intersection, suggesting that the spreading plate boundary in the Famous Rift is itself very narrow, and is located near the center of the inner floor.

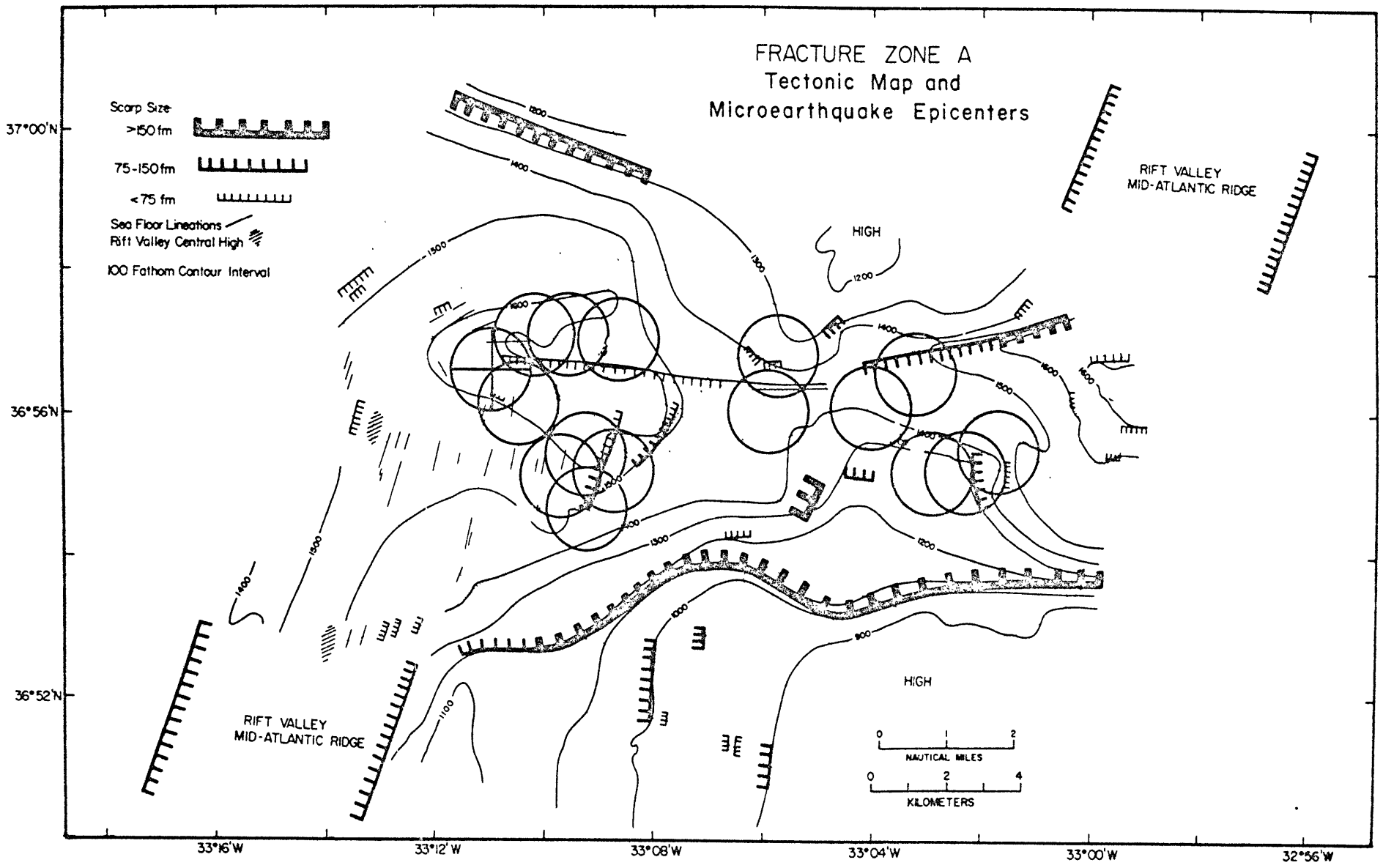
FRACTURE ZONE A
Tectonic Map and
Microearthquake Epicenters
Scarp Size
>150 fm
75-150 fm
<75 fm
Sea Floor Lineations
Rift Valley Central High
100 Fathom Contour Interval
RIFT VALLEY
MID-ATLANTIC RIDGE
HIGH
RIFT VALLEY
MID-ATLANTIC RIDGE
HIGH
NAUTICAL MILES
KILOMETERS
37°00'N
36°56'N
36°52'N
33°16'W
33°12'W
33°08'W
33°04'W
33°00'W
32°56'W

Figure 22B. U.S. Navy mult-beam bathymetric chart of FZB (Phillips and Fleming, in prep.) with epicenters from Reid and Macdonald (1973) superposed. Heavy contours are at 50 fathom intervals, light contours at 10 fathom intervals. This map shows the narrow east-west cleft of FZB cutting across the north-south ridge which bisects the FZB valley (Figure 1B). Note that the epicenters fall right on this narrow cleft within the 2 km. location accuracy, suggesting that this is the active transform fault trace. The cleft is only 2 km. wide compared to the 20 km. width of the FZB transform valley.

FRACTURE ZONE B

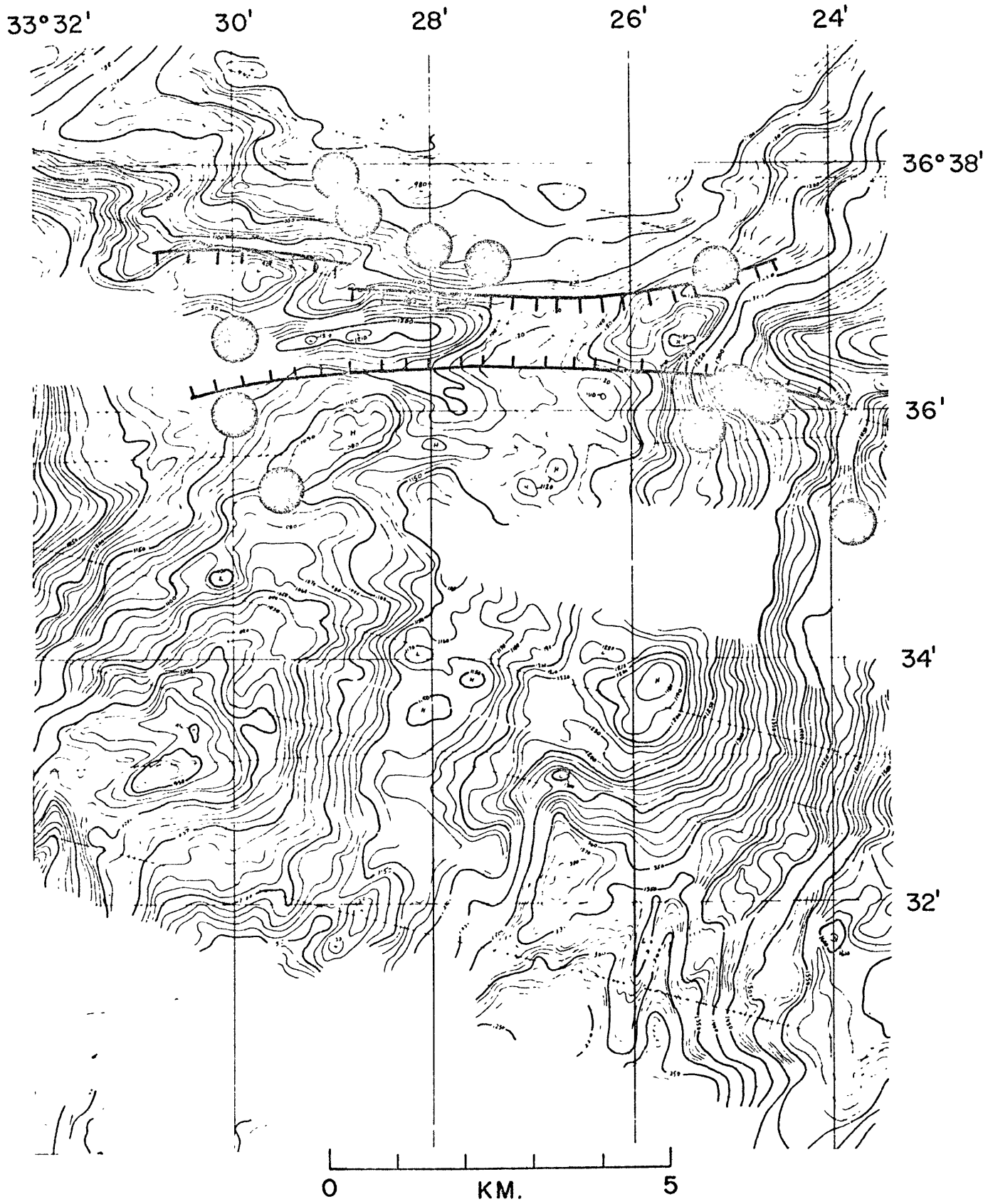

The FZB transform valley is from 10 km to more than 15 km wide. Again the microearthquakes define a narrow, linear band through the transform valley (Fig. 15). A detailed chart of FZB shows that the transform valley is divided by a north-south ridge between 33°24' and 33°30'W. On the north side of the transform valley (36°37'N), this north-south ridge is transected by a 1 km wide east-west trough. Within the 2 km accuracy of location, the microearthquakes fall right on this narrow east-west cleft continuing into the Famous valley intersection (Fig. 22B). Thus, in both FZA and FZB, the active transform fault is a narrow, approximately 1 km wide boundary within a broad transform valley. Furthermore, N 17°E lineations associated with the spreading plate boundary, continue to within 1 km of the active fault. This suggests that the transform fault is a very narrow plate boundary, perhaps a single fault, over short intervals of time. However, the very existence of the broad transform valleys suggests that over millions of years, the transform fault may migrate perpendicular to its strike over a zone at least 10 to 15 km wide. Disturbance of magnetic anomalies north of FZB also suggests migration of the transform fault (Macdonald, in prep.). Currently the FZA active fault lies near the axis of the transform valley.

The FZB transform fault is on the north side of the transform valley in the narrow trough.

The transform fault earthquake distribution has important implications for the median valley. The sharp intersections of the active transform faults with the Famous Rift at both ends suggest that the median valley accreting boundary itself must currently be a well-defined zone less than a few km wide. The earthquakes do not extend very far into the south Famous Rift intersection where the floor is five times wider than in the Famous Rift. This suggests that the accreting plate boundary is not narrowly defined where the floor is wide, and the the present plate boundary may be on the east side of the south Famous Rift. Furthermore, the current position of the FZB transform fault and the overlapping of the Famous and south Famous rifts, suggest that the south end of the Famous Rift is an inactive appendage. It is relict from a period when transform fault B was further south and was severed from the Famous Rift by the north migration of FZB.

g. Tectonic influence of neighboring fracture zones on the Famous Rift

Where major block faults extend for tens of kilometers, they plunge toward the fracture zones. On the west side of the

Figure 23. Longitudinal dip (or bending) of the west inner and outer walls toward FZA and FZB. Data from deep-tow profiles with some supplementary data from U.S. Navy narrow-beam bathymetric charts (Phillips and Fleming, in prep.). Dashed line shows distance midway between FZA and FZB. Triangles show the computed effect on elevation of lateral heat conduction across the fracture zone near the west inner wall/FZA interesection.

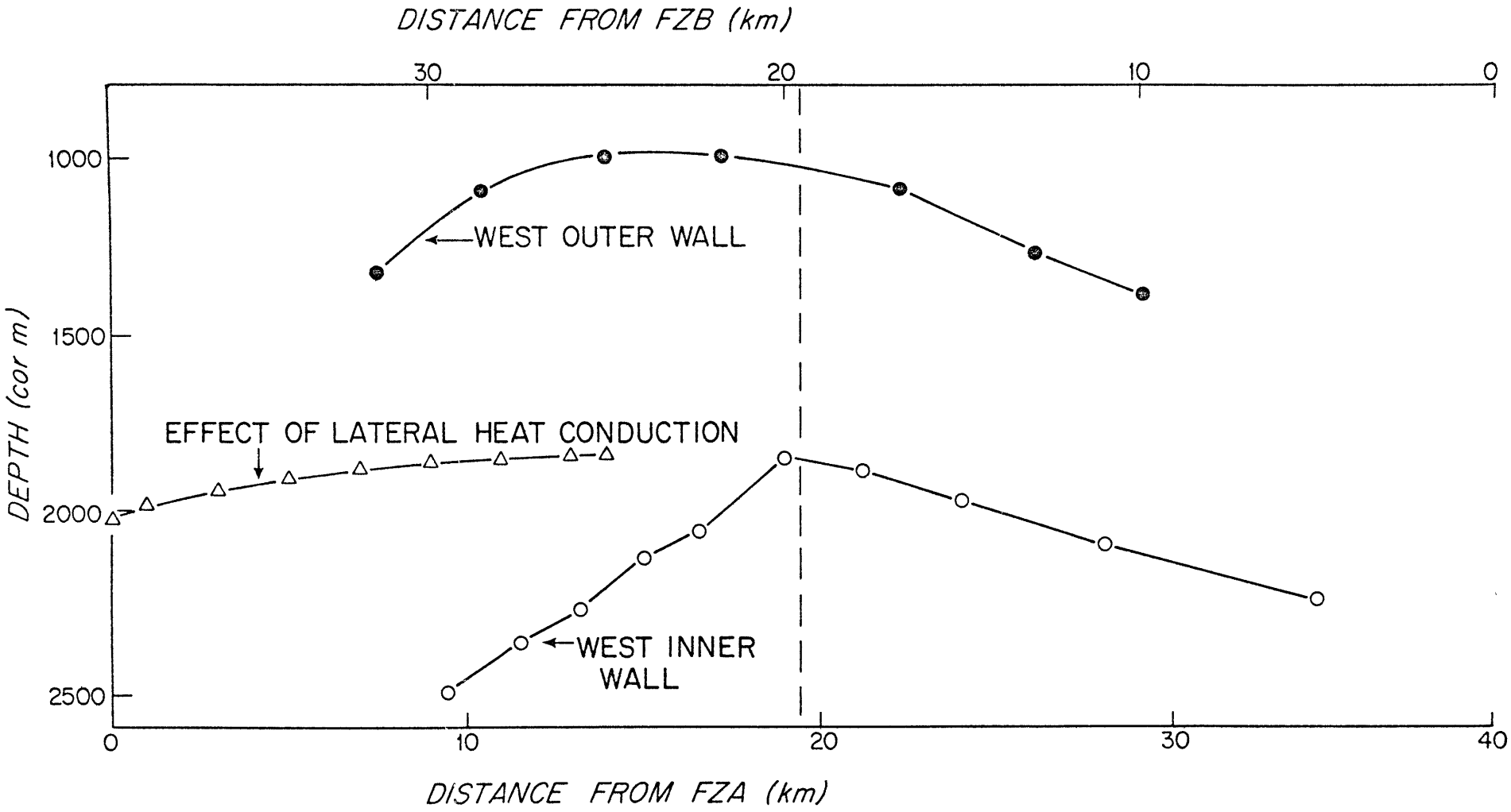
DISTANCE FROM FZB (km)
30
20
10
0
1000
1500
2000
2500
DEPTH (cor m)
WEST OUTER WALL
EFFECT OF LATERAL HEAT CONDUCTION
WEST INNER WALL
0
10
20
30
40
DISTANCE FROM FZA (km)

valley, single major blocks in the inner and outer walls can be traced over 20 km (Fig. 3). (This was not possible on the east side of the valley due to extensive relay faulting in the inner wall and poor coverage of the outer wall.) The blocks plunge toward the fracture zones about a bending point midway between fracture zones A and B (Fig. 23). This suggests that much of the vertical relief of the fracture zone valleys is accommodated by north-south bending of the rift valley walls, as well as by normal faulting along east-west faults bordering the fracture valley (e.g. at 36°54'N). More importantly, the plunging of the blocks sugests that the tectonic influence of neighboring fracture zones extends throughout the entire length of the 45 km long rift. North or south of the mid-point of the median rift the blocks immediately plunge toward the nearest fracture zone.

Small faults in the inner floor also cut across bathymetric contours, plunging toward the nearest fracture zone. The faults do not bend around, following the contours, as the transform-spreading intersection is approached.

One possible mechanism for the bending is lateral heat conduction across the fracture zone between crust of different ages and a resulting anomaly in elevation of the block edges.

Lateral heat conduction and resulting elevation changes due to thermal contraction were computed at various points across the fracture zones assuming a vertical boundary. A maximum of 1° of plunge can be accounted for this way, compared to the 2.8° to 3.8° of plunge observed (Fig. 23). Another possible mechanism is mechanical coupling of lithosphere of different ages, the older cooler lithosphere holding down the edge of the adjacent younger lithosphere.

h. Oblique spreading

Precise mapping of the Famous Rift and the adjoining transform faults shows that the rift is spreading obliquely (Figs. 3, 9). The active transform fault trends are N 90°E for both FZA and FZB, forming an oblique angle of 17° with the N 17°E trend of the valley (Figs. 3, 22). The transform fault trends agree within 2° of the predicted trends using the America-Africa poles of Pitman and Talwani (1972), Morgan (1968), and LePichon (1968). A tightly constrained fault plane solution on the Oceanographer FZ also shows current east-west (N 86°E) transform motion (Sykes, 1967), even though the gross trend of the fracture zone is S 75°E (Fig. 1). The tectonic grain of the inner floor is overwhelmingly N 17°E even down to a scale of meters (Figs. 9, 10). Thus even on a

fine scale there is no indication of readjustment within the rift to an orthogonal system. Magnetic data and the trends of fracture zones to the south suggest that oblique spreading has been stable here for some time, even through a change in spreading direction (Macdonald, in prep.).

i. Relationship between the Famous and south Famous rifts

The Famous Rift has an asymmetric but orderly structure consisting of a narrow inner floor, inner walls, terraces, then outer walls. The accreting plate boundary is currently narrow and well defined lying near the axis of the inner floor.

The south Famous Rift is far less orderly. The inner floor is 10 to 14 km wide, five to six times the width of the Famous inner floor. A narrow terrace is developed on the east side followed by an outer wall. However, there is no terrace or outer wall on the west side. Instead, the rift mountains begin just past the inner wall. The current position of active volcanism is not along the center of the inner floor. Sediment distribution, topography, microearthquake distribution, magnetic studies and dredge samples all suggest that the current plate boundary and locus of volcanism is on the east side of the floor near the east inner wall. This plus the uniform distribution of volcanic highs throughout the wide

floor suggests that volcanic extrusion may occur anywhere within the floor with essentially equal probability.

The nearly ubiquitous occurrence of a median valley on slow spreading ridges and numerous theoretical models suggest that the median valley is a steady state feature (Sleep, 1969; Deffeyes, 1970; Lachenbruch, 1974; Anderson and Noltemier, 1974). The contrasting structures of the Famous and south Famous rifts indicate that the median valley may be steady state only in existence and not in form. The width of the inner floor and the structure of the inner walls, terraces and outer walls may be constantly changing. The variation of these parameters reflects the width of the zone of active block faulting, and determines the width of the active volcanic zone (the zone in which volcanic extrusion may occur with essentially equal probability).

References and Bibliography, Chapter 2

Anderson, R.N., and H.C. Noltimier, A model for the horst and graben structure of mid-ocean ridge crests based on spreading velocities and basalt delivery to the oceanic crust, Geophys. J.R. astr. Soc., 34, 137, 1973.

Ballard, R.D., W.B. Bryan, J.R. Heirtzler, G. Keller, J.G. Moore, and Tj. van Andel, Manned submersible observations in the FAMOUS area Mid-Atlantic Ridge, Science, in press.

Ballard, R., and T.H. van Andel, Project FAMOUS: the Mid-Atlantic Rift valley at 36-37°N, morphology and tectonics of the inner rift valley at 36°50'N on the Mid-Atlantic Ridge, in prep. for Bull. Geol. Soc. Amer. dedicated issue on FAMOUS.

Bellaiche, G., J.L. Cheminee, J. Francheteau, R. Hekinian, X. Le Pichon, H.D. Needham, and R.D. Ballard, Rift Valley's inner floor: first submersible study, Nature, 250, 558-560, 1974.

Brundage, W.L., H.S. Fleming and N. Cherkis, Preliminary Naval Electronics Laboratory, LIBEC/FAMOUS Lineations Report, June, 1974.

Bryan, W.B., and J.G. Moore, Project FAMOUS: The Mid-Atlantic Rift valley at 36-37°N, volcanism, petrology and geochemistry of the basalts of the inner floor of the rift valley at 36°50'N on the Mid-Atlantic Ridge, in prep. Bull. Geol. Soc. Amer. dedicated issue on FAMOUS.

Deffeyes, K.S., The Axial Valley: A steady state feature of the terrain, in The Megatectonics of Continents and Oceans, H. Johnson and B.L. Smith, eds., Rutgers Univ., New Brunswick, New Jersey, p. 194, 1970.

de Sitter, L.U., Structural Geology, New York, New York, McGraw-Hill, 551 p., 1964.

Detrick, R.S., Fracture zone A, Mid-Atlantic Ridge 37°N: A near-bottom geophysical study, Scripps Institute of Oceanography Ref. 74-26, 10 p., 1974.

Detrick, R., J.D. Mudie, B.P. Luyendyk and K.C. Macdonald, Near-bottom observations of an active transform fault: Mid-Atlantic Ridge at 37°N, Nature, 246, 59, 1973.

Francis, T.J.G., A new interpretation of the 1968 Fernondiva caldera collapse and its implications for mid-ocean ridges, Geophys. J. R. astr. Soc., 39, 601, 1974.

Francis, T.J.G., and I.T. Porter, Median valley seismology: the Mid-Atlantic Ridge near 45°N, Geophys. J.R. astr. Soc., 34, 279, 1973.

Ivers, W.D., and J.D. Mudie, Towing a long cable at slow speeds: A three-dimensional dynamic model, Mar. Tech. Soc. J., 7, 23, 1973.

Keller, G.H., S.H. Anderson, D.E. Koelsch, and J.W. Lavelle, Near-bottom currents in the Mid-Atlantic Ridge Rift Valley, Canadian Journal of Earth Sciences, 12, 703, 1975.

Klitgord, K., and J. Mudie, The Galapagos spreading center: A near-bottom geophysical survey, Geophys. J. R. astr. Soc., 38, 563, 1974.

Lachenbruch, A.H., A simple mechanical model for oceanic spreading centers, J. Geophys. Res., 78, 3395, 1973.

Larson, Roger L., Near-bottom geologic studies of the East Pacific rise crest, Bull. G.S.A., 82, 823, 1971.

Laughton, A.S., and J.S. Rusby, Long range sonar and photographic studies of the median valley in the FAMOUS area of the Mid-Atlantic Ridge near 37°N, Deep-Sea Research, 22, 279, 1975.

Le Pichon, X., Sea-floor spreading and continental drift, J. Geophys. Res., 73, 3661, 1968.

Luyendyk, Bruce P., and Ken C. Macdonald, Physiography and structure of the Famous rift valley inner floor observed with a deeply towed instrument package, in prep. Bull. Geol. Soc. Amer. dedicated issue on FAMOUS.

Macdonald, Ken C., Near-bottom-magnetic anomalies, asymmetric spreading, oblique spreading, and tectonics of the accreting plate boundary on the Mid-Atlantic Ridge (37°N), in prep. Bull. Geol. Soc. Amer. dedicated issue on FAMOUS.

Macdonald, Ken C., B.P. Luyendyk, J.D. Mudie and F.N. Spiess, Near-bottom geophysical study of the Mid-Atlantic Ridge median valley near lat. 37°N: Preliminary observations, Geology, 211, 1975.

Moore, J.G., Mechanism of formation of pillow lava, American Scientist, 63, 269, 1975.

Moore, J.G., H.S. Fleming and J.D. Phillips, Preliminary model for extrusion and rifting at the axis of the Mid-Atlantic Ridge, 36°48'North, Geology, 2(9), 437-440, 1974.

Morgan, W.J., Rises, trenches, great faults and crustal blocks, J. Geophys. Res., 73, 1959, 1968.

Needham, H.D., and J. Francheteau, Some characteristics of the rift valley in the Atlantic Ocean near 36°48' North, Earth and Planet. Sci. Lett., 22, 29-43, 1974.

Osmaston, M.F., Genesis of ocean ridge median valleys and continental rift valleys, Tectonophys., 11, 387, 1971.

Phillips, J.D., and H.S. Fleming, The Mid-Atlantic Ridge west of the Azores 35°-39°N, in prep. Bull. Geol. Soc. Amer. dedicated issue on FAMOUS.

Pitman, W.C., III, and M. Talwani, Sea-floor spreading in the North Atlantic, Bull. Geol. Soc. Amer., 83, 619, 1972.

Reid, I., and K.C. Macdonald, Microearthquake study of the Mid-Atlantic Ridge near 37°N using sonobuoys, Nature, 246, 88-90, 1973.

Sleep, N.H., Sensitivity of heat flow and gravity to the mechanism of sea floor spreading, J. Geophys. Res., 74, 542, 1969.

Spiess, F.N., and R.C. Tyce, Marine Physical Laboratory deep-tow instrumentation system, Scripps Inst. Oceanography Ref. 73-4, 1973.

Spindel, R.C., S.B. Davis, K.C. Macdonald, R.P. Porter and J.D. Phillips, Microearthquake survey of median valley of the Mid-Atlantic Ridge at 36°30'N, Nature, 577-579, 1974.

Sykes, L.R., Mechanism of earthquakes and nature of faulting on the mid-ocean ridges, J. Geophys. Res., 72, 2131, 1967.

Sykes, L.R., and M.L. Sbar, Intraplate earthquakes, lithospheric stresses and the driving mechanism of plate tectonics, Nature, 245, 298, 1973.

Thorarinsson, S.T. Einarsson and G. Kjartansson, On the geology and geomorphology of Iceland, Geografiska Annaler, XLI, 135, 1959.

van Andel, Tj.H., and P.D. Komar, Ponded sediments of the Mid-Atlantic Ridge between 22° and 23° North latitude, Geol. Soc. Am. Bull., 80, 1163, 1969.

Walker, G.P.L., Some aspects of Quaternary volcanism in Iceland, Leicester Lit. Philos. Soc., 151, 25, 1964.

Weidner, D.J., and K. Aki, Focal depth and mechanism of mid-ocean ridge earthquakes, J. Geophys. Res., 78, 1818, 1973.

CHAPTER III

NEAR-BOTTOM MAGNETIC ANOMALIES, ASYMMETRIC SPREADING, OBLIQUE SPREADING AND TECTONICS OF THE ACCRETING PLATE BOUNDARY ON THE MID-ATLANTIC RIDGE (37°N)

1. INTRODUCTION

Although the Mid-Atlantic Ridge (MAR) is one of the most extensively studied spreading centers on earth, its magnetic anomaly pattern and fine scale tectonic history has remained obscure. In most areas of the ridge crest province of the central and north Atlantic, only the central anomaly and anomaly 5 are readily identifiable (Loncarevic and Parker, 1970; Aumento et al., 1971; Phillips et al., 1969; Pitman and Talwani, 1972). The magnetic anomaly pattern often remains ambiguous for intensive surveys with 2 km line spacings (at 26°N, MacGregor et al., submitted) even where three-dimensional inversion techniques accounting for topographic effects have been used (at 45°N, S.P. Huestis, personal comm.).

In 1973 we conducted a near-bottom geophysical study of the Famous area (MAR near 37°N) on R/V KNORR Cruise 31 of the Woods Hole Oceanographic Institution, using the deep-tow instrument package of the Marine Physical Laboratory of the

Figure 1A. Regional setting of the Famous area and the long deep-tow traverse (E-E''') into the east rift mountains. (chart courtesy of W. Perry)

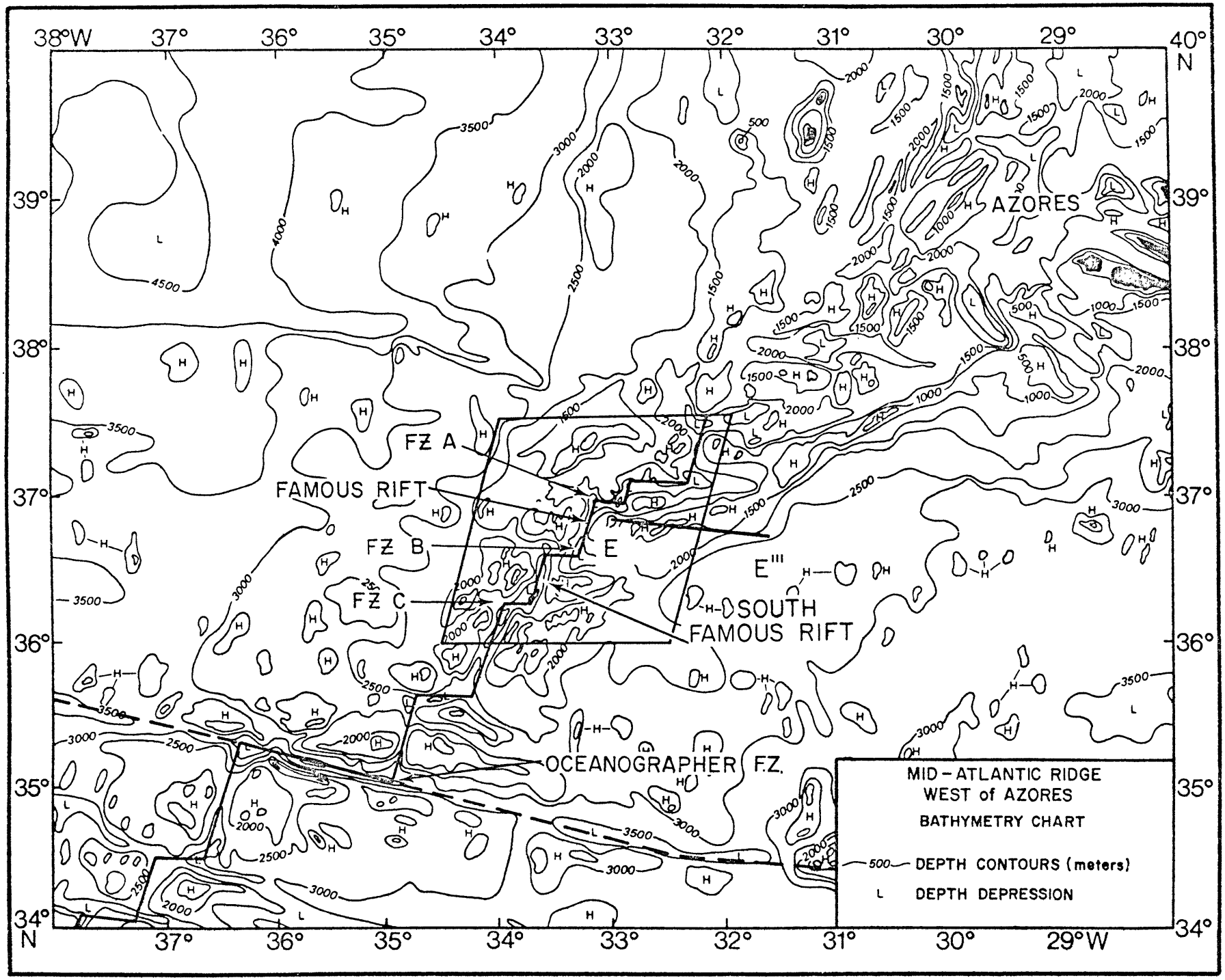
38°W
37°
36°
35°
34°
33°
32°
31°
30°
29°
40° N
39°
38°
37°
36°
35°
34° N
AZORES
FZ A
FAMOUS RIFT
FZ B
E
E'''
FZ C
SOUTH FAMOUS RIFT
OCEANOGRAPHER F.Z.
MID-ATLANTIC RIDGE
WEST of AZORES
BATHYMETRY CHART
500 DEPTH CONTOURS (meters)
L DEPTH DEPRESSION

Figure 1B. 100 fm. (uncor.) interval chart of the Famous area (courtesy of J.D. Phillips). Deep-tow tracks used in magnetic anomaly analysis are shown by solid lines. DSDP sites 332 and 333 are shown.

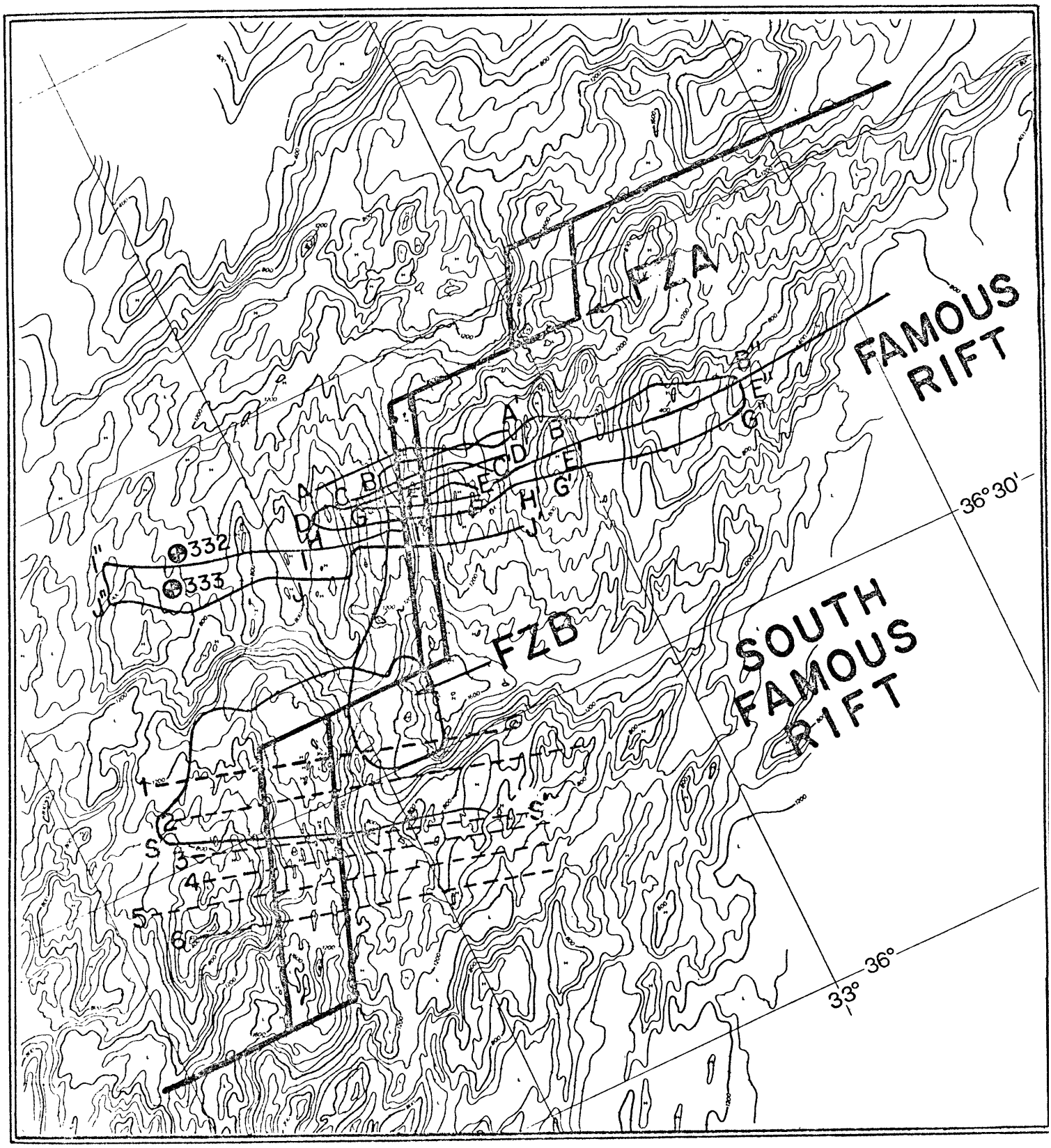
FZA
FZB
FAMOUS RIFT
SOUTH FAMOUS RIFT
36° 30'
33° 36'
A
B
C
D
E
F
G
H
I
J
332
333

Scripps Institution of Oceanography (Spiess and Tyce, 1973). The median valley segments studied are each approximately 45 km long and trend N 17°E. They are offset about 15 to 20 km by two east-west transform faults, FZA and FZB (Fig. 1). The Famous Rift Valley between FZA and FZB was the primary focus of the near-bottom magnetic studies. Macdonald et al. (1975) divide the Famous Median Valley into four physiographic provinces: 1) the outer walls that bound the valley; 2) the terraces; two relatively flat regions which lie between the inner and outer walls; 3) the inner walls, and 4) the inner floor. The structure of the Famous Rift has been discussed in detail by Macdonald and Luyendyk (in prep.), Luyendyk and Macdonald (in prep.), Ballard and van Andel (in prep.), Bryan and Moore (in prep.), Phillips and Fleming (in prep.), Macdonald et al. (1975), and Needham and Francheteau (1974). The south Famous Rift, south of FZB, is less thoroughly studied, but provides an interesting comparison with the Famous Rift magnetic studies as it has a single rather than a double median valley structure (Figs. 2, 3). The structure of south Famous Rift is discussed by Macdonald and Luyendyk (in prep.), and Laughton and Rusby (1975).

Figure 2. Geophysical profile D-D' across Mt. Venus in the Famous Rift. (C is the edge of the Brunhes anomaly and J is the Jaramillo). Dashed lines are inferred faults. Numbers are the maximum depth of each sediment pond in meters. Vertical exaggeration is 2X. Note the sharp maximum in crustal magnetization centered over Mt. Venus and the highly asymmetric location of anomaly boundaries.

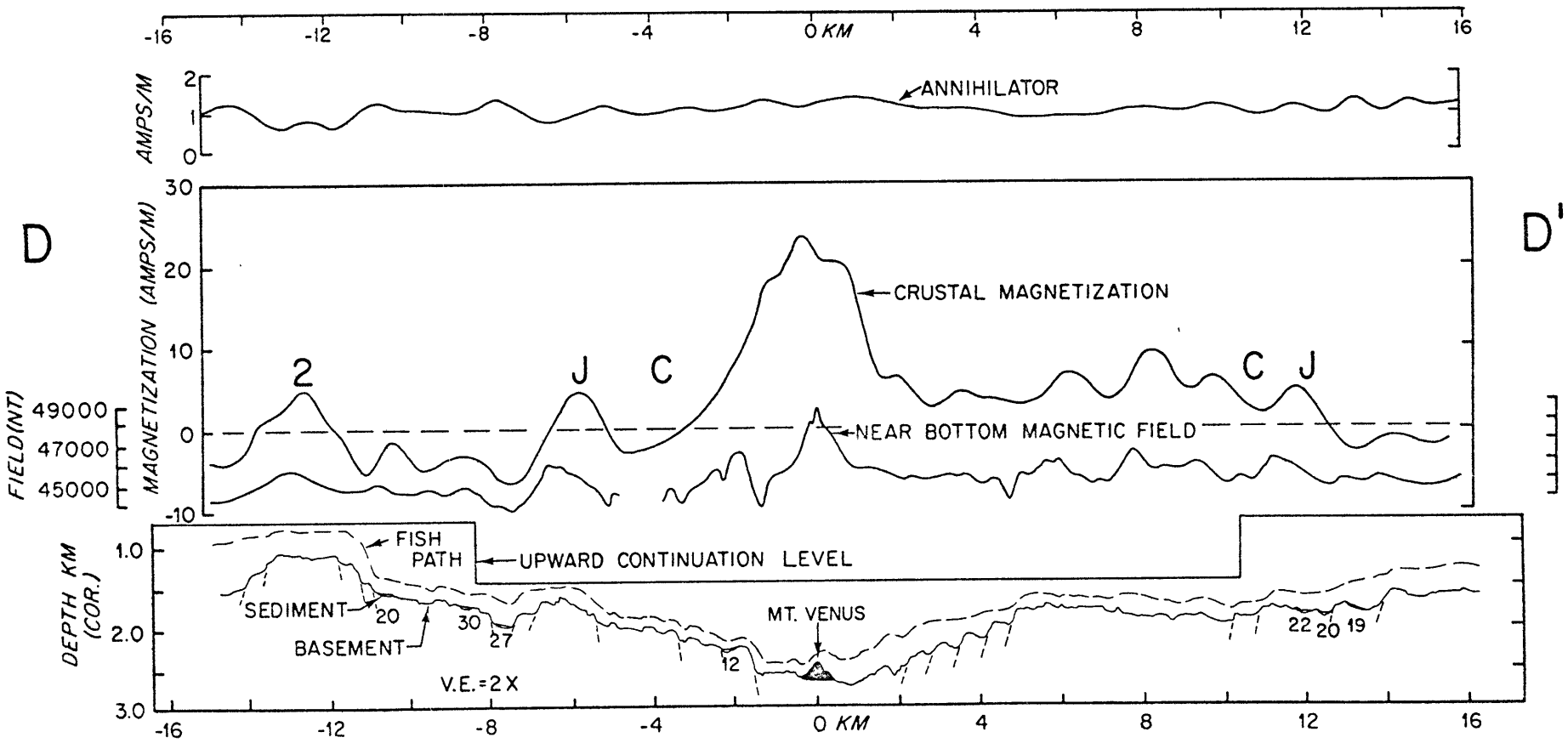
-16
-12
-8
-4
0 KM
4
8
12
16
AMPS/M
2
1
0
ANNIHILATOR
D
D'
30
20
10
0
-10
MAGNETIZATION (AMPS/M)
CRUSTAL MAGNETIZATION
2
J
C
C
J
FIELD(NT)
49000
47000
45000
NEAR BOTTOM MAGNETIC FIELD
DEPTH KM (COR.)
1.0
2.0
3.0
FISH PATH
UPWARD CONTINUATION LEVEL
SEDIMENT
BASEMENT
20
30
27
12
MT. VENUS
22
20
19
V.E.=2X

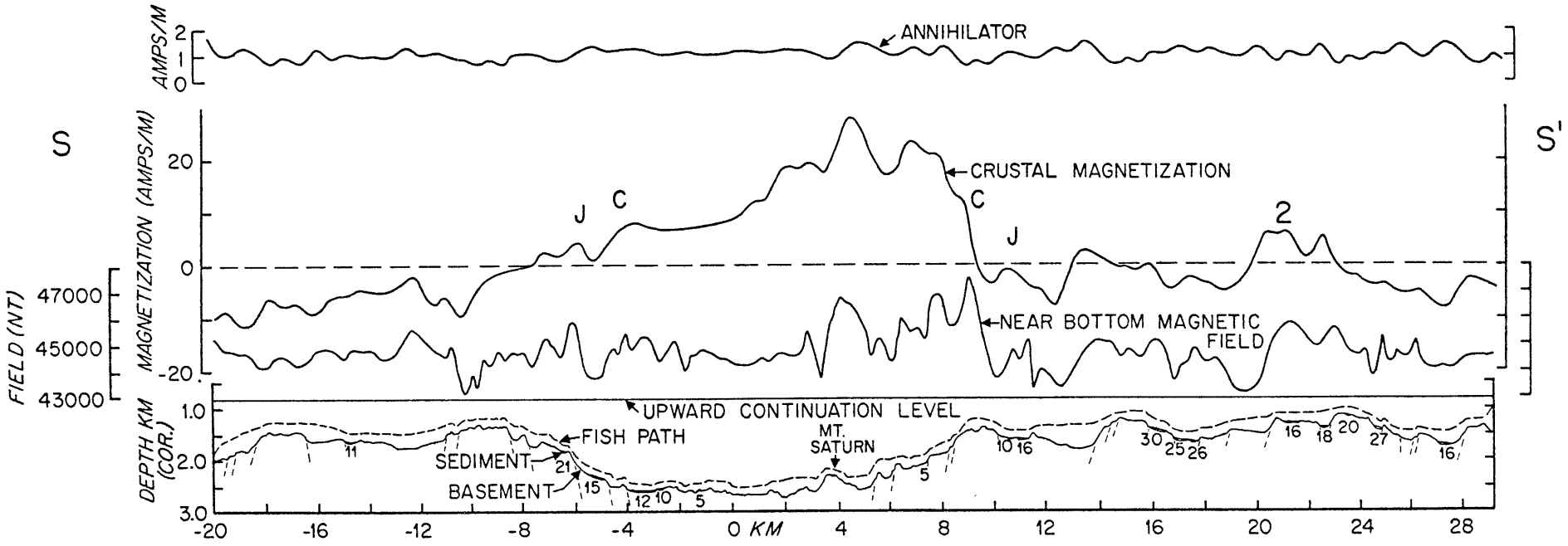
AMPS/M
2
1
0
ANNIHILATOR
S
S'
MAGNETIZATION (AMPS/M)
20
0
-20
J
C
CRUSTAL MAGNETIZATION
C
J
2
NEAR BOTTOM MAGNETIC FIELD
FIELD (NT)
47000
45000
43000
UPWARD CONTINUATION LEVEL
DEPTH KM (COR.)
1.0
2.0
3.0
FISH PATH
SEDIMENT
BASEMENT
MT. SATURN
11
21
15
12
10
5
5
10
16
30
25
26
16
18
20
27
16
-20
-16
-12
-8
-4
0 KM
4
8
12
16
20
24
28

The major objectives were to study the complications in the magnetic anomaly pattern, and to use the high resolution near-bottom magnetic data to investigate crustal accretion processes near the ridge crest and the fine scale tectonic history of the Mid-Atlantic Ridge. Anomalies 1 through 5 have been identified including many minor events. Highly asymmetric spreading occurs in the median valley region. The sense of asymmetry reverses in the rift mountains, resulting in a time-averaged symmetric spreading history. Oblique spreading may be stable for the Mid-Atlantic Ridge at 37°N and perhaps for other slow spreading ridges. A narrow, highly magnetized zone lies along the valley axis marking the present locus of crustal accretion. An abrupt decrease in magnetization amplitude occurs with age within the median valley. Small zones of negatively magnetized crust have been found in the valley floor within the Brunhes normal epoch. Volcanism appears to be highly episodic, and is confined almost entirely to the valley inner floor. The width of transition between normally and reversely magnetized crust is found to be periodic in time and reflects a time-varying rift valley structure. A tectonic model is developed for the Mid-Atlantic Ridge which is consistent with these observations and with the

detailed structure and morphology deduced from deep-tow studies discussed in the preceding paper (Macdonald and Luyendyk, in prep.).

2. NEAR-BOTTOM MAGNETIC DATA

The deep-tow instrument package (fish) is equipped with a proton precession magnetometer and is towed 50 to 200 m above the seafoor (Spiess and Tyce, 1973). The field is sampled approximately every 30 seconds, and interpolated at equal sample intervals of 50 m and 100 m for data analysis. Narrow-beam echo sounders give precise depth of the fish and the sea-floor; 4.0 kHz sonar provides sediment penetration up to 100 m; and side-looking sonar provides detailed information on the shape and linearity of topography within 500 m on either side of the fish. In addition, a surface tow magnetometer sampled the field at 1-minute intervals.

In an area within 12 km of the Famous Rift axis, two to four transponders were used to navigate the fish with a relative accuracy of better than 50 m. Forty satellite fixes were used to locate the transponder in latitude and longitude with an accuracy of about 200 m. Outside the transponder net the fish was located using a cable trajectory computer program (Ivers and Mudie, 1973) in conjunction with satellite navigation

with accuracies of 500 m to 1000 m. In this study latitude is shifted 0.7' west in order to match the base map used in the submersible studies.

3. DATA ANALYSIS: DIRECT MODELING AND INVERSION

In the first stage of analysis, the magnetic field was computed along the fish path for the measured basement topography using a computer program by Atwater and Mudie (1973). The remanent magnetism is assumed to be parallel to a geocentric axial dipole direction, and topography is assumed to be two dimensional. Medium scale relief, the primary sources of topographic anomalies, are linear for several km (Macdonald et al., 1975). Side-looking sonar records show that even small scale step faults and volcanic features are generally at least four times as long as the height of the fish above the bottom (Macdonald and Luyendyk, in prep.). The two-dimensional assumption fails where the fish passes over the extreme end of a lineated topographic feature. In such cases errors on the order of a factor of two in calculated anomaly and magnetization may occur (Miller and Macdonald, in prep.). Side-looking sonar records indicate that this special situation rarely occurs and that the effects are very localized.

A constant 500 m magnetic layer thickness was used in most of the modeling. This is equivalent to assuming that most of the relief is of faulted origin, an assumption verified by Macdonald and Luyendyk (in prep.). Obvious large scale volcanic features were modeled using a flat bottom, assuming a volcano to be riding on top of a faulted layer (Fig. 9). There is little difference between the calculated anomalies for the uniform thickness and flat bottom models, even over large volcanic features since the fish is usually much closer to the layer top than 500 m. The short wavelength magnetic anomalies are essentially unaffected by regional or even local changes in magnetic layer thickness. The short wavelength (200-1000 m) signal is almost entirely of topographic origin, dominated by the top and essentially unaffected by the bottom of the magnetic layer. This property enabled us to use direct modeling along the fish path as a prospecting tool to determine the magnetization of individual volcanic and faulted features.

For detailed studies of the magnetic anomalies and polarity transition zones, the near bottom field data was upward continued assuming two dimensionality to a level datum above the topography (Parker and Klitgord, 1972) and then inverted.

A regional gradient, determined from the International Geomagnetic Reference Field (IAGA, 1969), was subtracted from the data before inversion. A Fourier method for calculating potential anomalies (Parker, 1973) was used iteratively to solve for the source magnetization, given the observed field and topography (Parker and Huestis, 1974). The following assumptions were made: magnetization parallel to a geocentric axial dipole field direction, no vertical variation in magnetization, two-dimensional topography (infinite parallel to the ridge crest), and a constant magnetic layer thickness of 500 m (this assumption is discussed later). An inversion profile over Mt. Venus in the Famous Rift is shown in Figure 2.

Inversion of anomalies, like downward continuation, results in amplification of high and low wave numbers (Parker and Huestis, 1974). High-pass and low-pass filters with cosine tapers were used to suppress this amplification while minimizing the effect of side lobes in the data (Schouten and McCamy, 1972; Parker and Huestis, 1974). The filtering passed unattenuated all wavelengths between 1 km and 50 km with cosine tapers between 0.5-1.0 km and 50-∞ km. The near-bottom data provides a considerable improvement in resolution over surface tow data, which is dominated by noise at wavelengths less than

3 to 4 km (Miller et al., 1974). On the 130 km traverse on the east flank (Fig. 1) long period oscillation made it desirable to use a high-pass filter with a cosine taper between 50 km and 100 km. The wavelength of this noise was greater than the 130 km profile length, and may have been caused by errors in the regional field, or diurnal variation. This phenomenon was also observed by Klitgord (1974) in inverting deep tow magnetic data in the Pacific, and by Schouten and McCamy (1972).

Even with the assumptions mentioned earlier, the crustal magnetization derived from inversion is non-unique. For any given topography, there exists a magnetization distribution, the annihilator, which will produce no external field (Parker and Huestis, 1974). For example, an infinite slab with flat topography has an annihilator which is any constant magnetization. Since the annihilator produces no external field, any multiple of it may be added to the magnetization solution. The annihilator is valuable because it defines the non-uniqueness in such a way that independent geologic and geophysical observations may be introduced to arrive at a relatively unambiguous solution. For example, positive and negative anomaly magnetizations may be set approximately equal (away from the central anomaly) assuming that the intensity of the

earth's magnetic field has not changed drastically for long periods of time. Magnetization along track may be found by direct modeling of topographic features using near-bottom magnetic data and matching the amplitudes of the observed and calculated fields (shown later). Magnetization values for nearby dredge samples, submersible samples, and DSDP cores may be used to fix the solution at certain points. Finally, the amount of annihilator in the solution is constrained by spreading rates and the appearance or disappearance of key anomalies. Adding the wrong amount of annihilator can introduce artificial accelerations and decelerations in seafloor spreading with a correlation of fast or slow spreading with positive or negative polarities. When all these geologic factors are considered, the final magnetization solution (including annihilator) is quite tightly constrained.

4. INVERSION SOLUTIONS AND ANOMALY IDENTIFICATION

The major anomalies out to anomlay 3 can be clearly identified on both flanks of the Famous Rift (Fig. 4). The Brunhes normal epoch and the Jaramillo anomaly are distinct on the west side but merge somewhat on the east side (Fig. 4b). The Jaramillo is clearly recorded on both sides of the south Famous Rift. Rarely is the Jaramillo event recorded clearly

Figure 4A. Inversion solutions for the Famous Rift and rift mountains within 50 km. of the axis projected perpendicular to the valley trend. (1 amp/m= .001 emu/cm^3). Note the sharp magnetization maximum along the inner floor which decreases to the south, negative polarity material along the axis on J"-J', asymmetry of the anomaly locations which reverses sense at anomaly 2, the location of DSDP site 332 on a polarity transition, the slight clockwise rotation of anomalies at 2', and the contrast in anomaly fidelity between I"-I' and J"-J' in the west rift mountains. Inversion solution for the south Famous Rift is shown at the bottom for comparison.

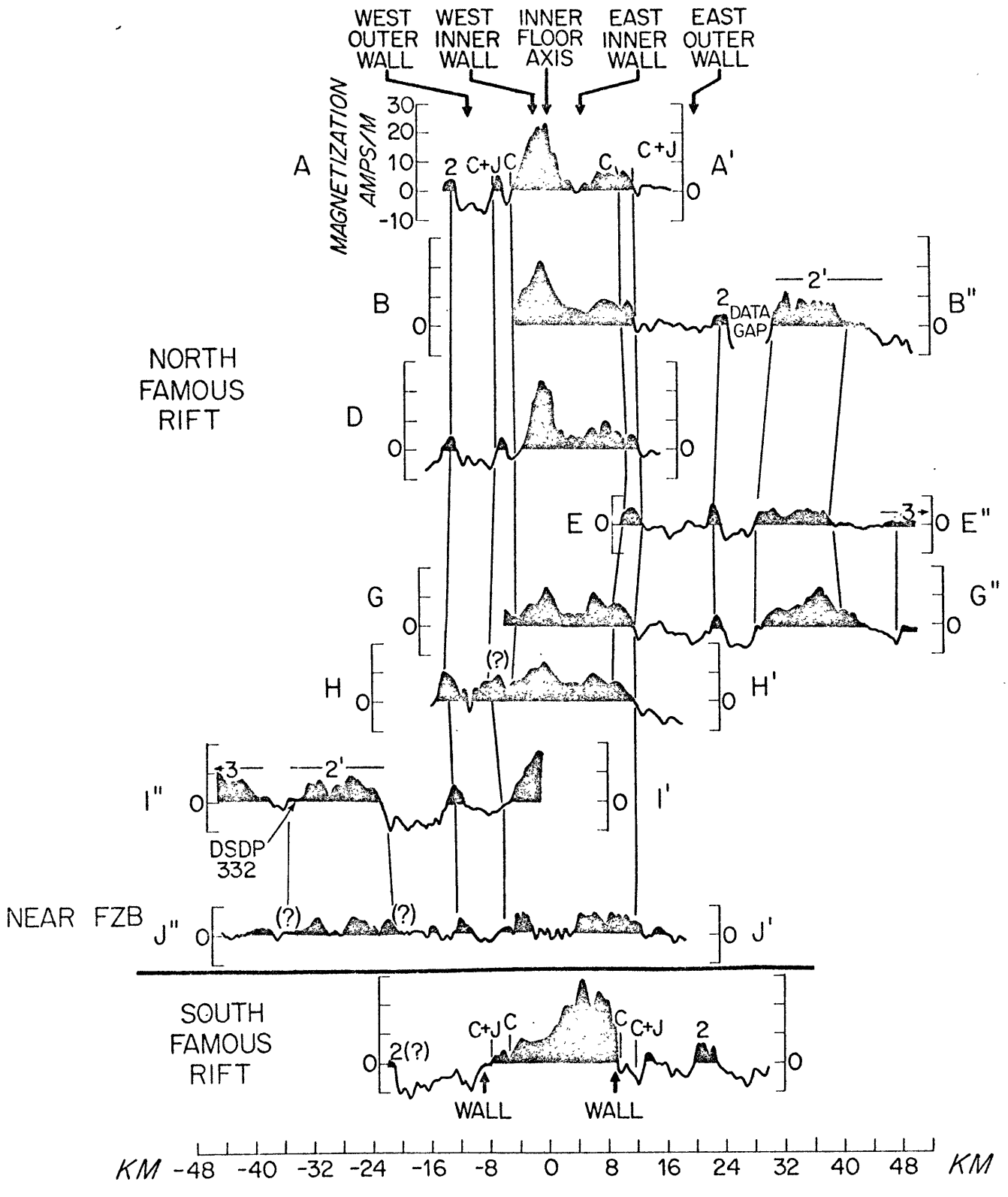
WEST OUTER WALL
WEST INNER WALL
INNER FLOOR AXIS
EAST INNER WALL
EAST OUTER WALL
MAGNETIZATION AMPS/M
30
20
10
0
-10
A
A'
2
C+J
C
C
C+J
B
B"
2'
2
DATA GAP
NORTH FAMOUS RIFT
D
E
E"
3
G
G"
H
H'
(?)
I"
I'
3
2'
DSDP 332
NEAR FZB
J"
J'
(?)
(?)
SOUTH FAMOUS RIFT
2(?)
C+J
C
C
C+J
2
WALL
WALL
KM -48 -40 -32 -24 -16 -8 0 8 16 24 32 40 48 KM

Figure 4B. Topography corresponding to the inversion solutions. Distance from Famous Rift axis in km. Vertical exaggeration is 4X. Numbers are magnetizations in amps/meter as determined by direct modelling (see text and Figures 9, 10). Direct modelling yields the magnetization for particular topographic features while inversion yields the average magnetization through a 500m thick layer. Circled numbers are magnetizations opposite in sign to the inversion solutions indicating volcanism away from the ridge axis and, in places, wide polarity transition zones (see text).

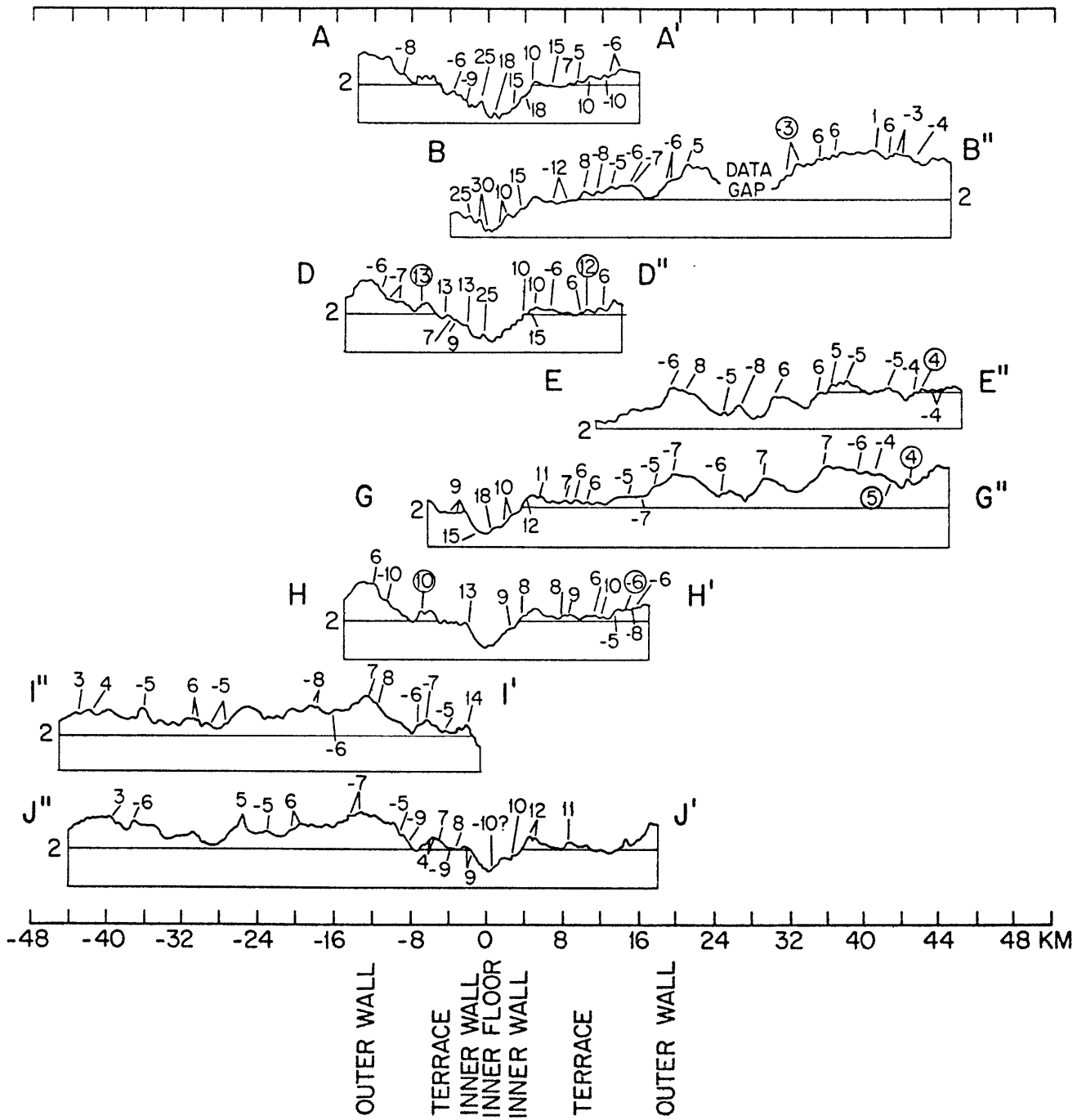
A
A'
B
B"
DATA GAP
D
D"
E
E"
G
G"
H
H'
I"
I'
J"
J'
2
-48 -40 -32 -24 -16 -8 0 8 16 24 32 40 44 48 KM
OUTER WALL
TERRACE
INNER WALL
INNER FLOOR
INNER WALL
TERRACE
OUTER WALL

Figure 5. Long geophysical profile into the east rift mountains. Inversion solution and anomaly identification is as shown. Numbers denote magnetization of the topography in amps/m determined from direct modelling for comparison with inversion solution. An opposite polarity feature at about 100 km. (circled number) indicates volcanism away from the axis.

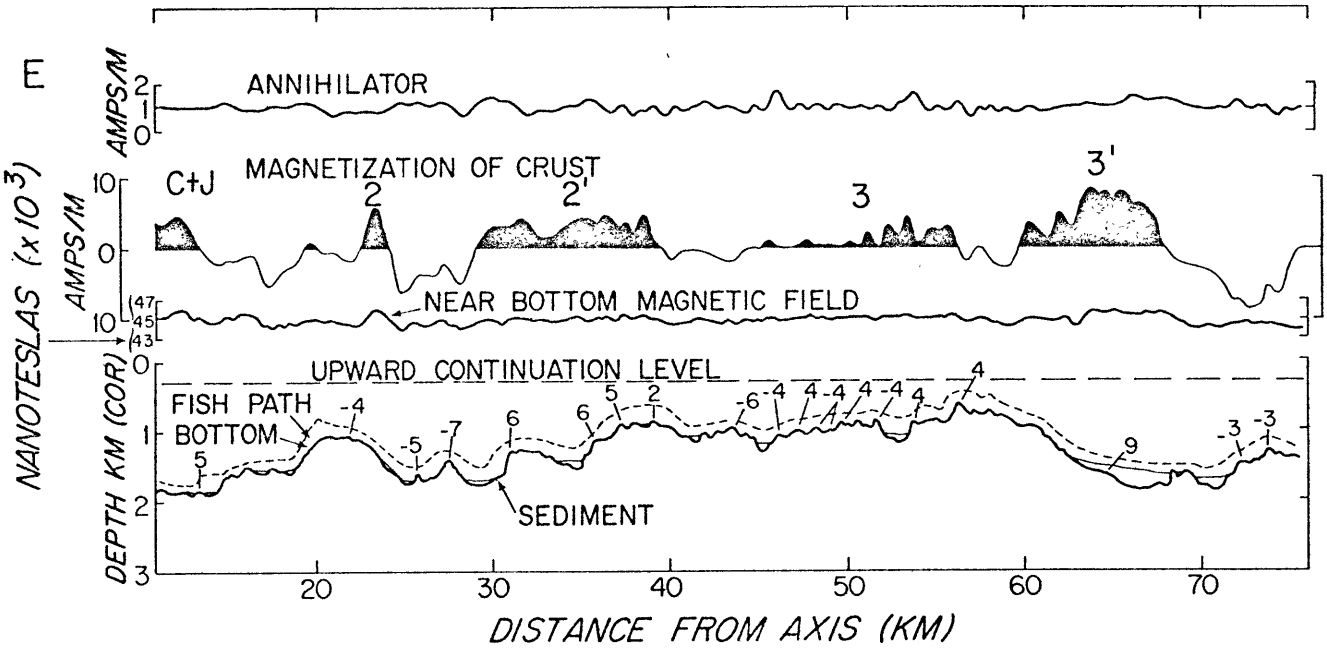
E
ANNIHILATOR
AMPS/M
2
1
0
C+J
MAGNETIZATION OF CRUST
2
2'
3
3'
10
0
10
AMPS/M
47
45
43
NEAR BOTTOM MAGNETIC FIELD
NANOTESLAS (x 10 3)
UPWARD CONTINUATION LEVEL
FISH PATH
BOTTOM
SEDIMENT
DEPTH KM (COR)
0
1
2
3
20
30
40
50
60
70
DISTANCE FROM AXIS (KM)

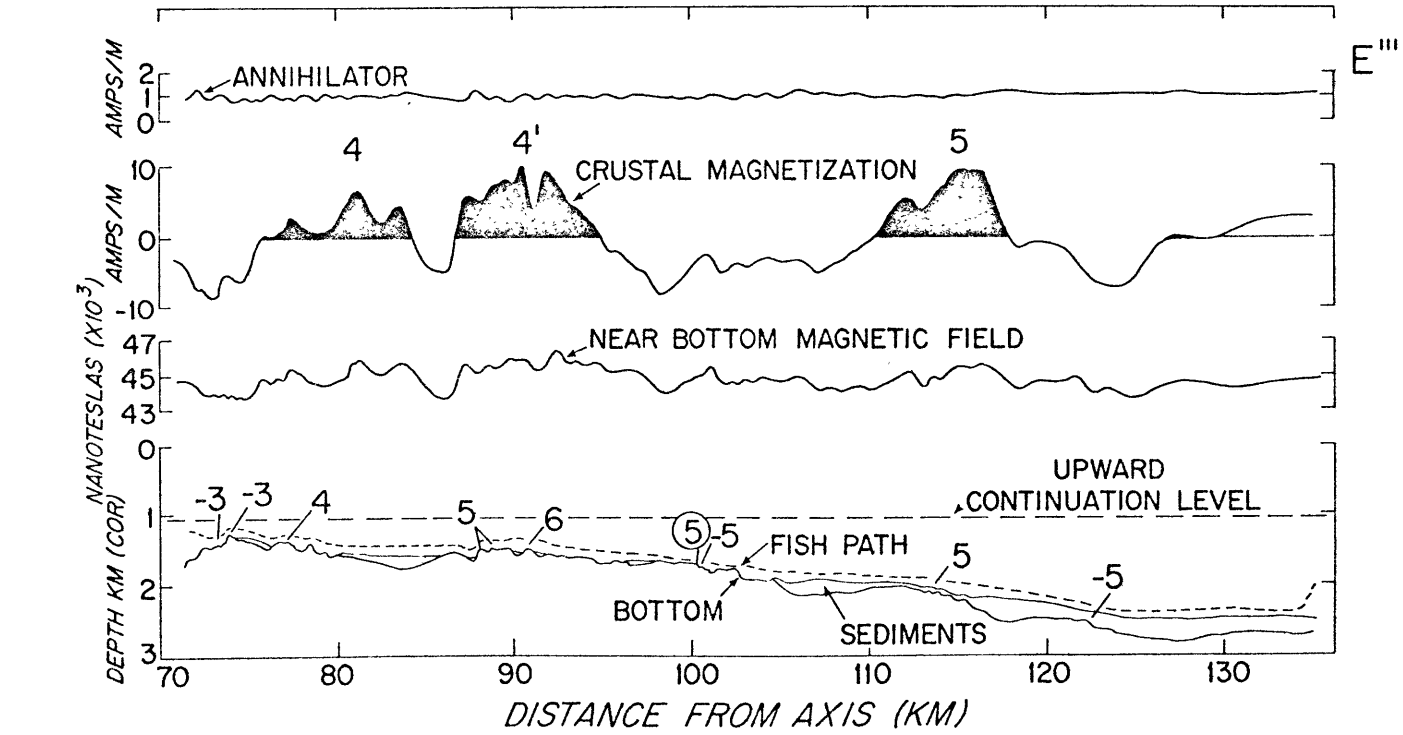
E'''
ANNIHILATOR
AMPS/M
2
1
0
4
4'
5
CRUSTAL MAGNETIZATION
10
0
-10
AMPS/M
NANOTESLAS (X10 3)
NEAR BOTTOM MAGNETIC FIELD
47
45
43
UPWARD
CONTINUATION LEVEL
FISH PATH
BOTTOM
SEDIMENTS
DEPTH KM (COR)
0
1
2
3
70
80
90
100
110
120
130
DISTANCE FROM AXIS (KM)

on slow spreading ridges, because of a finite crustal emplacement width and the short duration of the event (discussed later). Anomaly 2 occurs at the top of the outer walls on both sides of the rift, showing that the outer walls are isochrons despite their asymmetric location relative to the axis. Anomaly 2' is clearly recorded including the Kaena and Mammoth events on the west flank (Fig. 4a, I"-I'). On the long traverse into the east rift mountains, anomalies out to 5' are identifiable (Fig. 5). Anomaly 3 is severely attenuated and minor events are not resolvable in 3 or 3'. Anomalies 4 and 4' however are distinctly recorded including shorter events (see bottom of Fig. 6 for polarity time scale).

There are some fascinating aspects of the inversion solutions (Figs. 4, 5) which will be discussed: 1) the location of anomaly boundaries is highly asymmetric with respect to the axis, skewed toward the east out to anomaly 2 where the sense of asymmetry reverses. 2) A sharp magnetization maximum occurs along the axis of the Famous Rift, and along the east side of the south Famous Rift. 3) On profile J"-J' (Fig. 4) negatively polarized material occurs within the Brunhes normal near the axis of the inner floor. 4) There is a variation in the fidelity of anomaly recording in the crust

and in the widths of positive to negative polarity transitions. 5) DSDP site 332 may have been drilled in a transition zone between the Gauss and Gilbert epochs rather than in negative polarity crust as supposed (JOIDES, 1975). 6) The disturbing influence of FZB on the magnetic anomalies may extend as far as 15 km north of the presently active transform fault. 7) There is a slight clockwise rotation of the anomalies at anomaly 2' (profile B-B").

5. ASYMMETRIC SPREADING

The Mid-Atlantic Ridge in the Famous area has the highest degree of asymmetric spreading reported with rates of 7.0 mm/yr to the west and 13.4 mm/yr to the east, nearly a factor of two difference (Fig. 6). At anomaly 2 (1.7 m.y.b.p.) the sense of asymmetry reverses with half-rates changing to 13.3 mm/yr to the west and 10.8 mm/yr to the east. The total spreading rate changes only slightly from 20.3 mm/yr to 24.2 mm/yr. The beginning and end of anomaly 2 fall distinctly on different velocity lines, suggesting that the entire change in spreading velocity and asymmetry occurred in less than 0.15 m.y. This suggests that major plates can respond almost instantaneously (geologically) to a change in stress pattern.

Figure 6. Magnetic anomaly picks establishing asymmetric spreading rates and rate changes in the Famous area. (A composite of all near-bottom magnetic data, not just a single profile.) The time scale used is that of Talwani et.al. (1971) through anomaly 5, and Heirtzler et.al. (1968) older than anomaly 5. Note the change in the sense of asymmetric spreading at anomaly 2. Also note that the change in spreading rate occurs entirely within anomaly 2, i.e., in less than 0.15 my. Within the 95% confidence interval the velocity determinations all have uncertainties of less than 0.6 mm/yr.

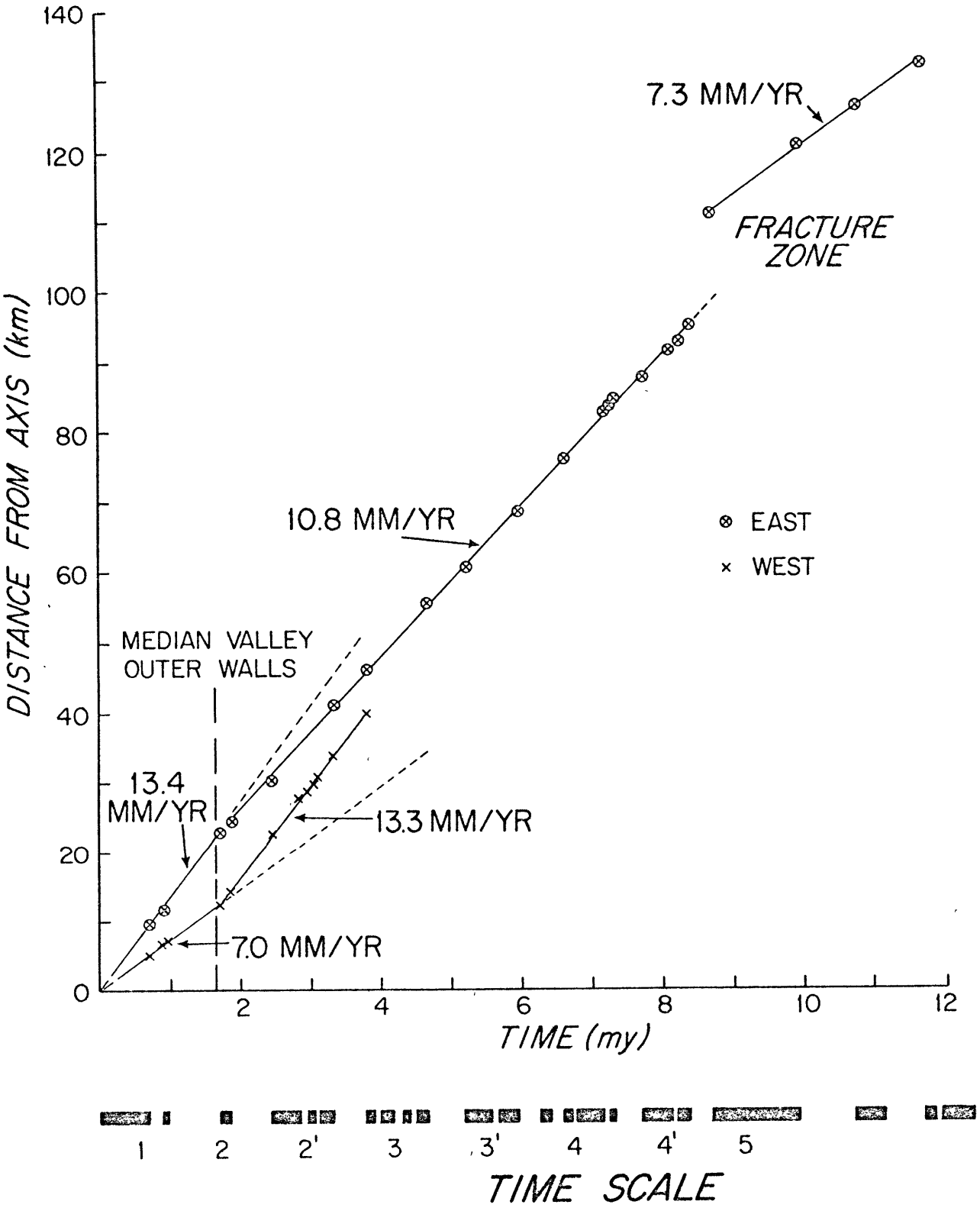
140
120
100
80
60
40
20
0
DISTANCE FROM AXIS (km)
7.3 MM/YR
FRACTURE ZONE
10.8 MM/YR
EAST
WEST
MEDIAN VALLEY
OUTER WALLS
13.4
MM/YR
13.3 MM/YR
7.0 MM/YR
2
4
6
8
10
12
TIME (my)
1
2
2'
3
3'
4
4'
5
TIME SCALE

Detailed analysis of surface magnetic data between 35° and 39° on the Mid-Atlantic ridge suggests that the spreading rate has been symmetrical at 10 mm/yr for the last 10 m.y. (Phillips et al., 1975). However, deep-tow data suggests that the grossly symmetrical spreading pattern is composed of highly asymmetric spreading episodes which reverse in sense, resulting in symmetry when integrated over long periods of time. Asymmetric spreading for crust 0-5 m.y. old in the Atlantic has also been reported at 45°N (Loncarevic and Parker, 1971), 37°N (Needham and Francheteau, 1974; Greenewalt and Taylor, 1974), 26°N (MacGregor et al., submitted) and at 6°-8°S (van Andel and Heath, 1970). In these cases, however, the degree of asymmetry measured was somewhat less and a reverse in asymmetry was not detected.

The extreme asymmetry in spreading rate is reflected in nearly every aspect of median valley structure (Macdonald and Luyendyk, in prep.). The outer walls are asymmetrical about the valley axis resulting in a median valley half-width of 11 ±1 km on the west side and 20 ±1 on the east (Fig. 4). The east and west inner walls are asymmetric in location and in structure. The west inner wall is a single major step composed of a series of steeply faulted slivers, while the

east inner wall consists of several wide steps less steeply faulted and with a more gradual average slope (Fig. 4b). Furthermore, the horizontal crustal extension in the inner floor and walls is approximately twice as great to the east as to the west, suggesting that asymmetric spreading entails asymmetric crustal extension as well as asymmetric crustal accretion (Macdonald and Luyendyk, in prep.). Within the inner floor the lineation of central highs and lows is slightly offset to the west, and the density of faulting is nearly twice as great on the east side of the floor (Luyendyk and Macdonald, in prep.). Chemical analyses of basalts collected from the ALVIN indicate an asymmetry in the concentration of SiO_2, K_2O, FeO and TiO_2 about the inner floor axis (Bryan and Moore, in prep.). In addition, the sediments thicken less rapidly with distance to the east (Macdonald and Luyendyk, in prep.). The asymmetry of the outer walls, inner walls, sediment thickness, distribution of small faults within the inner floor, and extension rates represent a time frame of tens of thousands of years to millions of years. This suggests that the process of asymmetric spreading is continuous on a very fine scale in time and in space. It is not accomplished by discrete ridge jumps of more than a few hundred meters as is often assumed.

Between anomalies 4' and 5 there is an 11 km discontinuity in the anomaly pattern (Figs. 5b, 6). Either this gap represents a short episode of spreading at 53.3 mm/yr between spreading rates of 10.8 mm/yr and 7.3 mm/yr or a short (11 km) fracture zone offset was crossed. Crossing of a fracture zone is more likely because of the extreme spreading acceleration required otherwise. The down-faulted bathymetry and increase in sediment thickness also suggests a fracture zone crossing (Fig. 5b). The spreading rate of 7.3 mm/yr on the older side of the fracture zone is much slower than the average half-rate of 11 mm/yr and may reflect a highly asymmetric spreading situation similar to the present.

Spreading is also asymmetric on the south Famous Rift with rates of 8.8 mm/yr to the west and 11.8 mm/yr to the east (assuming the center of the floor is the average center of spreading). The total opening rate is the same as that for the Famous Rift (20.6 mm/yr) as required by plate tectonics. (The two rifts are far from the pole of opening and adjacent to each other). The difference in asymmetric rates for the north and south Famous rifts results in the growth of the FZB transform fault by 3.6 mm/yr.

6. OBLIQUE SPREADING

The rift valleys in and near the Famous area are not orthogonal to nearby transform faults (Fig. 1). Fine scale topography as well as microearthquakes form east-west lineations in FZA and FZB (Reid and Macdonald, 1973; Detrick et al., 1973). More than 700 fine scale tectonic lineations (faults and fissures) mapped in the rift inner floor have a pronounced N 17°E strike (Luyendyk and Macdonald, in prep.). There are a few north-south lineations in the inner floor, but they form part of a nearly symmetrical Gaussian distribution of lineation strikes which has a median of N 17°E and a standard deviation of only 6°. Since the lineation pattern is normally distributed about N 17°E, it is misleading to interpret observation of a few north-south lineations as evidence for readjustment to orthogonal spreading as some workers have done (Phillips and Fleming, 1975). The magnetic maximum along the inner floor axis is caused by crust less than 0.2 m.y. old (discussed in the next section), and it also has a N 17°E trend (Figs. 3, 8). This is independent evidence that even the youngest crust in the inner floor is created in a direction oblique to the nearest transform faults.

How long has the spreading been oblique? Deep-tow and surface magnetic data indicate that magnetic anomalies back to 2' trend about N 17°E. Between anomalies 2' and 3' (2.5-5.2 m.y.b.p.) the magnetic lineations rotate to N 35°E (Fig. 7). (Bird and Phillips (in press) report a N 35°E trend for the anomalies for 0-9 m.y.b.p., however, it appears that the time interval they used in stacking the anomalies was too large to determine the correct trend for anomalies less than 3 m.y. old). The magnetic anomalies are offset right-laterally back to anomaly 3. Between anomalies 3 and 3' the magnetic lineations are continuous, suggesting an age of 3.7-5.2 m.y. for fracture zones A and B (Fig. 7). This age is consistent with the growth rate for the FZA transform fault determined earlier. Thus, the fracture zones and magnetic anomaly trends indicate that spreading has remained oblique at about 17° in its present configuration for about 3 to 5 m.y.

To investigate oblique spreading prior to the existence of FZA and FZB we must study fracture zone trends to determine the history of spreading directions relative to magnetic anomaly trends. The nearest major fracture zone, the Oceanographer trends N 75°W (Fox et al., 1969). However, epicenters associated with the Oceanographer F.Z. trend east-west (Barazangi

Figure 7. Summary of large scale magnetic lineations in the Famous area. Shaded areas show positively magnetized crust determined by inversion of deep-tow data; anomaly numbers are as shown. Dashed lines indicate the axes of anomalies outside the deep-tow study area determined from surface magnetic data (Phillips and Fleming, 1975). Note the clockwise rotation of anomalies between 2' and 3', and the change near anomalies 3 and 3' from offset to continuous anomaly trends across FZA and FZB. Lines with tick marks denote the outer walls of the Famous Rift.

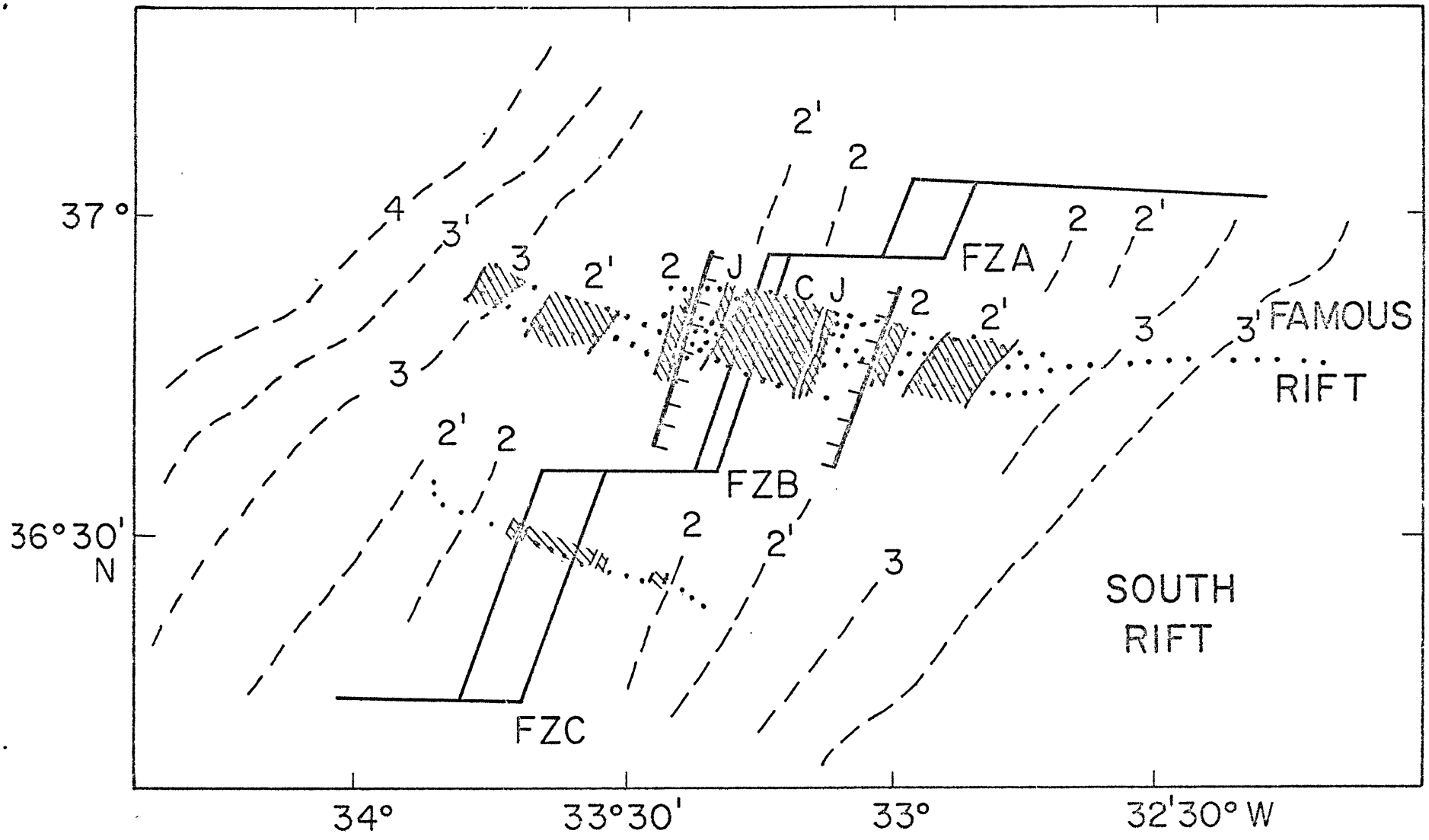
37°
36°30'
N
34°
33°30'
33°
32'30° W
FZA
FZB
FZC
FAMOUS
RIFT
SOUTH
RIFT
J
C J
4
3'
3
2'
2
3
2'
2
2'
2
2'
3
3'
2'
2
2
2'
3

and Dorman, 1969), and Sykes (1967) determined a tightly constrained focal mechanism solution showing N86E trending strike slip. Thus the present transform fault azimuth for the Oceanographer F.Z. agrees with that for FZA and FZB, while the overall N75W trend of the fracture zone reflects a previous spreading direction. FZA and FZB were probably created at the time of this change which dates the change in spreading direction at 3.7 to 5.2 m.y.b.p.

Thus both the fracture zones and the magnetic anomalies seemed to have changed direction at about the same time. The magnetic trends change to N35E between anomalies 2' and 3' (2.5-5.2 m.y.b.p.), while the fracture zones changed from east-west to N75W in trend between 3.7 and 5.2 m.y.b.p. Thus the plate boundary configuration was 20° oblique, prior to the change in spreading direction and the existence of FZA and FZB. The implications are surprising: 1) spreading in the Famous area is stably oblique at present; 2) the spreading pattern has had a stable obliqueness of 17° in the present configuration for 3-5 m.y., 3) spreading was oblique in this area before 3-5 m.y.b.p. even through a change in

spreading direction, 4) the amount of obliqueness has remained essentially constant at 17° to 20°.

Several recent theories on ridge crest tectonics are based on the observation and/or assumption that spreading centers and adjoining transform faults form orthogonal systems (Lachenbruch and Thompson, 1973; Lachenbruch, 1973; Oldenburg and Brune, 1975). While this observation is well documented for fast spreading centers, it is not for slow spreading centers. The mid-Atlantic ridge, a classic slow spreading center, has been studied in detail at 6°-8°S (van Andel and Heath, 1970), 22°-23°N (van Andel and Bowin, 1968), 26°N (McGregor and Rona, 1975), 37°N (FAMOUS), 43°N (Phillips et al., 1969), 45°N (e.g. Aumento, et al., 1971) and from 60°-62°N (Talwani et al., 1971). Only on the Reykjanes ridge and in the Famous area is there detailed information on the adjoining transform faults. In both cases the spreading is oblique. Recently it has been found that the Reykjanes ridge is breaking obliquely at 18° (Atwater, pers. comm.). On other slow spreading centers, only the Juan de Fuca ridge (Chase et al., 1970) and the Gulf of Aden (Laughton et al., 1970) have been studied in detail including the transform faults and they are both oblique. It may be said that the mid-Atlantic ridge at 60°-62°N,

and 37°N, and the Gulf of Aden and Juan de Fuca ridge are all anomalous. They are all near proposed hotspots. However, it may be more than coincidence that oblique spreading prevails for every slow spreading center where the angle with the adjoining transform faults is well known. The angle of obliqueness is generally 15°-20°. A symmetric stress distribution is essential to both Lachenbruch's (1973) and Oldenburg and Brune's (1975) theories. It may be that proximity of hotspots creates a non-symmetric stress distribution which disrupts orthogonality. It may also be that oblique spreading of 15°-20° is stable for slow spreading centers.

7. Magnetization of Crust in the Rift Inner Floor

A sharp, narrow maximum in crustal magnetization occurs near the axis of the inner floor (figs. 4, 8). The maximum exceeds 20 amps/m (1 amp/m = 0.001 emu/cm^3). It is highest in the north end of the inner floor coinciding with large volcanic features such as Mt. Mercury, Mt. Pluto and Mt. Venus. A contour map of magnetization (fig. 8) is derived from magnetic data filtered with a cosine taper between

Figure 8. Magnetization in the Famous Rift inner floor contoured from the inversion solutions (5 amp/m contour interval). Volcanic highs noted by outward hatchurs, central depressions by inward hatchurs. Note the magnetization maximum centered along the inner floor axis and the decrease in magnetization toward the south. The maximum is greatest over the central highs, but is still present over the central lows.

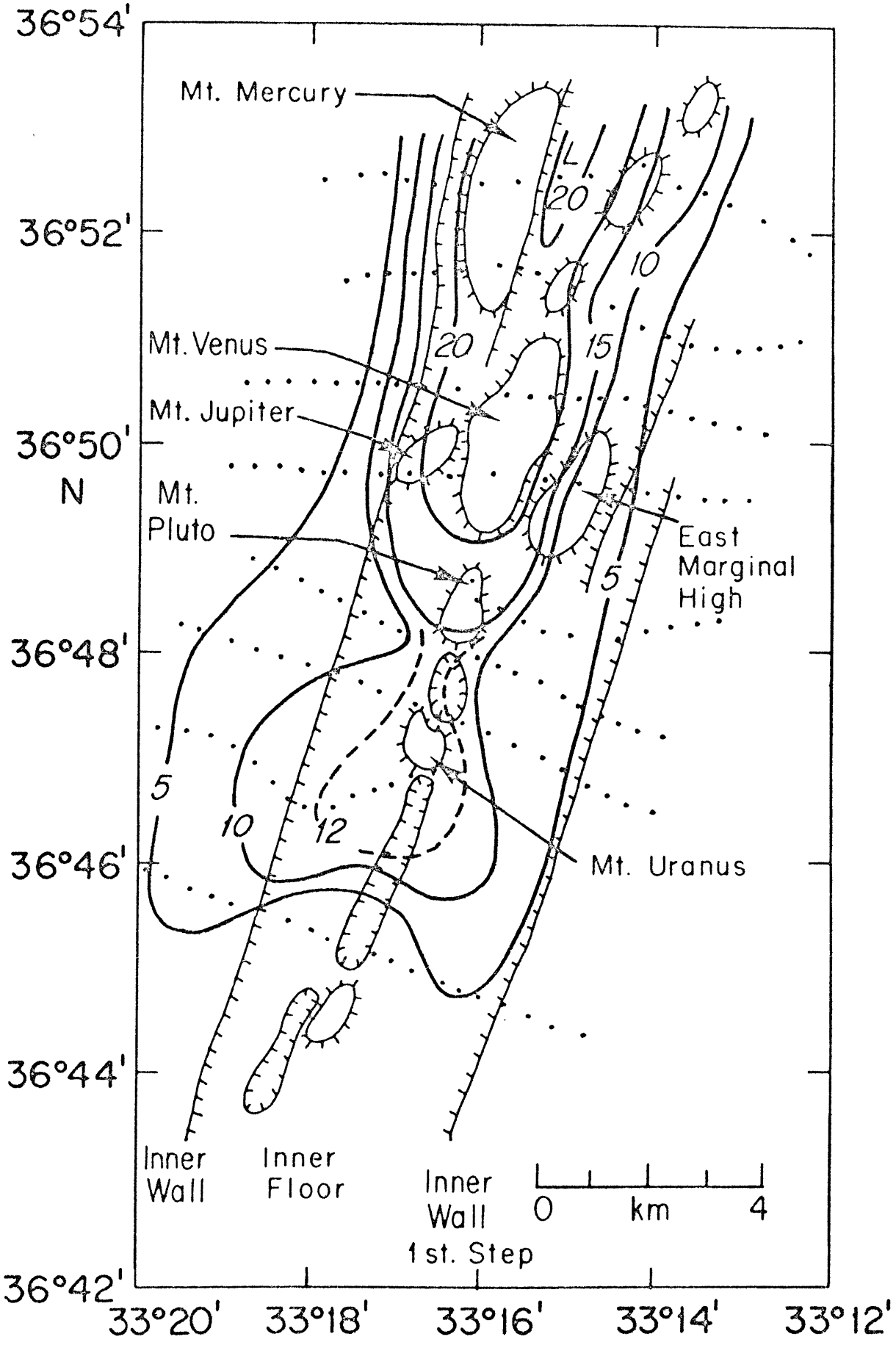
36°54'
36°52'
36°50'
N
36°48'
36°46'
36°44'
36°42'
33°20'
33°18'
33°16'
33°14'
33°12'
Mt. Mercury
Mt. Venus
Mt. Jupiter
Mt. Pluto
East Marginal High
Mt. Uranus
Inner Wall
Inner Floor
Inner Wall 1st. Step
0 km 4
5
10
12
15
20

500-1000 m, so the results are somewhat smoothed. Direct modeling for topographic features indicates that some of the volcanoes have magnetizations of 25-30 a/m (figs. 9, 10, 11). Correlation of the magnetization maximum with topography suggests that large volcanoes near the inner floor axis are the present site of crustal accretion and extrusion. The maximum is only 2-3 km wide and falls off rapidly. Samples gathered from submersibles support the inversion results, indicating that Mt. Venus and Mt. Pluto are capped by fresh pillow basalts only 10^2 to 10^4 years old (Belliache et al., 1975; Bryan and Moore, in prep.), young enough so that the magnetic minerals have suffered little alteration (Johnson et al., 1975). The maximum in magnetization continues as far south as 36°46'N (fig. 8). It continues but decreases in amplitude with the disappearance of large central highs and the dominance of central depressions along the inner floor axis. The fact that the maximum continues suggests that the lavas in the central lows are also young, while the decrease in amplitude suggests that the volume of freshly extruded pillows is smaller.

The width of the active volcanic zone inferred from crustal magnetization is very narrow, less than 2-3 km.

Magnetic measurements of rocks collected by submersible agree closely with the inversion solutions with an average magnetization of 23 $\pm$ 10 amps/m (Johnson et al., 1975). However, submersible samples and deep-tow direct modelling (discussed later) do not show the decrease in magnetization within the inner floor shown by inversion. Perhaps this is because near-bottom modelling and rock samples measure only the magnetization of the top of the crust. In addition side-looking sonar data suggests that volcanism occurs throughout the inner floor, even though the major locus of volcanism is within hundreds of meters of the floor axis (Macdonald and Luyendyk, in prep.). Thus, most of the inner floor is likely to have a veneer of fresh highly magnetized basalts, while the average magnetization integrated over a 500 m thick layer shows a maximum along the axial accretion zone because of the greater volume of fresh volcanics.

In the south Famous Rift the magnetization maximum is centered over Mt. Saturn, 4 km east of the axis of the floor (figs. 3, 4a). Correlation with Laughton and Rusby's sonographs (1975) indicates that Mt. Saturn is 3.5 km long, 1.5 km wide, and 300 m high, nearly the same dimensions as Mt. Venus. Apparently the most recent zone

of volcanism is centered near Mt. Saturn very close to the east wall. Sediment and side-looking sonar data also suggest a recent volcanic zone near the east wall (Macdonald and Luyendyk, in prep.).

8. Decay of Crustal Magnetization

Since the short wavelength component of the near-bottom magnetic anomaly is almost totally topographic in origin (Atwater and Mudie, 1973), one can measure the magnetization of topographic features by modelling this anomaly and matching the measured and computed field amplitudes (figs. 9, 10). The layer thickness was usually assumed to be 500 m, however, the amplitude of the computed anomaly is almost unaffected by the assumed thickness or variations in thickness of the layer (as long as the thickness is greater than 300 m) (e.g., fig. 10). Topography was assumed to be linear, and most of the volcanic and faulted features are quite linear, but for those that are not, the amplitude matching method will produce a minimum estimate of magnetization.

Magnetization of topographic features indicates that the intensity falls off to 1/e its initial value in less than 0.6 m.y. (fig. 11). A rapid decay rate is supported

Figure 9. Direct modelling of topographic anomalies along the fish path. The magnetic layer is assumed to be 500 m. thick and assigned a uniform magnetization as shown. Calculated and observed field amplitudes are matched by adjusting the magnetization intensity, while holding thickness and magnetization direction constant. Age of the crust is also shown.

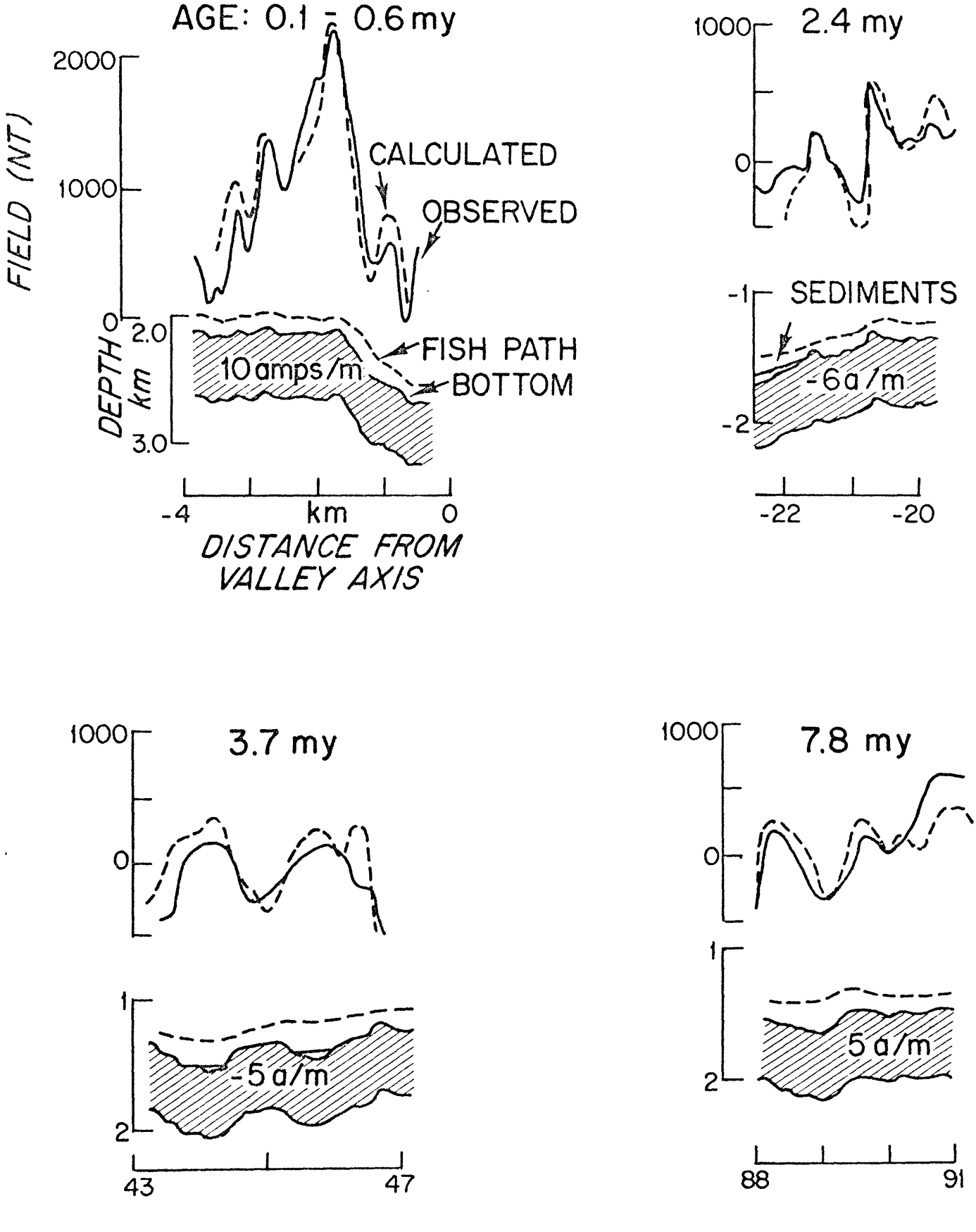
AGE: 0.1 - 0.6 my
FIELD (NT)
2000
1000
0
CALCULATED
OBSERVED
DEPTH km
2.0
3.0
10 amps/m
FISH PATH
BOTTOM
-4
km
0
DISTANCE FROM VALLEY AXIS
1000
2.4 my
0
-1
SEDIMENTS
-6 a/m
-2
-22
-20
1000
3.7 my
0
1
-5 a/m
2
43
47
1000
7.8 my
0
1
5 a/m
2
88
91

Figure 10. Direct modelling over the Mt. Mercury area. The field was calculated for both a constant 500 m. thickness and a flat bottom (variable thickness) model. The dotted line shows the flat bottom model results. Even for a large volcanic feature like Mt. Mercury, there is little difference between a constant thickness (purely faulted) and a flat bottom (volcanic) model.

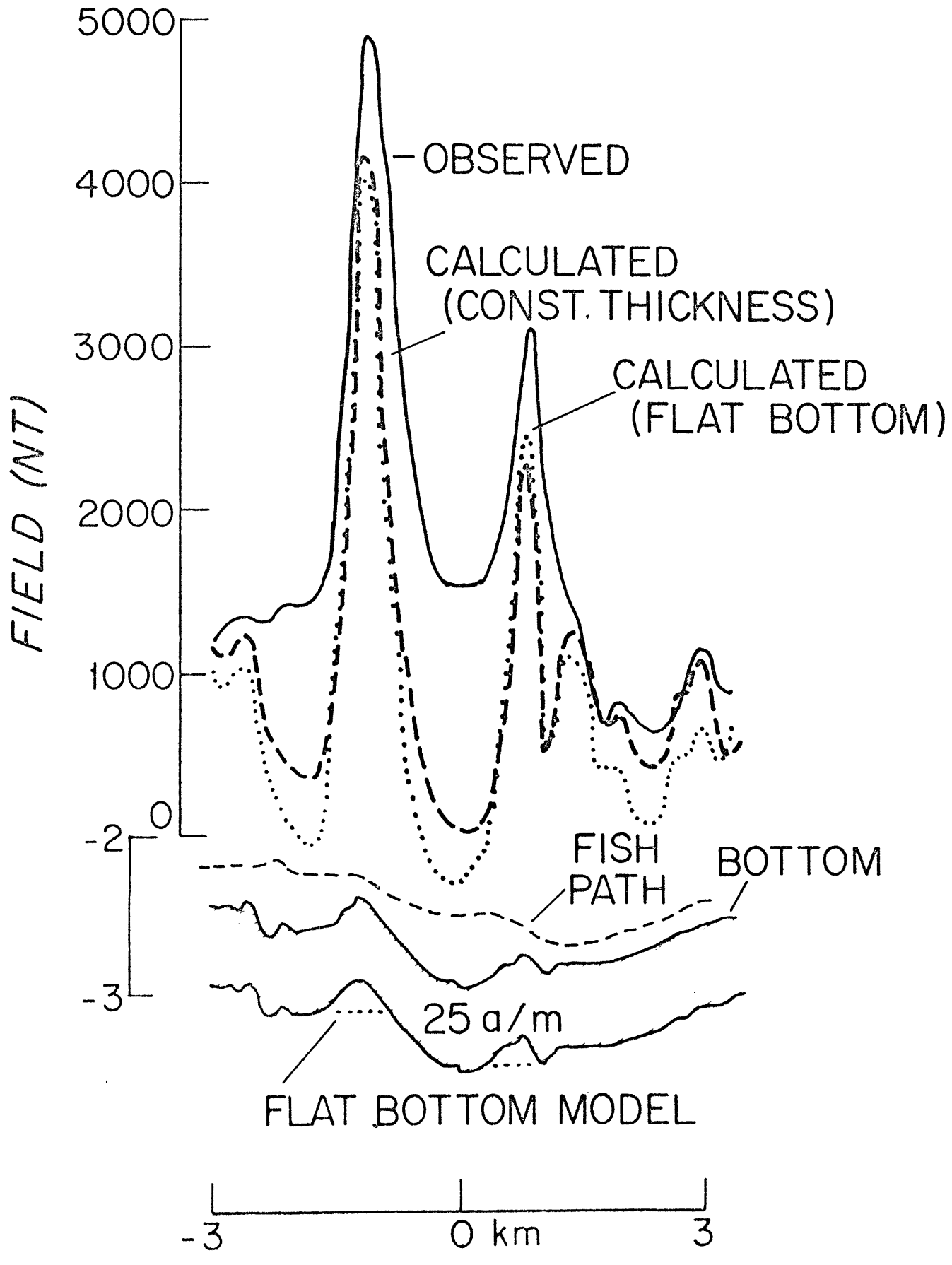
5000
4000
3000
2000
1000
0
-2
-3
FIELD (NT)
OBSERVED
CALCULATED
(CONST. THICKNESS)
CALCULATED
(FLAT BOTTOM)
FISH
PATH
BOTTOM
25 a/m
FLAT BOTTOM MODEL
-3
0 km
3

Figure 11. Magnetization of topography as a function of age derived from direct modelling. There is no obvious difference between volcanic and faulted topography except in the youngest crust where large scale faulted relief has not yet developed. Triangles are 0.2 m.y. averages out to 1 m.y.b.p., 0.5 m.y. averages out to 3.5 m.y.b.p., and 2 m.y. averages out to 10 m.y.b.p. Error bars are 4 standard errors in length.

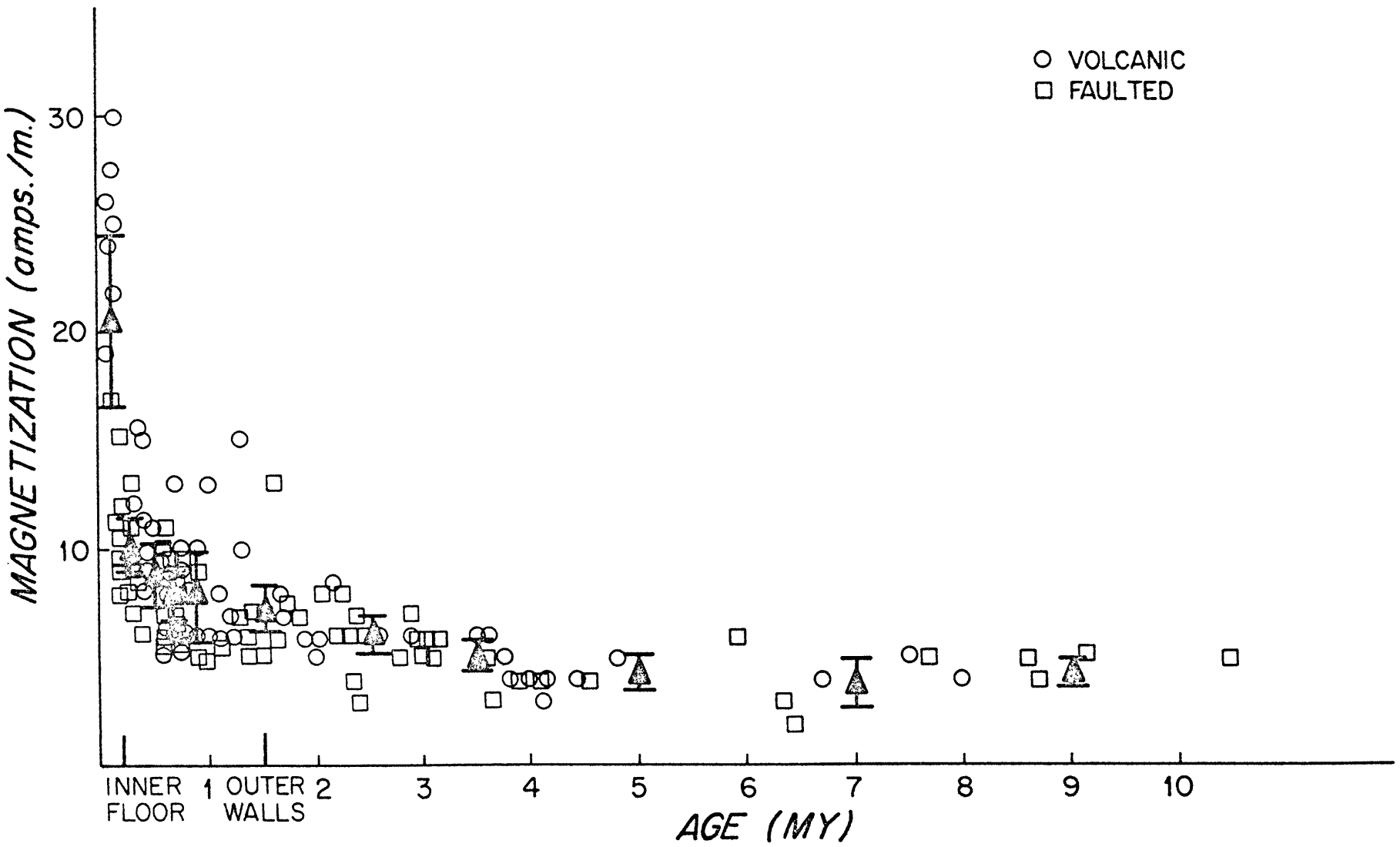
VOLCANIC
FAULTED
MAGNETIZATION (amps./m.)
30
20
10
INNER FLOOR
1
OUTER WALLS
2
3
4
5
6
7
8
9
10
AGE (MY)

by the inversion studies. On the west side of the magnetic maximum in the south Famous Rift, the intensity decreases to 1/e its maximum value in 4.8 km or 0.5 m.y. (fig. 3). In the Famous Rift, and on the east side of the south Famous Rift the decay rate appears to be even more rapid, but this may be caused in part by the proximity of Brunhes/Matuyama boundary. Since the zone of crustal accretion has a finite width (discussed later), 0.5-0.6 m.y. is an upper limit for the decay time of crustal magnetization to 1/e its initial value. This rate of decay is more rapid than that derived by experimental work on individual basalt pillows. Marshall and Cox (1972) suggest that 0.7 m.y. is required for the titanomaghemite alteration front to advance only 1 cm into a given pillow.

In the terraces and rift mountains the decay rate becomes much slower, the average intensity decreasing from 7-8 a/m to 4 a/m between 0.6 m.y. and 5 m.y. The magnetization seems to reach equilibrium after 5 m.y. at a value of 4 a/m (fig. 11). The values obtained for magnetization from the near bottom anomalies are in close agreement with dredge and submersible samples. Johnson et al. (1975) report a value of 23 $\pm$ 10 a/m for the rift inner floor and average values of 4.5 to 5.5 a/m are found for a

large collection of dredge samples over older crust (Irving, 1970; Lowrie, 1974). JOIDES (1975) reports averages of 2-4 amps/m for 4 sites in crust 3.5 to 16 m.y. old.

Macdonald and Luyendyk (in prep.) and Luyendyk and Macdonald (in prep.) report extremely intense fracturing of young oceanic crust. Intense faulting occurs less than 1 km from the valley axis and exceeds densities of 25 faults per km^2 in crust less than 0.2 m.y. old. Tensional cracks 1 to 25 m wide are also common and closely resemble the gjas of Iceland (Walker, 1964; Luyendyk and Macdonald, in prep; Ballard and van Andel, in prep.). Such intense fracturing exposes the magnetic layer to seawater, provides channels for circulation, and thus provides a rapid mechanism for the oxidation of titanomagnetite to titanomaghemite. This fracturing mechanism may facilliatate the rapid decay of magnetization in the first 0.6 m.y. by both exposing the crust to seawater and chemical alteration, and by mechanically disrupting and reorienting pieces of crust. Subsequent decay occurs at a much slower rate because few new cracks are opened in older crust beyond the inner walls.

9. Thickness of the Magnetized Layer

Given the magnetization of the crust, the long wavelength magnetic anomaly measured at the sea surface can be used to determine the thickness of the source layer (Atwater and Mudie, 1973). The most problematical assumption is that the magnetization be constant with depth in the crust, set equal to the magnetization determined from short wavelength magnetic anomalies. Given this limitation, the magnetic anomaly was computed for various crustal magnetizations, adjusting the layer thickness so that the amplitude of the calculated and observed (sea level) magnetic anomalies matched (fig. 12). A layer thickness of about 700 m matches the deep-tow and dredge magnetizations best. Using similar techniques, Atwater and Mudie (1973) and Talwani et al. (1971) deduced layer thicknesses of 500 m and 400 m respectively. The 700 m estimate presented here may still be a minimum estimate if the magnetization is found to decrease with depth in the crust, particularly if deep-seated instrusive sources are magnetically important (Cox et al., 1972).

A 500 m layer thickness assumption was used in most of the inversion calculations. If a layer thickness of 700 m had been used the magnetizations would all be approximately

Figure 12. Crustal magnetization from deep-tow (solid line, triangles with 4 standard error bars from Figure 11) and from dredge samples at 45°N (dashed line, Irving, 1970). Plain solid lines indicate the magnetization required for a magnetic layer of uniform thickness in order to match the amplitude of the surface tow magnetic anomalies. A 0.7 km. thickness fits best.

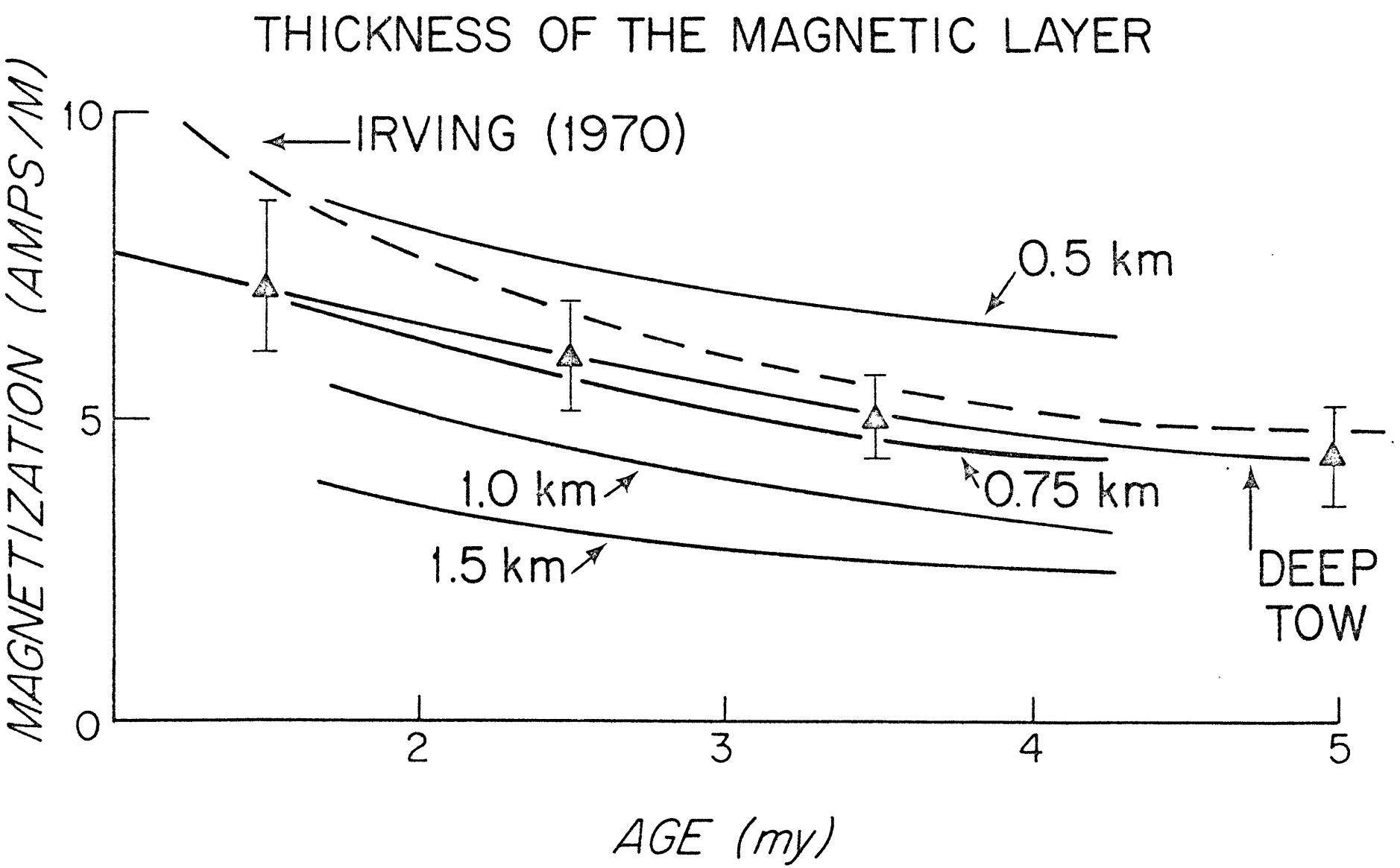
THICKNESS OF THE MAGNETIC LAYER
MAGNETIZATION (AMPS/M)
10
5
0
IRVING (1970)
0.5 km
0.75 km
1.0 km
1.5 km
DEEP TOW
2
3
4
5
AGE (my)

30% smaller (the relation between magnetization and source thickness is not linear). A 700 m thick layer would result in closer agreement between inversion magnetizations and those derived from topographic effects.

10. Volcanoes, Lips and Volcanism Outside the Inner Floor

Macdonald and Luyendyk (in prep.) noted that many topographic features with the same sizes, shapes and elongations as the inner floor volcanic highs are superposed on top of block-faulted relief outside the inner floor. Their lobate morphology and symmetrical cross sections suggest that they are volcanic. The origin of these volcanic features is an important question. In particular, are they created within the inner floor where most of the crust is emplaced, or are they eruptions in older crust away from the axis?

The extent to which volcanism occurs away from the inner floor is difficult to determine. Disturbances in water temperature are transient and rapidly dissipated. Disturbance of the sediment cover is rapidly masked by active downslope transport and redistribution of sediments (Macdonald and Luyendyk, in prep.). The most useful tool available is near

bottom magnetic data. Any volcanic activity outside the inner floor will either be recorded as an anomaly opposite in polarity to its surrounds, or as an amplitude perturbation in the magnetization. The case of opposite polarity crust is easily detectable in near-bottom magnetic data. If the crust is assigned a polarity consistent with the seafloor spreading anomaly measured over it, a topographic feature with opposite polarity will have an anomaly 180° out of phase with the calculated anomaly. If an eruption occurs in older crust which has the same polarity as the ambient field, detection is more difficult. The method of matching amplitudes of observed and calculated fields should show a high in the local magnetization.

Of nearly 170 topographic features analyzed only 7 or about 4% had magnetizations indicative of formation outside the valley floor. Conservatively assuming that the detection method outlined above is about 50% effective, not more than 8% of the extrusive volcanism occurs away from the accreting plate boundary in the inner floor.

This conclusion is also supported by topographic data as follows. Macdonald and Luyendyk (in prep.) note that an unusually high percentage of volcanic features are perched

at the edges of the fault scarps forming "lips" on the top of the block faults (fig. 13). If volcanoes were distributed randomly in the median valley, only 30% would be lips whereas they are observed 62% of the time (Macdonald and Luyendyk, in prep.). The occurrence of volcanic lips supports the concept that most volcanism occurs in the inner floor. If volcanoes originated outside the floor, their placement with respect to block faults should be random. If there were any systematic relationship between faulting and volcanism, the volcanoes would tend to erupt along fractured fault planes at the base of faults rather than systematically routing conduits to the tops of the scarp edges. This suggests that volcanic lips originate in the inner floor as central highs which are transported out on block faults (fig. 13). As discussed by Macdonald and Luyendyk (in prep.), and Ballard and van Andel (in prep.), the crust should tend to fail along either edge of the central high since the crust should be thinnest at that point (a minimum point between thickening of the crust due to the relief of the central high versus thickening of the crust with age (Parker and Oldenburg, 1973). Thus the inner floor volcanic features and central highs are transported out of the inner floor on block faults. They become a lasting part of the topography and account for nearly all (92%) of the volcanic terrain outside the inner floor.

Figure 13. How a central high may become a lip; profile across Mt. Venus at 4X vertical exaggeration shown as an example (A). a) The crust fractures near the edge of the central high where the crust is thinnest (dashed line, see text). b) The central high is transported laterally then uplifted by block faulting. Notice the similarity in morphology of this hypothetical lip to that of observed lips in the inner wall in this profile.

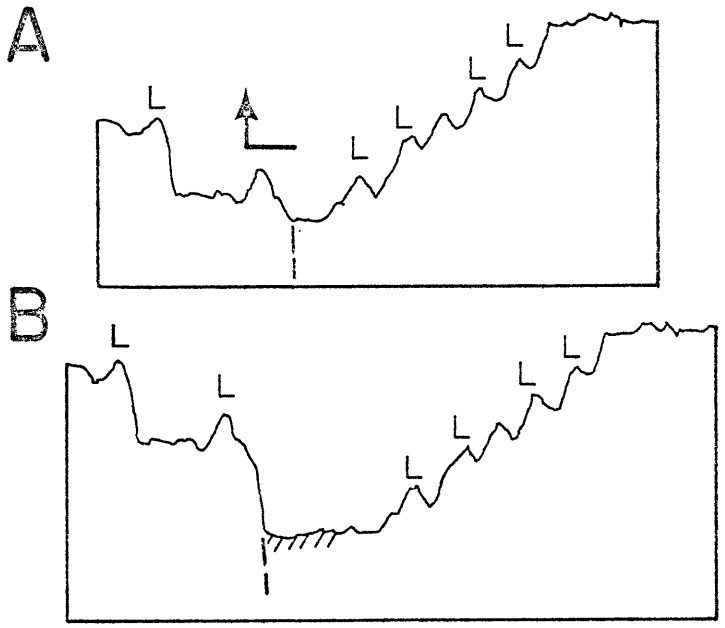
A
L
L
L
L
L
L
B
L
L
L
L
L
L

11. Fracture Zones and the Accreting Plate Boundary

Tectonics of the Famous Rift is not independent of the tectonics of FZA and FZB. Although microseismicity and detailed bathymetry suggests that the active transform fault boundary is only 1 to 2 km wide, the transform valleys are up to 16 km wide (Macdonald and Luyendyk, in prep.; Reid and Macdonald, 1973; Detrick et al., 1973). Macdonald and Luyendyk (in prep.) note that the major block faults of the rift valley outer and inner walls appear to bend toward FZA and FZB about a point of flexure midway between the two fracture zones.

The magnetic anomalies also reflect tectonic influence of the transform faults. On profile I'-I" in the west rift mountains, magnetic anomalies through 3 are clearly recorded in the crust (fig. 4a). On the return traverse 6-8 km closer to FZB (J"-J', fig. 4a), the anomalies are barely identifiable. This traverse is 15 km north of the present location of FZB (fig. 1). There is no evidence of significant volcanism away from the valley floor on this traverse which might disrupt the anomalies. Thus migration of FZB may be responsbile for disturbances in the anomaly pattern. If this is true, then FZB has migrated as far as 15 km from its present location.

This type of lateral migration of transform faults may create and destroy portions of the adjacent spreading centers. For example, northern migration of FZB from its present location would lengthen the south Famous Rift and create an inactive appendage at the south end of the Famous Rift. It appears that this has indeed happened. The N17E trending topographic depression of the Famous Rift extends 8 km south of transform fault B (fig. 1B) and is apparantly an inactive appendage.

12. Negatively Magnetized Crust in the Inner Floor

The inversion of near-bottom magnetic anomalies at the south end of the Famous Rift reveals negative polarity crust in the inner floor within the Brunhes normal epoch (fig. 14). If a very large amount of annihilator is added to the inversion solution, the negative zones may be removed. However, the boundaries of the central and Jaramillo anomalies disappear (the crust becomes positive through anomaly 2), and a relative minimum remains over the valley axis. In comparing the near-bottom field with the calculated field for positively magnetized topography, the observed and calculated fields are found to be nearly 180°

Figure 14. Geophysical profile across the south end of the Famous Rift showing negative polarity crust in the valley floor within the Brunhes epoch. Field measurements at 50 m. interpolation intervals were used for this inversion. Vertical exaggeration = 2X. (See text for details).

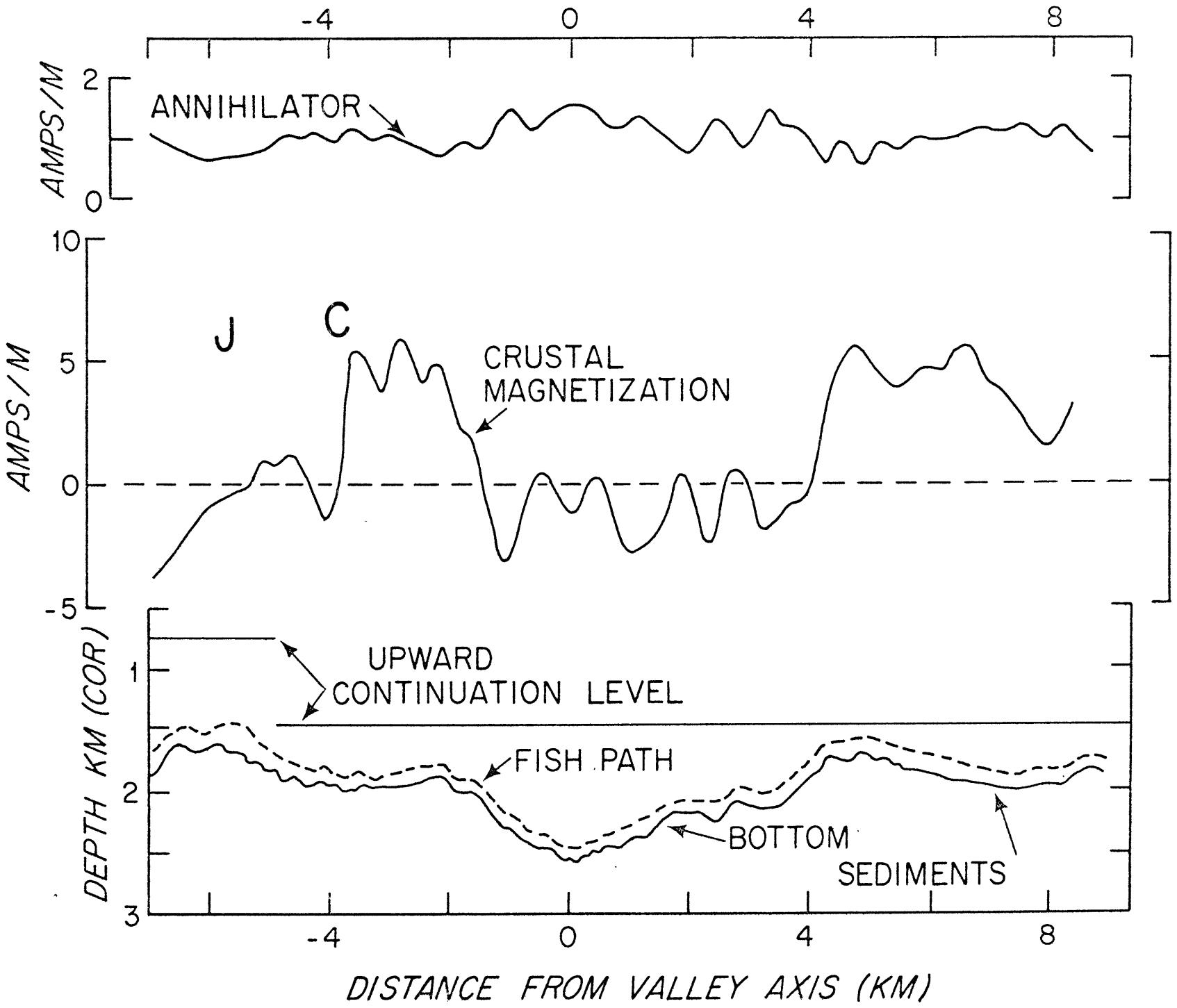
-4
0
4
8
AMPS/M
2
0
ANNIHILATOR
10
5
0
-5
J
C
CRUSTAL
MAGNETIZATION
DEPTH KM (COR)
1
2
3
UPWARD
CONTINUATION LEVEL
FISH PATH
BOTTOM
SEDIMENTS
DISTANCE FROM VALLEY AXIS (KM)

out of phase in 4 places corresponding closely to the negative zones in the inversion solution. Similar evidence also exists for a small amount of negatively polarized crust at the north end of the valley (fig. 4a, A-A', 4 km).

This surprising discovery has been subsequently documented by oriented basalt samples collected from the submersible ALVIN. Of 12 oriented samples collected in the inner floor, 5 show reverse polarity with an average inclination of -55° (Johnson, et al. 1975). Several reversely magnetized samples were also recovered from the Mid-Atlantic Ridge at 45°N using a rock drill (Ade-Hall et al., 1973). Thus the deep-tow inversion results appear to be real.

There are several ways in which negatively polarized crust could occur within the Brunhes normal epoch:
1) Hydrothermal activity can accelerate the alteration of titanomagnetite to titanomaghemite. However, it is difficult for alteration to result in reverse polarization, especially with steep inclinations. Furthermore, the reversely polarized samples appear to be unaltered (Johnson, personal comm.). 2) Self-reversal in some magnetic minerals is possible and has been observed in rare cases (Néel, 1951;

Nagata et al., 1952). However, the mechanisms are so obscure and the conditions so specialized that it is a most unlikely mechanism for negative polarity crust, especially over areas of thousands of square meters (Stacey and Banerjee, 1974). 3) A brief magnetic event during the Brunhes, such as the Blake event, may have been recorded in the crust (Greenewalt and Taylor, 1974). However, these events appear to last for such short periods of time (less than 10,000 years, Opdyke, 1972) that the probability of recording one over the large area concerned is extremely small. Furthermore, there are no prominent volcanic features in the relief to account for a recent eruption or recording of the Blake event. 4) A plausible, yet still disturbing explanation is that old crustal material (greater than 0.69 m.y. old) somehow has been left behind in the inner floor. The probability of negatively polarized crust occurring in the inner floor was calculated assuming the following: a) a normal distribution for crustal accretion, with a standard deviation of about 1 km (derived in the next section); b) transportation of crust out of the inner floor in units averaging 0.5 km in width (narrower fault slivers are found in the inner floor, but the major blocks of the inner wall average 0.5 to 1.0 km

wide. Also, major volcanic units such as lips average 500 m in width (Macdonald and Luyendyk, in prep.)); c) a Gaussian probability for lateral transport of crust , with a variance proportional to the number of unit widths needed to reach the Brunhes/Matuyama boundary. With these assumptions, there is a 14% probability of finding a 500 m wide negatively polarized crustal block in the inner floor. (A total of 5 approximately 500 m wide negatively polarized blocks were found out of 8 crossings of the floor.) Such a probability makes older crust being left behind seem like a reasonable mechanism. The probability is high largely because of the close proximity of the Brunhes/Matuyama boundary on the west side of the valley axis. Narrower blocks (or crustal units in which crust is transported) would decrease the probability (probabilities are 6% and 2% for 100 m and 10 m wide units, respectively). Still, the possibility of recording the Blake or other Brunhes epoch event certainly cannot be ruled out.

13. Polarity Transitions and the Zone of Crustal Accretion

The transition between positively and negatively polarized crust is of considerable importance because it reveals information about the dimensions of accreting plate

boundaries (e.g. Harrison, 1968; Atwater and Mudie, 1973). Two factors contribute to the width of a polarity transition: the time it takes for the earth's field to reverse, and the width over which new crustal material is accreted. During a reversal, the time required for the field intensity to decrease and increase again is about 10,000 years (Harrison and Somayaijulu, 1966; Dunn et al., 1971). For the spreading rates involved this time represents only 70 m to 140 m of spreading.

The polarity transition width is thus controlled primarily by the crustal emplacement width and the emplacement processes. We first discuss the processes. Atwater and Mudie (1973) found that if the crust is formed primarily by intrusion of dikes normally distributed about the spreading center, then $W = 4.6\,\sigma_D$, where W is the distance over which 90% of the transition occurs and σ_D is the standard deviation of the dike intrusion distribution. If the magnetic layer is formed only by lava flows normally distributed about a central fissure with standard deviation σ_F, then $W = 1.7\,\sigma_F$. Since the crust must be emplaced by both of these processes, the variance of the crustal formation distribution σ_C^2 is described by $\sigma_C^2 = \sigma_D^2 + \sigma_F^2$ (Atwater and Mudie, 1973). Widths of volcanoes in the Famous area suggest

that flows extend 20 m. to 600 m. from a central fissure (Macdonald and Luyendyk, in prep.; Ballard and van Andel, in prep.), so we let σ_F vary from 20 m. to 500 m. Dikes which feed the flows may occur anywhere within the inner floor which has a half width of 1 km. in the Famous Rift and 5.5 km. in the south Famous Rift, so we let σ_D vary from 1 km. to 5.5 km. Using Atwater and Mudie's (1973) experimental curves and taking the most extreme values for σ_D and σ_F, We find that $W = 4.3\ (\pm\ 0.3)\sigma_C$. Since by Gaussian statistics, 96% of the crust is emplaced within a distance of $4\sigma_C$ of the spreading axis, this means that the transition width between positively and negatively magnetized crust is approximately equal to the total width of the zone of crustal formation. This is an important result because several workers have assumed that the magnetic transition width is equal to one-half the width of the zone of crustal formation. Such an assumption is only correct if the entire magnetic layer is created by lava flowing from a single central vent. When a multiplicity of feeder dikes is considered, this assumption fails and the magnetic transition width rapidly approaches the crustal formation width.

Figure 15. Solid line is the magnetization solution for anomaly 2 from profile E-E'''. It is too narrow to reliably evaluate the polarity transition width directly from the inversion. The dashed lines are convolutions of a Gaussian filter with the Talwani time scale for various standard deviations (in km.). In this case a standard deviation of 0.5 km. fits best, equivalent to a transition zone 2.0 km. wide. (See text and Appendix 1 for detailed discussion of assumptions).

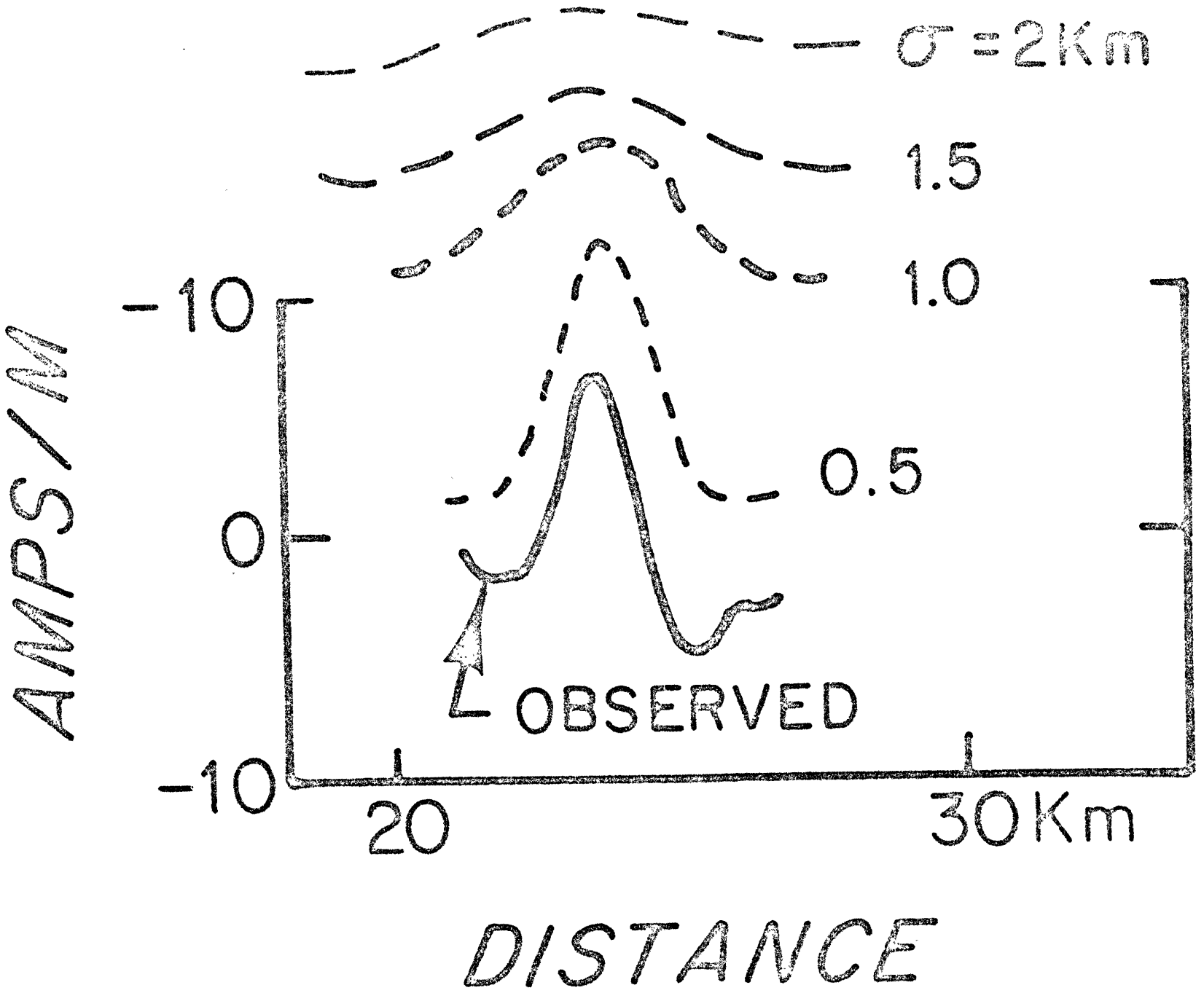
σ = 2Km
1.5
1.0
0.5
OBSERVED
-10
0
-10
AMPS / M
20
30Km
DISTANCE

The polarity transition width is taken to be the zone in which 90% of the magnetization change occurs as determined by inversion solutions (Figs. 4, 5). From the previous discussion, this transition width is a measure of the crustal accretion width at different times in the past. For anomalies of short duration, such as the Jaramillo, anomaly 2 and the events within anomaly 3, it is difficult to measure the distance between peaks and troughs in the magnetization accurately. As an independent method of checking these determinations, the Talwani time scale was convolved with a Gaussian emplacement filter (see Appendix 1 for discussion of this filter). The filtered time scale was compared with the amplitude and shape of the inversion solution for various different standard deviations of the filter. The transition width was set equal to 4 σ for the best fitting filter (Fig. 15). This method gave answers similar to those measured directly.

Most of the polarity transition zones are 1.0 to 2.0 km wide (Fig. 16). This agrees very closely with the present dimensions of crustal formation in the inner floor. The alternating central highs and lows form a lineation approximately 1.5 km wide, the magnetization maximum associated with the plate boundary is about 2 to 3 km wide (Fig. 8), and the

Figure 16. Histogram of polarity transition widths. Most of the transitions cluster around 1 to 2 km., but note that the survey lines are heavily biased toward younger crust.

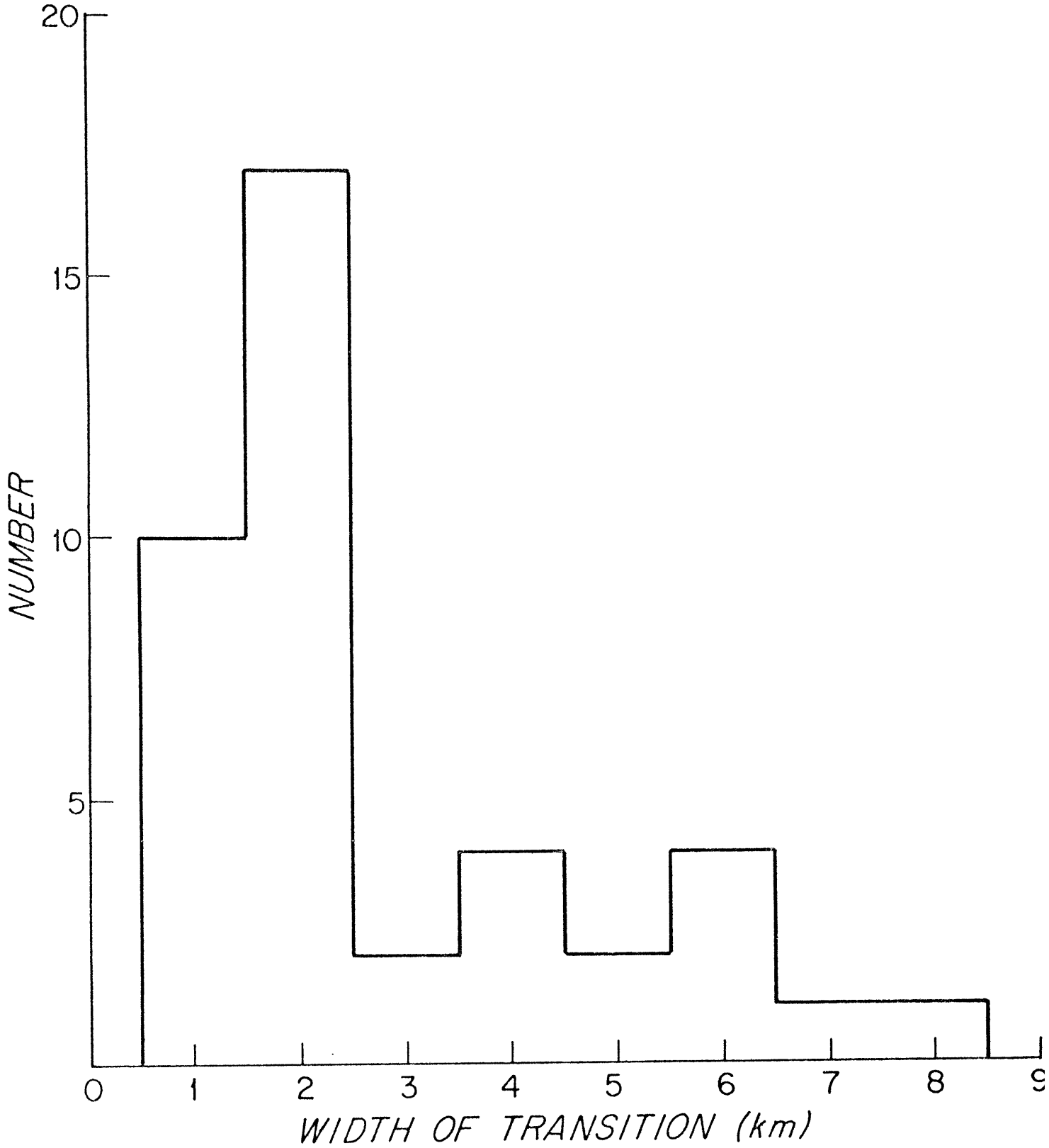
20
15
10
5
NUMBER
0
1
2
3
4
5
6
7
8
9
WIDTH OF TRANSITION (km)

Figure 17. The width of polarity transitions versus age of the crust. Circles are for the east side and squares for the west. X's are 1 m.y. averages out to 4 m.y.b.p. and 3 m.y. averages out to 10 m.y.b.p. Error bars are 4 standard errors in length. Time scale same as in Figure 6. Polarity transitions show an age dependence suggesting that the accreting plate boundary itself has changed in width and structure with time.

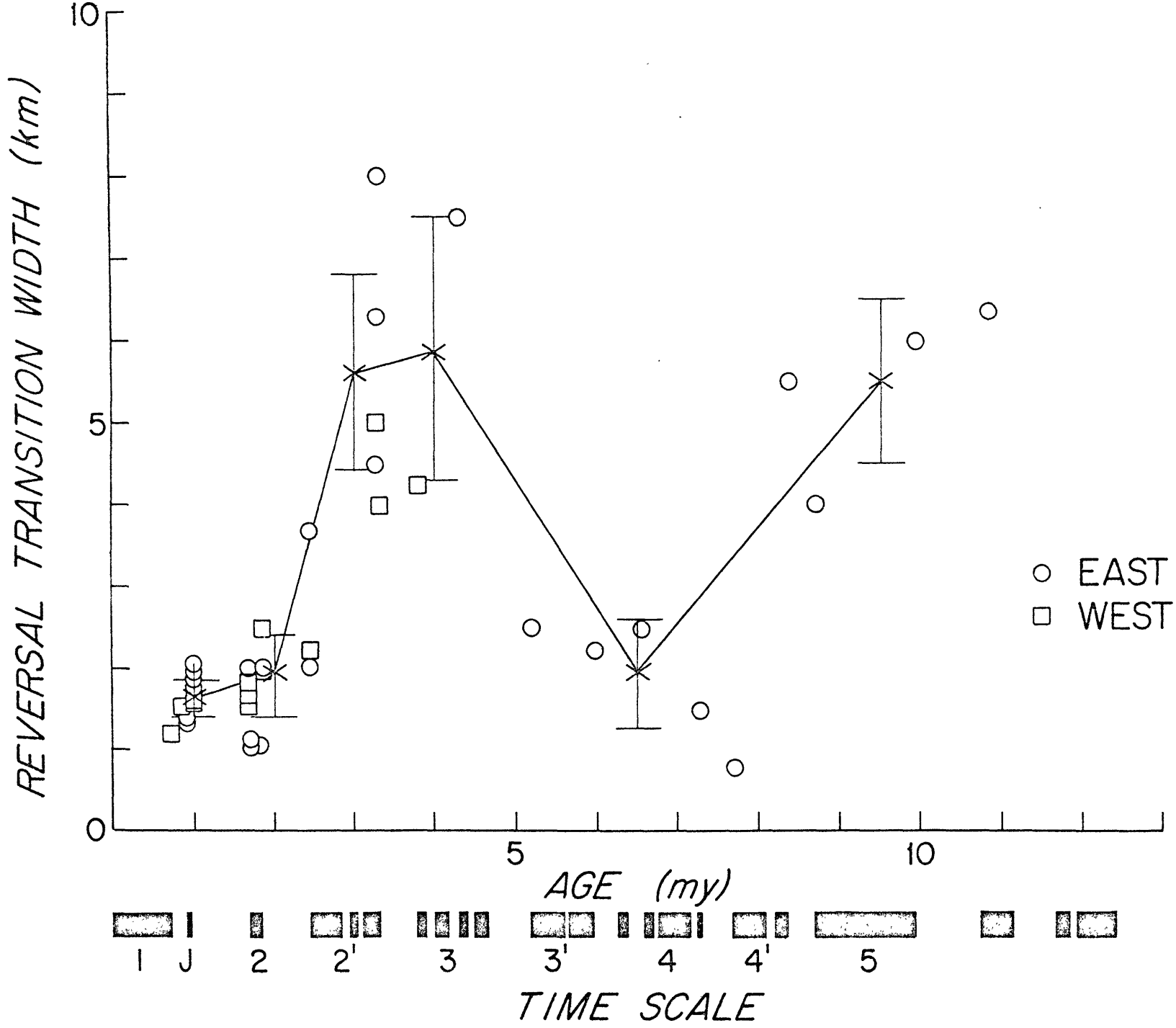
REVERSAL TRANSITION WIDTH (km)
10
5
0
5
10
AGE (my)
EAST
WEST
1
J
2
2'
3
3'
4
4'
5
TIME SCALE

inner floor itself varies in width from 1.0 to 3.0 km. There are, however, several transition widths as great as 8 km. Harrison (1974) has proposed that normal faulting may widen polarity transitions, however, for the largest faults observed this extension is less than 300 m. Since the survey focussed on the median valley, the transition determinations are biased for younger crust ($<$ 2 m.y. old).

Plotting the polarity transition widths against time to remove the age bias yields an interesting result: the transition widths vary with the age of the crust (Fig. 17). The transitions are narrow (1 - 2 km) from 0.7 to 2.5 m.y.b.p., wide ($>$ 5 km) from 2.5 to 4.5 m.y.b.p. and narrow again ($<$ 2 km) from 5 to 7.5 m.y.b.p. They appear to become wide again prior to 7.5 m.y.b.p. (Note that from 5 to 10 lines cross crust on both sides of the ridge axis 0 to 4 m.y. in age, and that the change in transition widths is seen on both flanks. Only one line on the east side traverses crust from 4 m.y. to 10 m.y. old.) In several places where wide transitions occur, direct magnetic modelling verifies the inversion results, revealing outliers of crust with the new polarity overlying crust of the older polarity (e.g. +43 km on E-E", G-G", Fig. 4). The change in transition width is not a simple increase with

age as might be caused by the alteration of magnetic minerals in the uppermost layer of a two-layer magnetic source model (Cox et al., 1972). This fluctuation cannot be a simple shift in the spreading center. A shift would smear out the transition on one side but not the other.

The fact that transition widths vary symmetrically about the ridge axis (Fig. 17) means that the width of the zone of crustal emplacement itself varies on a time scale of millions of years. This has never been observed before. The magnitude of the variation, 1 to 8 km, corresponds closely to extreme values for the width of the inner floor which varies from 1 to 3 km for the Famous Rift to 11 km for the south Famous Rift. We found earlier that more than 90% of the volcanism occurs within the inner floor. Thus the inner floor delimits the zone of crustal extrusion; volcanism seems to occur nearly everywhere within the inner floor, but beyond the inner floor boundaries (inner walls) the probability of volcanism falls off rapidly. At present, the south Famous inner floor is wide, and the site of crustal formation at Mt. Saturn is near the east wall (Fig. 3). The flat inner floor defines a zone 11 km wide in which crustal formation may occur, and polarity transitions for crust created in this type of environment will

tend to be wide, less than or equal to 11 km. The Famous inner floor confines major volcanic sites such as Mt. Venus to a very narrow zone, and when the valley is in this narrow configuration magnetic transitions will tend to be sharp and narrow, less than or equal to 2 km.

14. INVERSION SOLUTIONS NEAR DSDP SITE 332

Leg 37 DSDP site 332 was drilled in the Famous area (Fig. 1) in a negative anomaly between 2' and 3 corresponding to part of the Gilbert reverse polarity epoch (JOIDES, 1975). It was the first hole drilled over 500 m into oceanic basement, theoretically through most of the magnetic source layer (Atwater and Mudie, 1973; Talwani et al., 1971; Macdonald, in prep.). The dipole inclination in this area is 56°, however nearly all the inclinations for this hole are between ±20°, averaging -4°. Given the average intensities of 2 to 4 amps/m, a source layer over 2.5 km thick is needed to produce the magnetic anomaly observed at the sea surface (JOIDES, 1975). These same strange results occur at site 333 as well, which was drilled along the same isochron.

The fish passed only 1.9 km south of drill site 332 (profile I-I", Figs. 1b, 4). Projecting the drill site 1.9 km south onto the deep tow traverse indicates that hole 332 was

Figure 18. Inversion solution for crust near DSDP site 332 in the west rift mountains. Although the surface field and upward continued near bottom field show a negative anomaly over the DSDP site, inversion indicates that the site was located on a wide polarity transition zone between the Gilbert and Gauss epochs. The shift is largely due to the strike of the ridge. The site occurs on a transition regardless of whether a 0.5 km. or 2.0 km. layer thickness is used in the inversion.

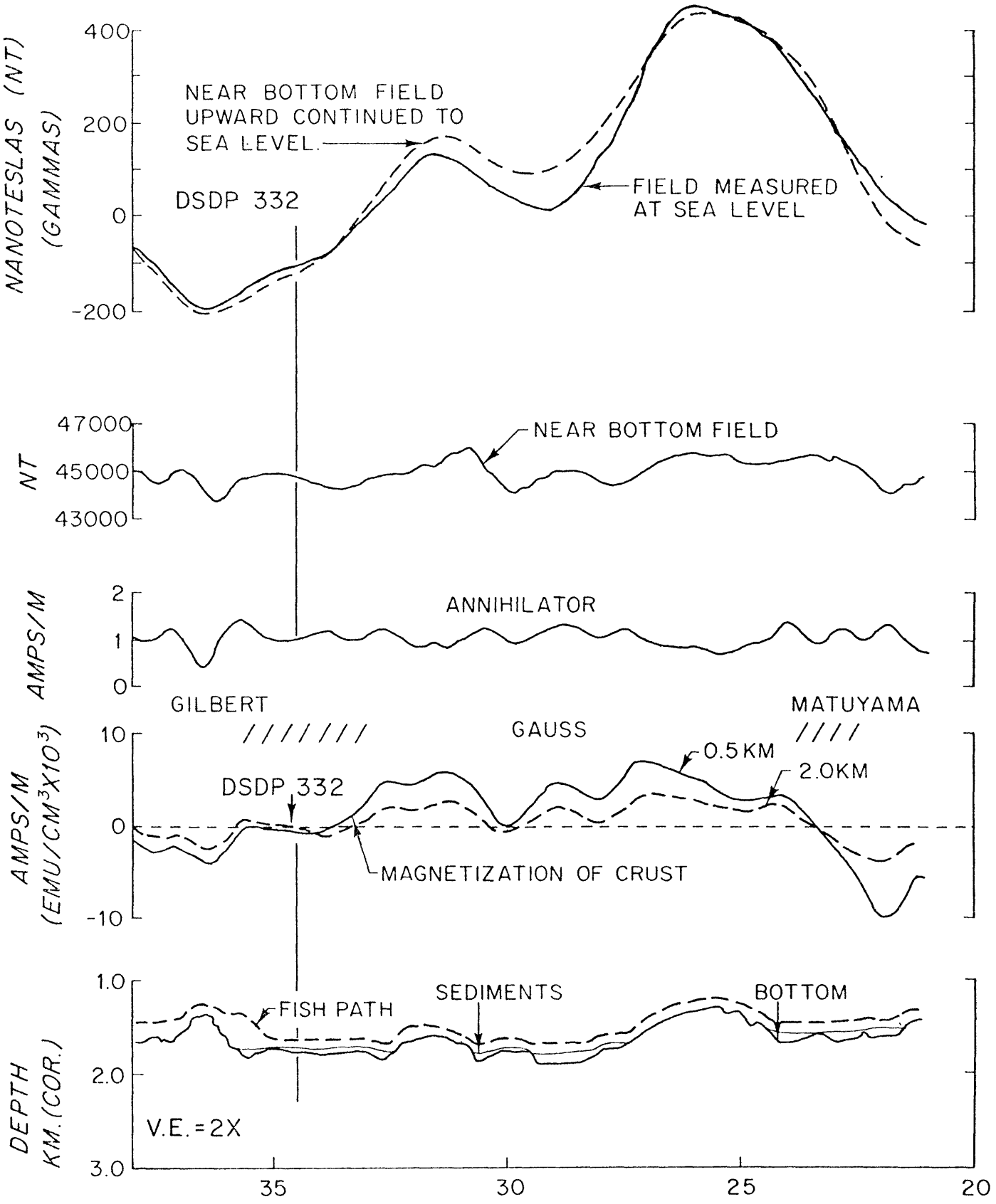
NANOTESLAS (NT)
(GAMMAS)
400
200
0
-200
NEAR BOTTOM FIELD
UPWARD CONTINUED TO
SEA LEVEL.
DSDP 332
FIELD MEASURED
AT SEA LEVEL
47000
45000
43000
NT
NEAR BOTTOM FIELD
2
1
0
AMPS/M
ANNIHILATOR
GILBERT
GAUSS
MATUYAMA
10
0
-10
AMPS/M
(EMU/CM3X10³)
DSDP 332
0.5KM
2.0KM
MAGNETIZATION OF CRUST
1.0
2.0
3.0
DEPTH
KM. (COR.)
FISH PATH
SEDIMENTS
BOTTOM
V.E.=2X
35
30
25
20
DISTANCE FROM VALLEY AXIS (KM)

Figure 19. Different multiples (shown by numbers) of the annihilator added to the solution near the DSDP site to show the range of possible solutions. If too little annihilator is added, the negative anomaly preceding 2' becomes too large and anomaly 2' almost vanishes. If too much annihilator is added the negative anomaly between 2' and 3 disappears. The spreading rates are also disturbed considerably by other choices of the annihilator showing a correlation of fast or slow spreading with positive or negative anomalies. The occurence of DSDP site 332 on a wide polarity transition is quite certain.

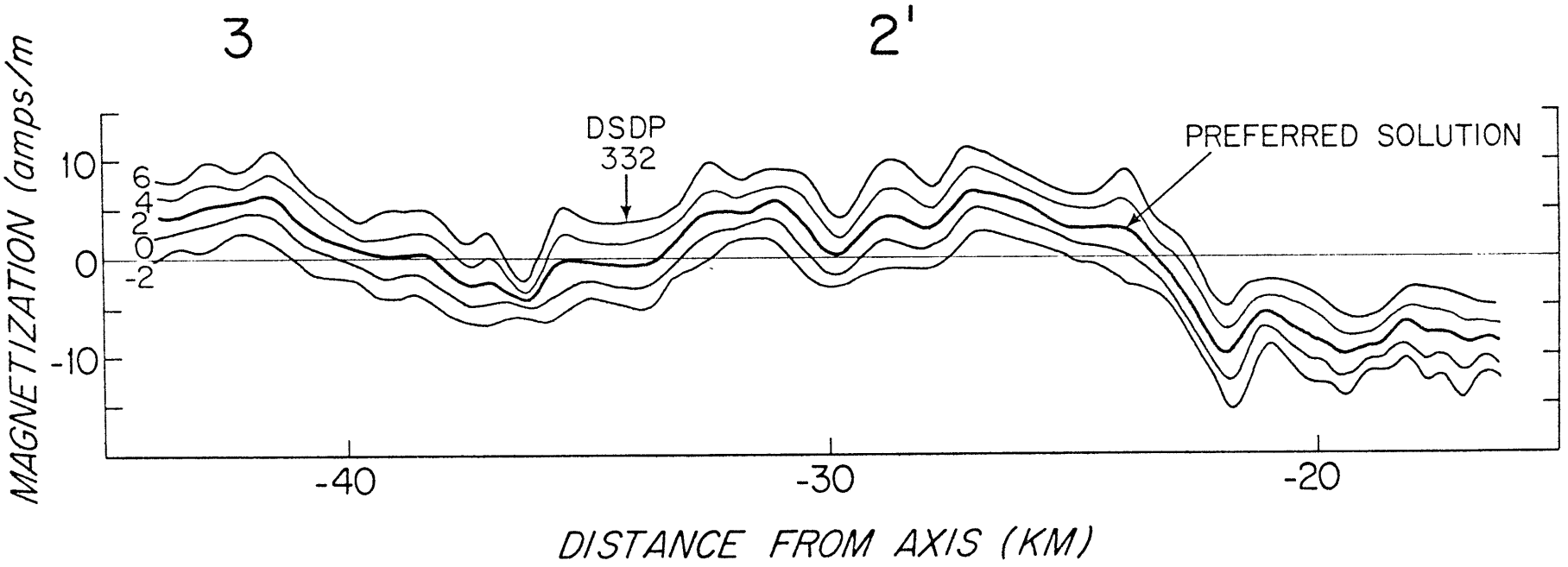
3
2'
DSDP
332
PREFERRED SOLUTION
6
4
2
0
-2
10
0
-10
-40
-30
-20
MAGNETIZATION (amps/m
DISTANCE FROM AXIS (KM)

not drilled in the negative anomaly between 2' and 3 as thought, but was drilled in the transition between the Gauss and Gilbert epochs (Fig. 18). The polarity transition here is broad, about 4 km. (justifying a 1.9 km. projection). The negative anomaly measured at the sea surface over the site is misleading because the strike of the ridge results in a phase shift to the east relative to the source (Fig. 18). The zero magnetization shown by the solution does not necessarily mean zero intensity but may also be near-horizontal inclinations in the source and/or a mixture of polarities. Crustal thicknesses of 0.5 km. and 2.0 km. were used in the calculations, and in both cases, the site is located on a wide polarity transition (Fig. 18). A number of different multiples of the annihilator were added to the solution (Fig. 19). For solutions which place the drill hole in positive crust, the negative anomaly between 2' and 3 nearly disappears. For solutions which place the site in negative crust, anomaly 2 becomes too small in amplitude and the negative anomaly preceding 2' becomes too large. In both cases the spreading rates are distorted for solutions with different amounts of annihilator, resulting in artificial accelerations and decelerations in spreading correlating with positive and negative anomalies. Profile J"-J' near hole 333 also shows a polarity transition "bench" in the solution.

In attempts to re-enter hole 332 several very shallow holes were drilled within 10 meters of the main hole, some recovering negative material, others positive. This supports the inversion results placing the site in a polarity transition zone.

There are several possible explanations for the anomalously shallow inclinations: 1) secular variation, 2) tectonic tilt, 3) unusual excursions or undetected short reversals in the paleofield, 4) a large episode of volcanism during the polarity transition. Secular variation can produce very shallow inclinations, however such perturbances last only for years to hundreds of years (Baraclough, 1972). A tectonic tilt of about 40° toward the north would cause these inclinations, but the regional tilt is only 3° toward the west and locally is zero.

As pointed out earlier field reversals generally require about 10,000 years, however, there is some evidence that the reversal between the Gauss and Gilbert epochs is unusual. Atwater and Mudie (1973) and Klitgord (1974) both observe an excursion or reversal in the field in deep tow magnetic anomalies only 0.05 m.y. after the Gauss/Gilbert reversal.

Atwater and Mudie (1973) propose that this event lasted less than 25,000 years. If this event is real, the probability of recording low intensities or shallow inclinations is approximately 3 times higher than if the Gauss/Gilbert reversal were a single isolated transition.

Episodes of volcanism during the polarity reversal(s) could account for the low inclinations. Ade-Hall and Ryall (1975) note that the basalts of hole 332 may be divided into 9 distinct lithologic groups. Each group has a distinct average inclination with very low standard deviation which is close to but statistically different from the inclinations of adjacent groups. These lithologic/inclination groupings may be explained by 9 separate volcanic eruptions, closely spaced in time, which sampled erratic field behavior during the Gauss/Gilbert reversal and/or the short duration event. Studies of volcanism in the valley inner floor indicate that major eruptions occur approximately every 1,000 to 10,000 years (Bryan and Moore, 1975; Moore et al., 1974). On the average, then, the 9 eruptions sampled would occur over 9 to 90 thousand years. Assuming that the event of Atwater and Mudie (1973) is a reversal, the field was in a transitional state for 30,000 years (a total of 3 polarity transitions).

Thus episodic volcanism at a rate consistent with observations in the inner floor, may account for the recording of shallow inclinations during the polarity reversal(s) at DSDP sites 332 and 333. Perhaps the shallow inclinations represent dominance of the non-dipole component of the field during the reversal(s) (Nagata, 1969; Parker, 1969).

15. DISCUSSION

Present and past configurations of the accreting plate boundary: At present, the accreting plate boundary is narrow and well-defined. In the Famous Rift it is expressed by a 1.5 km wide lineation of alternating central volcanoes and central depressions which lies near the axis of a 2-3 km wide inner floor. In the south Famous Rift, the present zone of crustal accretion (Mt. Saturn) is again about 1.5 km wide, but lies off to one side of a broad (11 km) inner floor. Magnetic and side-looking sonar evidence indicates that eruptions occur away from the 1.5 km wide volcanic zone, but that their volume is relatively very small.

Clearly the zone of crustal accretion cannot be so narrow and regular over long periods of time or else the Mid-Atlantic ridge would have beautiful, clear magnetic anomalies. In a few places on the Mid-Atlantic ridge and in the

Famous area, magnetic anomalies are clearly recorded, including short duration events. More often, for no obvious reason, anomalies are severely attenuated or unidentifiable even in study areas where closely spaced, high quality data is available (e.g. between anomalies 2 and 5 at 45°N, near anomaly 3 in the Famous area).

The variable and often poor quality of magnetic anomalies can be explained by a time-varying median valley structure. When the inner floor is narrow, the zone of crustal accretion and extrusion is also narrow and magnetic anomalies are clearly recorded, even at slow spreading rates. When the inner floor is wide, the zone of volcanism is also wide, and polarities are mixed over a broad zone, resulting in wide polarity transition zones and anomalies which are attenuated and poorly recorded (Fig. 17). This time-varying aspect of the crustal accretion zone has been overlooked by workers who try to relate the width of the crustal accretion zone to the spreading rate (Vine and Morgan, 1967; Blakely and Lynn, 1975).

Thus the median valley appears to have a varying structure: narrow inner floor (accretion zone) and wide terraces; or wide inner floor and narrow terraces. The two structures are epitomized at present by the north and south Famous rifts.

That one structure may evolve into the other is indicated by their simultaneous existence adjacent to each other and the variation in anomaly transition widths with age. However, the connection between the two structures is not necessarily continuous or steady state. Given the approximate spreading half-rates and valley half-widths, a continuous cycle of wide to narrow to wide inner floor would be repeated every 1.4 m.y. Figure 17 suggests that if there is any periodicity it is about 5 m.y. The variable structure cannot be controlled by large scale plate motions because both structures exist simultaneously side by side. The control must be local, caused by variations in the stresses which are responsible for the median valley, by the mechanics of intrusion of deeper crustal layers, or by local availability of magma.

The volcanic zone, which is the surface expression of the accreting plate boundary, lies within the inner floor (as shown earlier by the magnetization of topographic features). However, within the inner floor it may be relatively stationary, it may move from one side of the floor to the other in a regular way (oscillating sprinkler model), or it may shift about randomly. The oscillating sprinkler model is appealing because it can be used to explain asymmetric spreading.

If the accreting plate boundary migrates smoothly toward one side, the spreading rate becomes asymmetric, the slower half-rate being in the same direction as the migration. When the boundary reaches the edge of the floor it may migrate back, reversing the sense of asymmetry or jump back and begin the migration again. Models similar to this have been proposed by Sleep (submitted) and Bryan and Moore (in prep.). Evidence from the Famous area refutes this model on two grounds: 1) a smooth, slow migration of a narrow volcanic center would not produce the variation in polarity transition widths observed, the transition widths would remain approximately constant, and anomalies should always be clear, 2) the only concrete example available of a volcanic center within a wide inner floor, Mt. Saturn, is on the wrong side of the floor to produce the sense of asymmetry observed. A stationary volcanic zone within the inner floor may be rejected on similar grounds.

We thus favor a model in which the accreting plate boundary and zone of volcanism is confined to the inner floor, but may occur almost randomly anywhere within the floor. Plate tectonics requires that the total spreading rate increase with azimuth from the pole of opening, while the half-rates may vary widely from one segment of the ridge to another.

However, all observations on the Africa/North America plate boundary show faster spreading to the east (discussed earlier). This suggests that asymmetric spreading has a more global cause than the migration of the volcanic zone within each individual ridge segment. Furthermore, volcanism may occur anywhere within the inner floor, the crust is not committed to one plate or the other until it is uplifted by block faults forming the inner wall. Thus it is the distribution of block faulting and not the locus of volcanism which must be responsible for asymmetric spreading on a local scale.

It is important, especially with regard to the question of oblique spreading, to assess the influence of Azores triple junction. Phillips and Fleming (1975) note that a pronounced median valley continues up to 38°N, where it abruptly disappears. Rotation of anomalies 2' and 5 about the America/Africa rotation pole (Phillips and Forsyth, 1973) produces an almost perfect overlap of anomalies on opposite sides of the ridge south of 38°N and a gross misfit for anomalies north of 38°N (Phillips and Fleming, 1975). The Famous area is between 100 and 200 km south of this abrupt change in tectonics, so it is apparently unaffected by the triple junction.

It is thus unlikely that the 17 degrees of oblique spreading observed in the Famous area is caused by triple junction tectonics. It was shown earlier that oblique spreading is presently stable here, that there is no evidence of readjustment to an orthogonal system, and also that oblique spreading has been stable here for millions of years even through changes in the direction and asymmetry of spreading. Oblique spreading at approximately the same angle is also occurring at other slow spreading centers such as the Gulf of Aden (Laughton et al., 1970), the Juan de Fuca ridge (Chase et al., 1970), and the Reykjanes Ridge (T. Atwater, personal comm.). The assumption that slow spreading ridges and their transform faults form orthogonal systems should be reevaluated, especially with regard to theoretical tectonic models which rely on this assumption (e.g. Lachenbruch and Thompson, 1973; Lachenbruch, 1973; Oldenburg and Brune, 1975).

Generation of the magnetized layer, the roles of volcanism and faulting: If most of the magnetic layer is composed of pillow basalts produced by extrusive volcanism (e.g. Marshall and Cox, 1972) then more than 90% of the magnetic layer is created within the median valley inner floor.

The width of the volcanic zone in which anomalies are recorded depends critically on the width of the inner floor. Thus polarity transition widths and fidelity of magnetic anomalies vary through time with the structure of the median valley.

Results from DSDP hole 332 (Macdonald, submitted; and Ade-Hall and Ryall, 1975) and observations in the inner floor (Macdonald and Luyendyk, in prep.; Bryan and Moore, in prep.) suggest that volcanism is highly episodic. Volcanic events which may last only 10^{-2} to 10^{-1} years occur every 10^{3} to 10^{4} years. Thus, recording of the magnetic field by the crust is highly quantized and is represented by crustal units such as volcanoes and lips which are hundreds of meters wide.

In contrast, tectonic activity is essentially continuous even down to a time scale of days (Reid and Macdonald, 1973; Spindel et al., 1973; Macdonald and Luyendyk, in prep.). Intense faulting and fracturing of the crust commences within less than 1 km of the volcanic center. This is important for the freshly extruded crust is immediately exposed internally to seawater, accelerating the alteration of titanomagnetite. We have found that initially high magnetization values of 20 to 30 amps/m decay to 1/e in only 0.6 m.y. The decay rate slows drastically only a few km from the inner floor as few new fractures are opened in the crust.

16. CONCLUSIONS

1. The Mid-Atlantic Ridge in the Famous area is characterized by highly asymmetric spreading; 7.0 mm/yr to the west and 13.4 mm/yr to the east. The sense of asymmetry reversed at 1.7 m.y.b.p. Prior to 1.7 m.y.b.p. the rates were 10.8 mm/yr to the east and 13.4 mm/yr to the west. The grossly symmetric spreading previously reported for the Mid-Atlantic Ridge (e.g., Pitman and Talwani, 1972; Phillips et al., 1975) is probably composed of highly asymmetric episodes of spreading.

2. The reversal in asymmetric spreading and change in total spreading rate occurred almost instantaneously (geologically) in less than 0.15 m.y.

3. The Mid-Atlantic Ridge here is spreading obliquely at an angle of 17°. Detailed studies of the strikes of faults, fissures, recent volcanic zones, and fine scale magnetic trends, as well as microearthquake distribution all indicate that spreading is stably oblique. There is no indication of reorientation to an orthogonal system in the transform faults or in the rift inner floor. Oblique spreading has been stable for millions of years, even through a change in spreading direction. At least out to anomaly 5 (10 m.y.) the Famous area is sufficiently removed from the Azores triple junction

so that oblique spreading cannot be explained by its influence. Oblique spreading may be stable for many or even most slow spreading centers.

4. The accreting plate boundary is marked by a narrow (2-3 km) maximum in crustal magnetization. The axial magnetization maximum is highest in central volcanoes such as Mt. Venus and Mt. Pluto, and decreases but is still present in the central depressions. While volcanism may cover most of the inner floor with a veneer of recent lavas, the magnetization maximum delineates the major recent volcanic center. It lies near the center of the Famous Rift and well off to the east side of the south Famous Rift.

5. High magnetizations of the youngest crust (20 to 30 amps/m) decay very rapidly to 1/e in only 0.6 m.y. Most of the decay occurs in and near the inner floor where the crust is intensely fractured and faulted almost immediately after formation. This intense fracturing may accelerate the alteration of magnetic minerals through seawater contact and circulation, as well as cause mechanical disruption of the magnetized layer. This may also contribute to rapid cooling of the crust near the axis through hydrothermal circulation.

6. The magnetization of topographic features (from deep tow modeling), combined with surface tow magnetic anomalies suggests that the magnetized layer is 700 m thick. This is assuming constant magnetization with depth in the crust. Our thickness estimate is also close to that of JOIDES (1975) of 570 to 820m at sites 334 and 335. Our thickness estimate is 40% to 50% higher than those of Atwater and Mudie (1973) and Talwani et al. (1971).

7. Deep tow magnetic modeling of topographic magnetic anomalies suggests that over 90% of the volcanism and crustal accretion occurs within the inner floor. Central highs which mark the volcanic zone are transported out of the inner floor on block faults becoming a lasting part of the topography. They frequently occur as lips at the edges of fault blocks.

8. There are several zones in the inner floor, hundreds of meters wide, in which the crust is negatively polarized. The Blake or some other Brunhes epoch event may have been fortuitously recorded. Alternatively, highly asymmetric spreading places the Brunhes normal epoch boundary close enough to the inner floor on the west side so that Matuyama epoch crust may have been left behind in the inner floor (about a 14% probability).

9. The unusually low inclinations observed throughout the first deep DSDP hole (332) may be explained by its location on a wide polarity transition zone which may consist of more than one reversal. Results from the hole and from the inversion solution here suggests that volcanism is highly episodic and that the entire magnetized layer can be created in a short period of time. The deep hole here may be invaluable in studying the earth's magnetic field during a field reversal.

10. Polarity transition widths vary from 1 km to 8 km with time and appear to reflect a bi-stable median valley structure. The valley has either a wide inner floor and narrow terraces, in which case the volcanic zone is wide and magnetic anomalies are poorly recorded (wide transition widths); or it has a narrow inner floor and well-developed terraces, the volcanic zone is then narrow and anomalies are clearly recorded (narrow transition widths). The median valley of any ridge segment varies between these two structures with time.

11. The accreting plate boundary over short periods of time ($< 10^5$ years) is sharply defined in space (< 1.5 km). Over millions of years, however, the valley structure changes and the plate boundary may shift about inside a zone approximately 10 km wide.

12. Transform faults are also sharply defined in space (1 to 2 km wide) as delineated by microearthquakes and near-bottom mapping. However, over millions of years the faults migrate over a zone 10-20 km wide, a zone wide enough to disrupt lineated magnetic anomalies generated at the ridge crests.

References and Bibliography, Chapter 3

Ade-Hall, J.M., F. Aumento, P. Ryall, R. Gerstein, J. Brooke and D. McKeown, The Mid-Atlantic Ridge near 45°N, 21, magnetic results from basalt drill cores from the median valley, Can. J. Earth Sci., 10, 679, 1973.

Ade-Hall, J.M., and P.J.C. Ryall, Geomagnetic field inclinations recorded by the upper part of layer 2 in the vicintiy of the crest of the Mid-Atlantic Ridge near 37°N, (abstract) EOS, 56, 376, 1975.

Atwater, T.M., and J.D. Mudie, Detailed near bottom geophysical study of the Gorda Rise, J. Geophys. Res., 78, 8665, 1973.

Aumento, F., B.D. Loncarevic and D.I. Ross, Hudson geotraverses: geology of the Mid-Atlantic Ridge at 45°N, Phil. Trans. Roy. Soc. London, 268, 623, 1971.

Ballard, R., and T.H. van Andel, Project FAMOUS: the Mid-Atlantic Rift valley at 36-37°N, morphology and tectonics of the inner rift valley at 36°50'N on the Mid-Atlantic Ridge, in prep. for Bull. Geol. Soc. Amer. dedicated issue on FAMOUS.

Baraclough, D.R., Spherical harmonic analyses of the geomagnetic field for eight epochs between 1600 and 1910, Geophys. J.R. astr. Soc., 36, 497, 1974.

Barazangi, M., and J. Dorman, World seismicity maps compiled from ESSA, Coast and Geodetic Survey, epicenter data, 1961-1967, Bull. Seismol. Soc. Amer., 59, 369, 1969.

Bellaiche, G., J.L. Cheminee, J. Francheteau, R. Hekinian, X. Le Pichon, H.D. Needham and R.D. Ballard, Rift valley's inner floor: first submersible study, Nature, 250, 558-560, 1974.

Bird, P., and J.D. Phillips, Oblique spreading near the Oceanographer fracture zone, J. Geophys. Res., in press.

Blakely, R.J., Geomagnetic reversals and crustal spreading rates during the Miocene, J. Geophys. Res., 79, 2979, 1974.

Blakely, R.J., and W.S. Lynn, Wide zone of volcanic intrusion at the Nazca-Pacific plate boundary, (abstract) EOS, 56, 445, 1975.

Bryan, W.B., and J.G. Moore, Project FAMOUS: The Mid-Atlantic Rift valley at 36-37°N, volcanism, petrology and geochemistry of the basalts of the inner floor of the rift valley at 36°50'N on the Mid-Atlantic Ridge, in prep. Bull. Geol. Soc. Amer. dedicated issue on FAMOUS.

Chase, T.E., H.W. Menard and J. Mammerickx, Bathymetry of the North Pacific, Chart 4, Tech. Rep. Ser., TR-9, Inst. of Marine Resour., Univ. of Calif., San Diego, 1970.

Cox, A., R.J. Blakely and J.D. Phillips, A two-layer model for marine magnetic anomalies, (abstract) EOS, 53, 974, 1972.

Detrick, R., J.D. Mudie, B.P. Luyendyk and K.C. Macdonald, Near-bottom observations of an active transform fault: Mid-Atlantic Ridge at 37°N, Nature, 246, 59, 1973.

Dunn, J.R., M. Fuller, H. Ito and V.A. Schmidt, Paleomagnetic study of a reversal of the earth's magnetic field, Science, 172, 840, 1971.

Fox, J., A. Lowrie, Jr. and B.C. Heezen, Oceanographer fracture zone, Deep-Sea Res., 16, 59, 1969.

Greenewalt, D., and P.T. Taylor, Deep-tow magnetic measurements across the axial valley of the Mid-Atlantic Ridge, J. Geophys. Res., 79, 4401-4405, 1974.

Harrison, C.G.A., Formation of magnetic anomaly patterns by dyke injection, J. Geophys. Res., 73, 2137, 1968.

Harrison, C.G.A., Tectonics of mid-ocean ridges, Tectonophys., 22, 301, 1974.

Harrison, C.G.A., and B.L.K. Somayajulu, Behavior of the earth's magnetic field during a reversal, Nature, 212, 1193, 1966.

Heirtzler, J.R., G.O. Dickson, W.C. Pitman, III, E. Herron and X. Le Pichon, Marine magnetic anomalies, geomagnetic field reversals, and motions of the ocean floor and continents, J. Geophys. Res., 73, 2119, 1968.

IAGA Commission Two Working Group 4, Analysis of the geomagnetic field, International Geomagnetic Reference Field, 1965, J. Geophys. Res., 74, 4407, 1969.

Irving, E., The Mid-Atlantic Ridge at 45°N, 16, oxidation and magnetic properties of basalt; review and discussion, Can. J. Earth Sci., 7, 1528, 1970.

Ivers, W.D., and J.D. Mudie, Towing a long cable at slow speeds: a three-dimensional dynamic model, Mar. Tech. Soc. J., 7, 23, 1973.

Johnson, H.P., T. Atwater and E. Carter, Paleomagnetic and rock magnetic properties of basalts from the Mid-Atlantic Ridge at 36°N, (Abstract) EOS, 56, 375, 1975.

JOIDES, Sources of magnetic anomalies on the Mid-Atlantic Ridge, Nature, 255, 389, 1975.

Klitgord, K.D., Near-bottom geophysical surveys and their implication on the crustal generation process, sea-floor spreading history of the Pacific and the geomagnetic time scale 0 to 6 m.y.b.p., Ph.D. thesis, Univ. of Calif. at San Diego, 177 pp., 1974.

Lachenbruch, A.H., A simple mechanical model for oceanic spreading centers, J. Geophys. Res., 78, 3395, 1973.

Lachenbruch, A.H., and G.A. Thompson, Oceanic ridges and transform faults: their intersection angles and resistance to plate motion, Earth Planet. Sci. Lett., 15, 116, 1972.

Laughton, A.S., and J.S. Rusby, Long range sonar and photographic studies of the median valley in the FAMOUS Area of the Mid-Atlantic Ridge near 37°N, Deep-Sea Research, 22, 279, 1975.

Laughton, A.S., R.B. Whitmarsh and M.T. Jones, The evolution of the Gulf of Aden, Royal Soc. London Philos. Trans., ser. A., 267, 227, 1970.

Loncarevic, B.D., and R.L. Parker, The Mid-Atlantic Ridge near 45°N, XVII: magnetic anomalies and ocean floor spreading, Can. J. Earth Sci., 8, 883, 1971.

Lowrie, W., Oceanic basalt magnetic properties and the Vine and Matthews hypothesis, J. Geophys., 40, 513, 1974.

Luyendyk, Bruce P., and Ken C. Macdonald, Physiography and structure of the FAMOUS rift valley inner floor observed with a deeply towed instrument package, in prep. Bull. Geol. Soc. Amer. dedicated issue on FAMOUS.

Macdonald, Ken C., Deep-tow inversion solutions for crustal magnetization at DSDP site 332, submitted to international symposium on the nature of the oceanic crust.

Macdonald, Ken C., and B.P. Luyendyk, An intensive deep-tow study of the goemorphology and tectonics of the Mid-Atlantic Ridge (37°N), in prep. Bull. Geol. Soc. Amer. dedicated issue on FAMOUS.

Macdonald, Ken C., B.P. Luyendyk, J.D. Mudie and F.N. Spiess, Near-bottom geophysical study of the Mid-Atlantic Ridge median valley near lat. 37°N: preliminary observations, Geology, 211, 1975.

Marshall, M., and A. Cox, Magnetic changes in pillow basalts due to sea-floor weathering, J. Geophys. Res., 77, 6459, 1972.

McGregor, B.A., and P.A. Rona, Crest of the Mid-Atlantic Ridge at 26°N, J. Geophys. Res., 80, 3307, 1975.

McGregor, B.A., C.G.A. Harrison, J.W. Lavelle and P.A. Rona, Magnetic anomaly pattern on the Mid-Atlantic Ridge crest at 26°N, submitted J. Geophys. Res., 1975.

Miller, S.P., K.D. Klitgord and J.D. Mudie, Influence of geological and time varying sources on the spectra of marine magnetic anomalies, (abstract) EOS, 55, 231, 1974.

Moore, J.G., H.S. Fleming and J.D. Phillips, Preliminary model for extrusion and rifting at the axis of the Mid-Atlantic Ridge, 35°48'North, Geology, 2(9), 437-4401, 1974.

Nagata, T., Length of geomagnetic polarity intervals, (discussion of papers by A. Cox, 1968, 1969), J. Geomag. Geoelec., 21, 701, 1969.

Nagata, T., S. Uyeda and S. Akimoto, Self-reversal of thermoremanent magnetism of igneous rocks, J. Geomagn. Geoelectr., 4, 22, 1952.

Needham, H.D., and J. Francheteau, Some characteristics of the rift valley in the Atlantic Ocean near 36°48' North, Earth and Planet. Sci. Lett., 22, 29-43, 1974.

Neél, L., L'inversion de l'aimantation permanente des roches, Ann. Geophys., 7, 80, 1951.

Oldenburg, D.W., and J.N. Brune, An explanation for the orthogonality of ocean ridges and transform faults, J. Geophys. Res., 80, 2341, 1975.

Opdyke, N.D., Paleomagnetism of deep-sea cores, Rev. Geophys. Space Phys., 10, 213, 1972.

Parker, E.N., The occasional reversal of the geomagnetic field, Astrophys. J., 158, 815, 1969.

Parker, R.L., The rapid calculation of potential anomalies, Geophys. J. R. astr. Soc., 31, 447, 1973.

Parker, R.L., and S.P. Huestis, The inversion of magnetic anomalies in the presence of topography, J. Geophys. Res., 79, 1587, 1974.

Parker, R.L., and K.D. Klitgord, Magnetic upward continuation from an uneven track, Geophys., 37, 662, 1972.

Parker, R.L., and D.W. Oldenburg, Thermal model of ocean ridges, Nature, 242, 137, 1973.

Phillips, J.D., and H.S. Fleming, The Mid-Atlantic Ridge west of Azores, 35°-39°N, (Abstracts) EOS, 56, 374, 1975.

Phillips, J.D., and H.S. Fleming, The Mid-Atlantic Ridge west of the Azores 35-39°N, in prep. Bull. Geol. Soc. Amer. dedicated issue on FAMOUS.

Phillips, J.D., H.S. Fleming, R. Feden, W.E. King and R. Perry, Aeromagnetic study of the Mid-Atlantic Ridge near the Oceanographer Fracture Zone, Geol. Soc. Amer., in press.

Phillips, J.D., and D.W. Forsyth, Plate tectonics, paleomagnetism, and the opening of the Atlantic, Geol. Soc. Amer. Bull., 83, 1579, 1972.

Phillips, J.D., G. Thompson, R.P. Von Herzen and V.T. Bowen, Mid-Atlantic Ridge near 43°N latitude, J. Geophys. Res., 74, 3069, 1969.

Pitman, W.C., III, and M. Talwani, Sea-floor spreading in the North Atlantic, Bull. Geol. Soc. Amer., 83, 619, 1972.

Reid, I., and K.C. Macdonald, Microearthquake study of the Mid-Atlantic Ridge near 37°N using sonobuoys, Nature, 246, 88-90, 1973.

Schouten, H., and K. McCamy, Filtering marine magnetic anomalies, J. Geophys. Res., 77, 7089, 1972.

Sleep, N.H., Topography and tectonics of ridge axes, submitted to J. Geophys. Res.

Spiess, F.N., and R.C. Tyce, Marine Physical Laboratory deep-tow instrumentation system, Scripps Inst. Oceanography Ref. 73-4, 1973.

Spindel, R.C., S.B. Davis, K.C. Macdonald, R.P. Porter and J.D. Phillips, Microearthquake survey of median valley of the Mid-Atlantic Ridge at 36°30'N, Nature, 248, 577-579, 1974.

Stacey, F.D., and S.K. Banerjee, The Physical Principles of Rock Magnetism, Amsterdam, Elsevier, 195 pp., 1974.

Sykes, L.R., Mechanism of earthquakes and nature of faulting on the mid-ocean ridges, J. Geophys. Res., 72, 2131, 1967.

Talwani, M., C.C. Windisch and M.G. Langseth, Jr., Reykjanes Ridge Crest: a detailed geophysical study, J. Geophys. Res., 76, 473, 1971.

van Andel, Tjeerd, H., and Carl O. Bowin, Mid-Atlantic Ridge between 22° and 23° north latitude and the tectonics of mid-ocean rises, J. Geophys. Res., 73, 1279, 1968.

van Andel, Tjeerd H., and G. Ross Heath, Tectonics of the Mid-Atlantic Ridge, 6°-8° south latitude, Mar. Geophys. Res., 1, 5, 1970.

Vine, F.J., and W.J. Morgan, Simulation of mid-ocean ridge magnetic anomalies using a random injection model, (abstract) Program 1967 Ann. Meeting, Geol. Soc. Am., Nov. 1967.

Walker, G.P.L., Some aspects of Quaternary volcanism in Iceland, Leicester Lit. Philos. Soc., 151, 25, 1964.

APPENDIX I

THE USE OF GAUSSIAN FILTERS TO APPROXIMATE THE CRUSTAL EMPLACEMENT PROCESS

Where reversals in the time scale are too closely spaced, it is difficult to pick the polarity transition width directly from the inversion solutions. In such cases (e.g. anomaly 2, Fig. 15) a Gaussian filter was convolved with the Talwani et al. time scale (1971) and compared to the inversion solution for amplitude and shape.

There is, however, considerable confusion in the literature as to whether a half-Gaussian (e.g. Schouten and McCamy, 1972) or full-Gaussian filter (e.g. Blakely, 1974) more accurately represents the emplacement of the magnetic crust. The question is critical because the two filters have very different characteristics especially with regard to phase. The half-Gaussian filter is asymmetric and thus introduces a phase shift when convolved with the time scale. For the standard deviations and spreading rates appropriate to the Famous area, the asymmetric half-Gaussian filter will shift the observed anomaly transitions away from the valley axis 1.0 to 3.0 km. A full Gaussian filter is symmetric and will not introduce a shift. If there is a shift in the data, it

may be measured by plotting the distance between isochrons (anomalies) on either side of the ridge versus age (i.e., total spreading rate). The intercept on the distance axis is the outward shift. For the deep-tow data, the phase shift is 0 ±300 m. This result strongly favors a symmetric over an asymmetric filter, i.e., a full-Gaussian over a half-Gaussian filter.

The geology of the rift inner floor also supports a symmetric Gaussian type emplacement process. An asymmetric half-Gaussian emplacement process is equivalent to the crust being formed by extrusion from a single vent (Atwater and Mudie, 1973, Fig. 15). Dike emplacement and multiple feeders for the flows "stretch" the crust allowing older crustal material to be closer to the axis than newer material. The emplacement process thus becomes increasingly symmetric about the reversal boundary as dike emplacement gains importance. Using Atwater and Mudie's (1973) graphs, we find that even the narrowest possible intrusion widths and widest flow dimensions result in an emplacement distribution which is far more symmetric than asymmetric about the reversal boundary.

We conclude that a symmetric filter more accurately represents the intrusion process than an asymmetric filter. A full Gaussian is as realistic as any other symmetrical filter consistent with emplacement of material about a linear plate boundary.

APPENDIX II

MICROEARTHQUAKE STUDIES

(Reprinted from Nature, Vol. 246, No. 5428, pp. 88–90, November 9, 1973)

Microearthquake Study of the Mid-Atlantic Ridge near 37° N, using Sonobuoys

In view of the successful use of telemetering radio sonobuoys for detecting and locating microearthquakes in the Gulf of California[1], we carried out a similar survey of the Mid-Atlantic Ridge, in the region near latitude 37° N, during May and June of this year. Our object was to study the level and distribution of seismicity; in particular, we hoped to locate some earthquakes sufficiently accurately that we could associate them with local physiographic features, and draw conclusions about the present tectonic activity of this section of the ridge. Teleseismic study of the mid-ocean ridge suffers from two basic limitations: the epicentral locations are not sufficiently accurate to allow more than a general correlation of seismic activity with the median rift (where present) and with the transform faults offsetting the ridge segments[2], and it is not generally possible to locate earthquakes of magnitude less than about 4 (ref. 3). Ocean

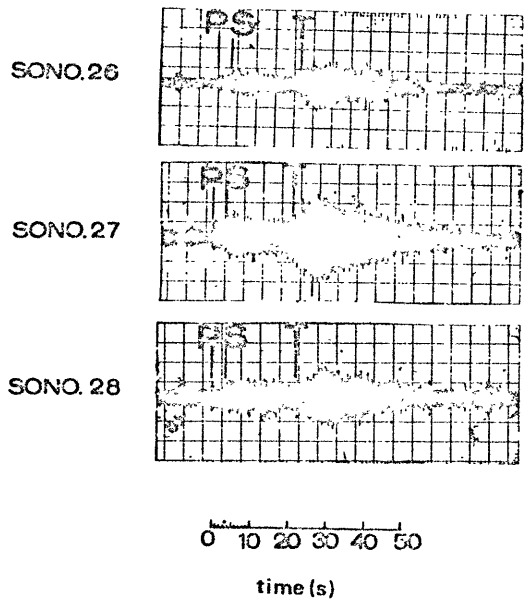

Fig. 1 Recording of a typical earthquake detected on sonobuoys. The epicentral distance is about 30 km. (This is not the original record but a replay off magnetic tape.)

bottom seismometers have also been used to study ridge seismicity, but the results to date have been fairly limited[4].

The study described here was undertaken as an ancillary program on cruise 31 (WHOI TOW 1) of RV Knorr (Woods Hole Oceanographic Institution). The main object of this cruise was a detailed survey of the area, using the Scripps Institution of Oceanography/Marine Physical Laboratory's deep-tow instrument package[5]. This, in turn, is part of a continuing intensive study of this section of the Mid-Atlantic Ridge (Project FAMOUS). As a result, the topography is well enough known to allow meaningful correlation with the seismicity.

The technique used was basically that described by Reid *et al.*[1] for the Gulf of California. Expendable sonobuoys[6] were monitored by onboard recording equipment. The sonobuoy positions were found by firing explosive charges to determine their range from the ship. Whenever possible, we tried to maintain an array of at least three sonobuoys operating, with a spacing of a few kilometres. We obtained fifty-nine epicentral locations, out of 104 earthquakes recorded during 11 d of favourable recording conditions. More than half the locations have an estimated error of 2 km or less.

Figure 1 shows the record of a typical event at a distance of about 30 km. We follow the phase identification and nomenclature of Reid *et al.*[1]. The P and S arrivals are the direct compressional and shear waves through the crust, and the T phase is interpreted as the wave travelling through the water layer from the epicentre. At distances less than about 10 km, S and T phases are not normally seen, and the observed phases are P and its reflections in the water column, designated P_1, P_2, and so on.

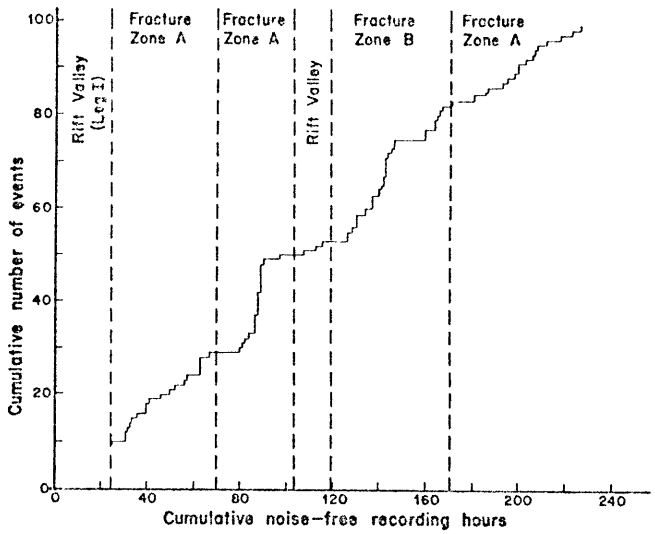

Fig. 2 Cumulative number of earthquakes recorded against cumulative number of low-noise recording hours. The dashed vertical lines indicate the successive sonobuoy arrays.

The results are summarised in Figs 2 and 3. Figure 2 is a plot of cumulative number of earthquakes recorded against cumulative number of low-noise recording hours, and Fig. 3 shows the located epicentres superposed on a bathymetric contour map of the area. As Fig. 3 shows, the study area includes a ridge segment with a well defined median rift, 45 km long and averaging 7 km width. This is terminated by two fracture zones, designated fracture zone A (to the north) and fracture zone B (to the south), which offset the ridge from its continuations. Figure 2 also shows in which part of the area the sonobuoy arrays were placed. On the first leg of the cruise, during which the main survey of the rift took place, the weather was consistently poor, resulting in a noise level too high for effective recording. During the second leg, operations were concentrated on the fracture zones, particularly fracture zone A, and this is reflected in Fig. 2 and in the density of epicentres in Fig. 3.

The seismicity seems to be quite uniform in time (Fig. 2) and the same for both fracture zones. The sample of rift seismicity is not sufficient to allow firm conclusions to be drawn, but it seems lower than the fracture zone seismicity. Figure 2 has been compiled from the raw data, with no corrections for earthquake magnitude or for distance from the array. But we believe Fig. 2 is a fair representation of the seismicity, at least for the fracture zones. We have not attempted any individual magnitude estimates; the detection threshold for a nearby event is about $M=0$, and we estimate most of the earthquakes recorded to be between $M=0$ and $M=1$. In contrast to the Gulf of California or the Galapagos spreading centre, where microearthquake swarms seem to predominate[1,7] there were only two or three swarm-like sequences[8] recorded, consisting of up to seven closely spaced events. The microseismicity, at ten events per day, is comparable with that on active sections of the

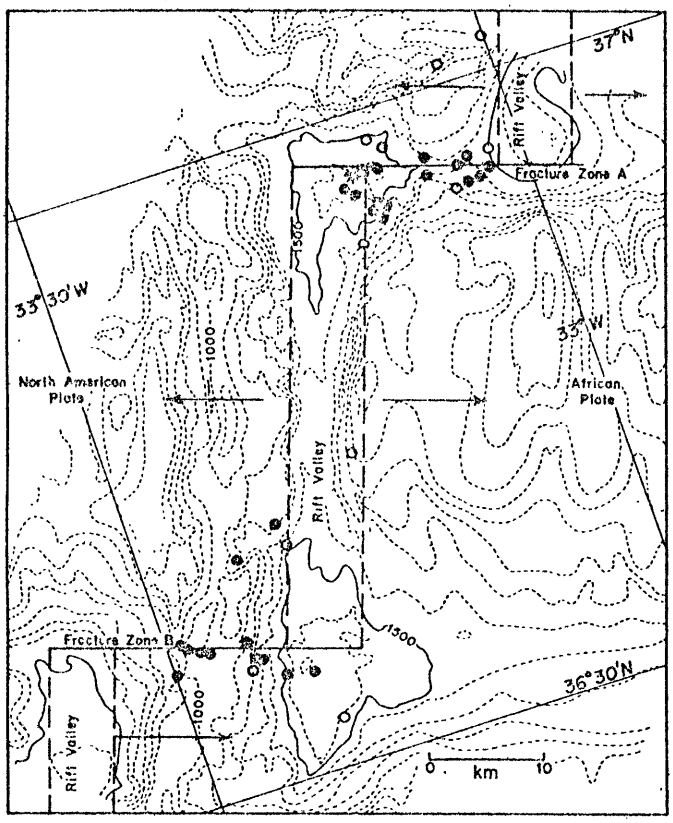

Fig. 3 Map of the best located epicentres, superposed on a bathymetric map of the area. The tectonic interpretation shown is a simplified approximation. ●, Good locations (generally with less than 2 km error); ○, less reliable locations (up to about 5 km error). The star-like symbol at the west end of fracture zone A represents a swarm-type sequence of about seven recorded events.

San Andreas Fault[9], and is consistent with the number of teleseismically detected earthquakes occurring along this section of the Mid-Atlantic Ridge[10].

Figure 3 demonstrates the excellent correlation of the seismicity with the fracture zones deducted from the topography. It clearly shows that most activity is restricted to the section of fracture zone between the rift segments, that is the section where transform faulting[11] is occurring. Along fracture zone B, the seismicity appears to delineate a simple transform fault, characterized by a narrow line of epicentres and narrow topographic notch (seen on the deep-tow data but not on the Fig. 3 map). Fracture zone A comprises a broader region of deformation, with a number of fault scarps and grabens (R. Detrick, personal communication). Most of the computed fracture zone A epicentres, however, lie within 1 km of a straight line, well inside the location uncertainty, which we estimate to be less than 2 km in most cases. This suggests that only one fault plane may be presently active. The active transform faults, as delineated by the seismicity, seem to be narrow and linear, even on a small scale. They are also active over their entire length, even over short time intervals. They show the usual approximate orthogonality to the ridge axis[12].

The junctions of the fracture zones with the median rift are characterized by topographic depressions. The deep-tow study showed that the depression at the junction of fracture zone A with the central rift is bounded on the north by a well defined fault scarp, which we interpret as the active transform fault. This scarp showed a high level of seismic activity, including the only located swarm, and we located one event on this scarp with particularly high accuracy (within 0.5 km). This suggests that active transform faulting continues well into the central rift valley, and hence, that the spreading centre plate boundary (or zone of intrusion), is itself a narrow feature within the central valley.

Because of the small sampling and, we believe, lower seismicity, there are hardly any reliable locations along the rift itself. Such evidence as there is suggests that the seismicity may be concentrated near the edge of the rift, and that there is essentially no activity outside the rift. This would be expected if normal faulting on the rift walls were the dominant source of rift earthquakes[13]. If the low microseismicity of the rift, particularly the low incidence of swarms, is real, then this is in sharp contrast to the Gulf of California and the Galapagos spreading centre, where the spreading segments are highly active[1,7]. This might indicate less volcanic activity on this slower spreading ridge[8].

We found it difficult to obtain accurate focal depths in this study, due to array limitations. In one case we found a focal depth of about 1 ± 1 km for a fracture zone A event. Other evidence, particularly the predominant T phase of many events, suggests an equally shallow source for most of the events recorded. In obtaining the epicentre locations, we have generally assumed zero focal depth and a P velocity of 5 km s^{-1}. This should not lead to appreciable errors in most cases. In general, the detailed seismicity and earthquake distribution seem to be in good agreement with current ideas on mid-ocean ridge plate tectonics.

We thank the Chief Scientists of the expedition, Drs B. P. Luyendyk, F. N. Spiess and J. D. Mudie, for accommodating and assisting this work and for allowing us to make use of the deep-tow data, and Dr J. D. Phillips for allowing us to use the bathymetric map of Fig. 3. This research was supported by National Science Foundation grants.

IAN REID

Institute of Geophysics and
Planetary Physics and
Scripps Institution of Oceanography,
University of California, San Diego,
La Jolla, California 92037

KEN MACDONALD

Department of Geology and Geophysics,
Woods Hole Oceanographic Institution,
Woods Hole, Massachusetts 02543
and
Department of Earth and Planetary Sciences,
Massachusetts Institute of Technology,
Cambridge, Massachusetts 02139

Received September 14, 1973.

1 Reid, I., Reichle, M., Brune, J., and Bradner, H., *Geophys. J. R. astr. Soc.* (in the press).
2 Sykes, L. R., Oliver, J., and Isacks, B., *The Sea*, 4 (edit. by Maxwell, A. E.), 353 (Interscience, New York, 1971).
3 Evernden, J. F., *Bull. seism. Soc. Am.*, 59, 1365 (1969).
4 Francis, T. J. G., and Porter, I. T., *Nature*, 240, 547 (1972).
5 Spiess, F. N., and Mudie, J. D., *The Sea*, 4 (edit. by Maxwell, A. E.), 205 (Interscience, New York, 1971).
6 Le Pichon, X., Ewing, J., and Houtz, R. E., *J. geophys. Res.*, 73, 2597 (1968).
7 Macdonald, K. C., and Mudie, J. D., *Geophys. J. R. astr. Soc.* (in the press).
8 Sykes, L. R., *J. geophys. Res.*, 75, 6598 (1970).
9 Brune, J. N., and Allen, C. R., *Bull. seism. Soc. Am.*, 57, 277 (1967).
10 Francis, T. J. G., *Earth planet. Sci. Lett.*, 4, 39 (1968).
11 Wilson, J. T., *Nature*, 207, 343 (1965).
12 Menard, H. W., and Atwater, T., *Nature*, 219, 463 (1968).
13 Sykes, L. R., *J. geophys. Res.*, 72, 2131 (1967).

Printed in Great Britain by Henry Ling Ltd., at the Dorset Press, Dorchester, Dorset

(Reprinted from Nature, Vol. 248, No. 5449, pp. 577–579, April 12, 1974)

Microearthquake survey of Median Valley of the Mid-Atlantic ridge at 36°30′N

MICROEARTHQUAKE activity in the median valley of the Mid-Atlantic Ridge near 36°30′N has been monitored using expendable radio-sonobuoy arrays. Similar techniques have been used by Reid *et al.*[1] in the Gulf of California, Macdonald and Mudie[2] near the Galapagos spreading centre and recently by Reid and Macdonald[3] near fracture zones A and B shown in Fig. 1 (ref. 4). This study provides area coverage not obtained by Reid and Macdonald whose experiment was confined to the fracture zone regions. A new method of sonobuoy position determination was used that provides relative buoy locations (locations with respect to each other) to within ±10 m. The ultimate positioning capability in latitude and longitude depends on the accuracy of the primary navigation system available. Satellite navigation can yield absolute positions to within ±100 m. An estimated actual accuracy of ±200 m is ascribed to the experiments reported here. Accuracy of this order allows correlation of epicentre locations with topographic features of similar scale size. Recently acquired bathymetric data (K. C. Macdonald and colleagues, in preparation) indicate that significant features of the ridge near 36°30′N, such as transform faults and valley walls, can be defined by scale sizes of some hundreds of metres. A total of 112 events definitely attributable to seismic activity were recorded in 72 h of listening, yielding an average rate of occurrence of 1.5 events h^{-1}.

FIG. 1 Bathymetric map of part of the Mid-Atlantic Ridge Epicentre locations obtained in this study are shown as large circles. Small circles represent epicentres determined by Reid and Macdonald[3]. Approximate location of fracture zones and median valley is shown. Contours are in uncorrected fathoms.

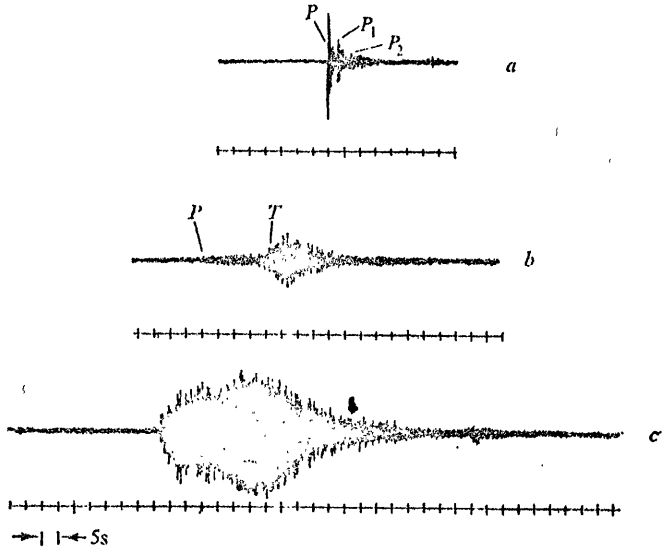

FIG. 2 Example of microearthquakes received with a single sonobuoy. Event *a* is less than 1 km horizontal range from the receiving hydrophone. *a*, 0231:30; *b*, 0156:40; *c*, 0154.

Arrays consisting of three US Navy AN/SSQ-57 calibrated sonobuoys, with 91.4-m hydrophone depth, were launched at three locations within the study area. The arrays approximated equilateral triangles with legs of 1.5 to 2 km. Sonobuoy positions were continuously monitored in real time by an acoustic navigation system originally designed to track the course of the submersible DSRV Alvin, but modified to track a moving hydrophone. The system uses either two or three bottom-moored acoustic transponders and a shipboard transmitter/receiver. (Two transponders make orientation with respect to the transponder baseline ambiguous; three transponders resolve the ambiguity. Often the ambiguity can be resolved from bathymetric data, or alternative navigation aides, thus allowing the use of only two transponders.) Determination of the position of a sonobuoy consists of first measuring the round trip travel time of an acoustic pulse emitted by the ship, received and retransmitted at a different frequency by each transponder and received aboard ship. This observation provides the one way travel time from ship to transponder, t_1. A second transmitted pulse is received by the transponders and retransmitted, but this time is received by the sonobuoy, thus determining the ship–transponder–sonobuoy acoustic travel time, t_2. The travel time from transponders to buoy is t_1–t_2. Slant ranges to the transponders are computed, corrections are made for sound velocity variation with depth (ray bending), and buoy position is resolved into a rectangular coordinate system whose origin is fixed with respect to the transponder net. Travel times can be determined to within 2 ms, thus establishing a limitation of about ±3 m in buoy positioning. In practice a sonobuoy fix can be obtained every 20 to 30 s. (The maximum round-trip travel time range of the navigation system was about 12 s.) Absolute positioning of the transponder net in latitude and longitude is done using satellite fixes.

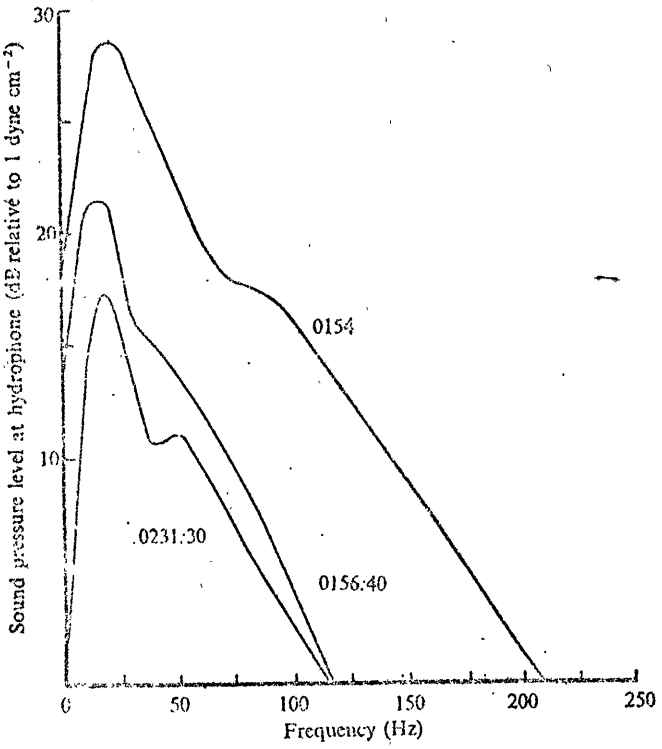

FIG. 3 Power spectra of three typical events (signal in excess of noise).

Seismic signals from the sonobuoy array elements were low pass filtered (0 to 500 Hz) and recorded on an f.m. analogue tape recorder with frequency response +0, −0.7 dB from d.c. to 5 kHz. An example of three events received by a single sonobuoy within an interval of about 40 min is shown in Fig. 2. The event depicted in Fig. 2*a* occurred within the bounds of the triangular array, less than 1 km away from all sonobuoys. First compressional wave arrival (P) and two reflections of that wave through the water column (P_1 and P_2) are clearly shown. Shear waves (S) and direct water waves (T) are not evident because of the proximity of the event. Figures 2*b* and 2*c* are more distant and exhibit prominent T-phase arrivals. These figures give an indication of the excellent recording conditions encountered. Sea states were typically 0 to 1/2 with wind and swell near zero. Ambient noise levels at 25 Hz were chiefly less than −10 dB with respect to 1 μbar. It is estimated that the array could detect microearthquakes of magnitude $M > -1$.

Power spectra of the events shown in Fig. 2 are shown in Fig. 3. These spectra have been corrected for the rising frequency response of the calibrated sonobuoys and represent an earthquake signal in excess of background noise. The spectra peak is about 15 to 25 Hz, rather greater than the typical peak frequencies of distant events[5]. This is not surprising since there is increased attenuation of high frequencies over long propagation paths. Measured peak pressures are comparable to an equivalent source strength of some 75 to 100 dB relative to 1 μbar at 1 m assuming spherical spreading over the entire transmission path.

Earthquake epicentre locations were determined by measuring the relative arrival times of the initial P wave on all three buoys. A horizontal, plane bottom was assumed, characterized by a compressional velocity of 5,000 ms^{-1}. When S-wave arrivals were distinct, S–P travel time differences were also used. The arrival times were solved iteratively for epicentre location using a computer. Geographical location accuracy is estimated to be within ±200 m, the major sources of error being the estimate of absolute latitude and longitude of the transponder navigation net, the assumed crustal compressional velocity of 5,000 m s^{-1} and the assumption of zero focal depth[3,6].

Although 112 events were recorded, only 29 had sufficiently distinct arrival times to allow accurate epicentre location. The small array dimensions (restricted by the range of the acoustic navigation net) made it impossible to locate events more than about 20 km away from the array. Thus it is difficult to compare the level of seismicity in the median valley with that near transform faults because virtually all recording time was over median valley segments. Reid and Macdonald measured about 0.5 events h^{-1} on fracture zones A and B, while we measured 1.5 events h^{-1}, but their system was less sensitive because of poor weather conditions and higher ambient noise levels.

All but two of the located events occurred along the boundary between the median valley floor and the median valley wall. Near-bottom, bathymetric profiles in the vicinity of the median valley both north and south of fracture zone B show that the median valley walls are constructed predominantly of normal faults (K. C. Macdonald *et al.*, unpublished). Since the microearthquakes in this study cluster at the edges of the median valley and not along the axis, the tremors are probably associated with the incipient and ongoing uplift of fault blocks forming the wall rather than with the dynamics of intrusion in the centre of the median valley. Indeed, the events located occurred only along the eastern edge of the median valley where the east rift wall begins, even though the array detection range was sufficient to detect events along the west wall and valley axis. This asymmetry is also apparent in the bathymetry and magnetics; the regional gradient of the rift walls is more gradual on the east side, and the axis of the central magnetic anomaly is offset several kilometres to the east (ref. 5 and H. D. Needham and F. Francheteau, to be published). Although our sampling is over a very short time interval, the seismicity distribution suggests that seafloor spreading activity here may be highly asymmetric, skewed towards the east at present.

This study was carried out as part of Project FAMOUS, during cruise 77 of RV Atlantis II in August 1973. We acknowledge the cooperation and assistance of W. B. Bryan, chief scientist of the cruise. This work was supported by a National Science Foundation grant and an Office of Naval Research contract.

R. C. SPINDEL

Woods Hole Oceanographic Institution

S. B. DAVIS

University of California, Santa Barbara, Santa Barbara, California 93106

K. C. MACDONALD
R. P. PORTER
J. D. PHILLIPS

Woods Hole Oceanographic Institution, Woods Hole, Massachusetts 02543

Received November 29, 1973.

1 Reid, I., Reichle, M., Brune, J., and Bradner, H., *Geophys. J. R. astr. Soc.*, (in the press).
2 Macdonald, K. C., and Mudie, J. D., *Geophys. J. R. astr. Soc.*, (in the press).
3 Reid, I., and Macdonald, K. C., *Nature*, (in the press).
4 Phillips, J. D., *Trans. Am. geophys. Union*, 54, 242 (1973).
5 Milne, A. R., *Bull. seism. Soc. Am.*, 49, 317 (1959).
6 Weidner, D. J., and Aki, Keiiti, *J. geophys. Res.*, 78, 1818 (1973).

Printed in Great Britain by Henry Ling Ltd., at the Dorset Press, Dorchester, Dorset